



UNIVERSITY OF
LEICESTER

**Quantifying oil palm-induced deforestation and land cover
change on Bugala island in Uganda using machine learning
and satellite remote sensing.**

by

Ivan Innocent Sekibenga

In submitting this thesis, I confirm that it is my own work.

**A thesis submitted to the School of Geography, Geology and the
Environment, University of Leicester in partial fulfillment of the
requirements for the degree of
Master of Science in Satellite Data Science.**

2023

Word count:14,230

Table of Contents

List of Figures	v
List of Tables	vii
Acknowledgments.....	viii
Abstract	ix
1. Introduction	1
1.1 Background on oil palm and its development in Uganda	1
1.2 Research Problem and Rationale	6
1.3 Aim and Research Objectives.....	9
1.4 Thesis Overview	9
2. Literature Review	10
2.1 Remote Sensing of Oil palm	10
2.2 Common machine learning algorithms for image classification.....	12
2.2.1 Random Forest Classifier	12
2.2.2 Support Vector Machine Classifier	13
2.2.3 The Maximum Likelihood Classifier	15
2.3 Thematic Accuracy Assessment	16
2.3.1 The Error matrix.....	17
2.3.2 The Kappa Coefficient.....	18
2.4 Comparison of accuracy of Machine Learning algorithms in oil palm mapping	19
2.5 Change Detection of oil palm induced land cover changes	21
3. Methodology.....	24
3.1 Study Area	24
3.2 Study Design.....	25
3.3 Data Acquisition and Pre-processing	27

3.4 Image Classification.....	28
3.4.1 Collection of Training samples	29
3.4.2 Training of machine learning classifiers	29
3.4.3 Classifying of Raster.....	29
3.5 Accuracy Assessment	30
3.6 Change detection	30
4. Results.....	31
4.1 Satellite Imagery.....	31
4.2 Objective1: Identification of the most accurate machine learning classifier	34
4.2.1 Summary of all Accuracy Assessment	34
4.2.2 Random Forest Classification and Accuracy Assessment of the 2002 image	34
4.2.3 Random Forest Classification and Accuracy Assessment of the 2016 image	37
4.2.4 Random Forest Classification and Accuracy Assessment of the 2022 image	39
4.3 Objective 2: Land cover areas and changes by class between 2002 and 2022	42
4.4 Objective 3: Oil palm induced Land cover class transitions.....	45
4.4.1 Land cover class transitions between 2002 and 2016 (14-year period)	45
4.4.2 Land cover class transitions between 2016 and 2022 (6-year period)	47
4.4.3 Overall Land cover class transitions between 2002 and 2022(20-year period).....	51
5. Discussion	57
5.1 Summary of the findings.	57
5.1.1 Objective 1: Identification of the most accurate machine learning classifier.....	57
5.1.2 Objective 2: Quantification of the areas of land cover classes in 2002, 2016 and 2022	57
5.1.3 Objective 3: Quantification of the major land cover transitions between 2002 and 2022	58
5.2 Comparison with published literature	58

5.3 Contributions of the study	59
5.4 Policy recommendations of the study	60
5.5 Gaps and recommendations for further research	61
5.6 Conclusion	62
6. References.....	63
7. Appendices.....	68
Appendix A : Support Vector Machine (SVM) confusion matrices	69
Appendix B : Maximum Likelihood (ML) confusion matrices	70
Appendix C : Support Vector Machine (SVM) classified maps.....	71
Appendix D : Maximum Likelihood (ML) classified maps	74

List of Figures

Figure 1.1: World vegetable oil production in tonnes between 1961 and 2020 (Source: Ritchie and Roser,2020).....	1
Figure 1.2: Oil palm production in millions of tonnes in 2020 (Source: Ritchie and Roser, 2020)	2
Figure 1.3: Oil palm production in tonnes in 2020 in the tropics (Source: Ritchie and Roser, 2020)	3
Figure 1.4: Oil palm mill operated by OPUL surrounded by its nucleus oil palm plantations. In the background is Lake Victoria (Source: Ministry of Agriculture, 2019).....	4
Figure 1.5: An out grower poses with freshly harvested oil palm bunches before transporting them to the OPUL mill. In the background are oil palm trees. (Source: Ministry of Agriculture, 2019)	5
Figure 2.1: Implementation of the Random Forest algorithm (Source: Rastogi,2020)	13
Figure 2.2: Implementation of the Support Vector Machine algorithm (Source: Kumar, 2022)	14
Figure 2.3: The Maximum Likelihood algorithm (Source: Nunez et al., 2019)	15
Figure 2.4: Calculation of producer, user and overall accuracies from the error matrix (Source: Congalton and Green ,2019)	17
Figure 2.5: Scales used for the interpretation of Kappa coefficient (Source: Foody,2020)	19
Figure 3.1: Location of Bugala island on Lake Victoria inside Uganda which is in Africa.	25
Figure 3.2: Methodology flow chart for the study design	26
Figure 4.1: 2002 Landsat 7 true colour image of Bugala island. (Source: USGS,2023)	31
Figure 4.2: 2016 Rapid Eye 5 true colour image of Bugala island. (Source: Planet Labs, 2022)	32
Figure 4.3: 2022 PlanetScope true colour image of Bugala island. (Source: Planet Labs, 2022)	33
Figure 4.4: Random Forest classifier generated areas of land cover classes for 2002 in km ² and percentages.....	35
Figure 4.5: Random Forest classified land cover map from the 2002 Landsat 7 image.....	36
Figure 4.6: Random Forest classified land cover map from the 2016 Rapid Eye 5 image	38
Figure 4.7: Random Forest classifier generated areas of land cover classes for 2016 in km ² and percentages.....	39

Figure 4.8: Random Forest classifier generated areas of land cover classes for 2022 in km ² and percentages.....	40
Figure 4.9: Random Forest classified land cover map from the 2022 PlanetScope image	41
Figure 4.10: Land cover class areas per class on Bugala island for 2002, 2016 and 2022	42
Figure 4.11: Land cover change areas by class between 2002 and 2016.....	43
Figure 4.12: Land cover change areas by class between 2016 and 2022.....	44
Figure 4.13: Map showing land cover transitions between 2002 and 2016.	46
Figure 4.15: Sankey diagram to visualize class area transitions between classes from 2002, through 2016 and up to 2022.	50
Figure 4.16: Map of areas that changed from Forest to other classes between 2002 and 2022.	51
Figure 4.17: Areas that changed from Forest to other classes between 2002 and 2022.	52
Figure 4.18: Map of areas that changed from Arable land to other classes between 2002 and 2022.	53
Figure 4.19: Areas that changed from Arable land to other classes between 2002 and 2022.	54
Figure 4.20: Map of areas that changed from Settlements to other classes between 2002 and 2022.	55
Figure 4.21: Areas that changed from Settlements to other classes between 2002 and 2022.	56

List of Tables

Table 1.1: The outcomes from the oil palm investment in Kalangala as of December 2018 (Source: Ministry of Agriculture, 2019)	6
Table 2.1: some applications of remote sensing to oil palm plantation monitoring	10
Table 3.1: Characteristics of Landsat 7, Rapid Eye 5 and PlanetScope imagery (Source: Planet Labs,2022; USGS,2023)	27
Table 4.1: Summary of Accuracy assessment results for the three classifiers on all the 3 images	34
Table 4.2: Random Forest based confusion matrix of classified map from 2002 image.	35
Table 4.3: Random Forest based confusion matrix of the classified map from 2016 image. .	37
Table 4.4: Random Forest based confusion matrix of the classified map from 2022 image. .	40
Table 4.5: Random Forest classifier derived class area changes between 2002 and 2022....	42
Table 4.6: Area transition matrix from 2002 to 2016	47
Table 4.7: Area transition matrix from 2016 to 2022	49
Table 4.8: Changed areas from forest to other classes.	52
Table 4.9: Changed areas from Arable land to other classes.	54
Table 4.10: Changed areas from Settlements to other classes.	56

Acknowledgments

I honor the Lord Jesus Christ for the gift of life and wisdom, without which I could accomplish nothing. I thank the Lord for enabling me to receive a Commonwealth Shared Scholarship that has enabled me to study this master's degree. I am forever grateful to the UK Commonwealth commission and University of Leicester for the offer of this full scholarship without which it would be impossible to study in the UK. I also express my heart felt gratitude to my supervisor, Professor Heiko Balzter who has been a guide and a rich resource of wisdom and mentorship while I was at the University of Leicester. The module he taught on satellite data analysis using Python and his passion for conservation of forests inspired me and birthed this dissertation topic. I also express my gratitude to the teams at Planet Labs and United States Geological Survey that gave me access to download their satellite imagery that has been the core of this research. Lastly, I am very grateful to my family; Lillian, Charis, Jireh and Jael for the moral support and prayers. I thank God for my special friends; Glorious, Isaiah, Matthew, Mutunrayo, Krishna, Jonas, Innocent, Lucman, Steven and Naya for the friendship during my stay in the UK. God bless you all.

Abstract

This study compared Random Forest, Support Vector Machine and Maximum Likelihood classifiers and established that the Random Forest classifier was the most accurate for classifying satellite imagery of land cover on Bugala island. The Random Forest classifier exhibited overall accuracies of 0.94, 0.86 and 0.83 for the 2002, 2016 and 2022 maps respectively.

The variations in land cover through time and space, and transitions from 2002 to 2022 were mapped and quantified using the Random Forest generated maps. Results show that between 2002 and 2022, Oil palm plantations have increased to 91.2km² at the expense of forests which have reduced by 74.2km²(43%). The desire by the government to allocate more land to Oil Palm Uganda Limited (OPUL) for oil palm plantations led to reduction in settlements by 16.6km² through eviction of illegal tenants. Overall, arable land increased by 12.9km² at the expense of forests.

Further, between 2002 and 2022, 64.6km² of forest were converted into oil palm plantations while 2km² of forest became settlements. An additional 29.5km² of forest was converted into arable land. 15.4km² of arable land were converted into oil palm plantations while 10.3km² of arable land transited into forests. An additional 2.3km² of arable land was converted into settlements. 5.7km² of settlements were converted into oil palm plantations. 7.9km² of settlements became arable land while 4.4km² of settlement transited into forest.

The study recommends increased monitoring and gazetting of forests into protected reserves and shifting of future oil palm plantation expansions to fallow land to minimise deforestation.

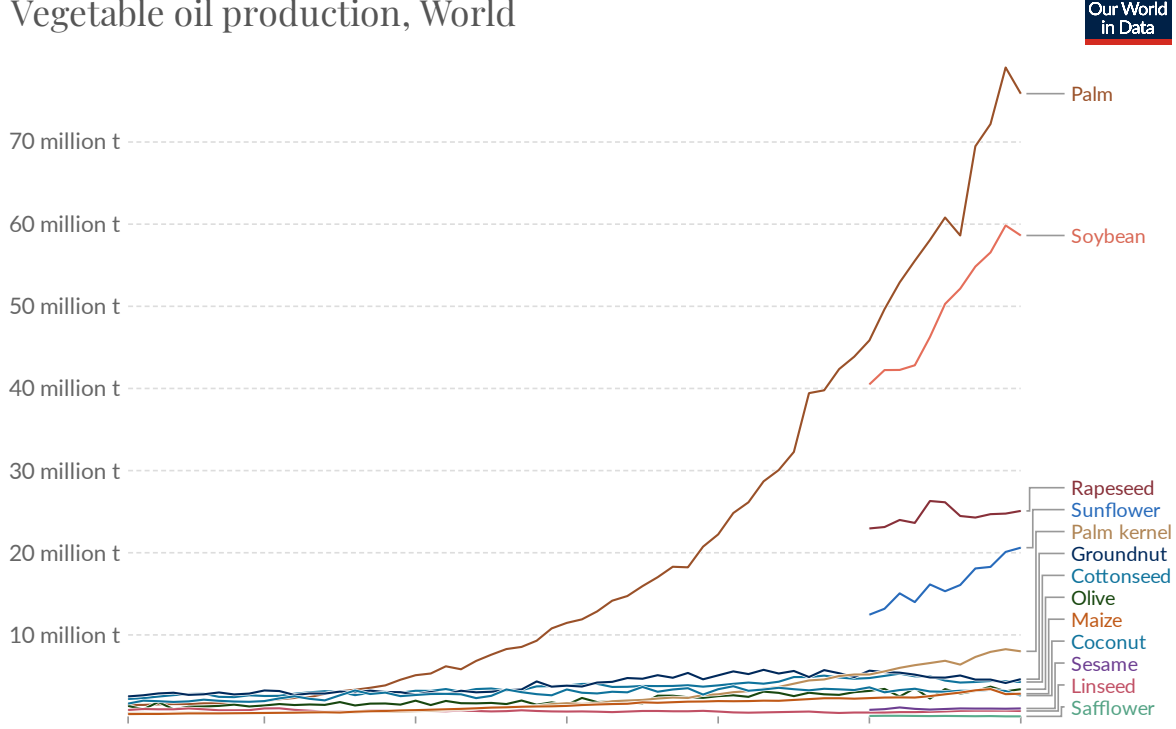
1. Introduction

In this chapter, the scope of this dissertation is inaugurated by providing a background to the research problem, rationale and motivation for the research investigation and the corresponding research aim and objectives.

1.1 Background on oil palm and its development in Uganda

Oil palm with scientific name, *Elaeis guineensis* is a perennial crop grown in tropical areas located inside 10 degrees North and 10 degrees South of the equator (Chong *et al.*, 2017; Otuba *et al.*, 2022). Globally, oil palm is the major source of vegetable oil (**Figure 1.1**) for cooking and frying globally and offers a much higher yield capacity of oil per hectare when compared to its competitors such as sunflower, rapeseed and soybean (Chong *et al.*, 2017; Otuba *et al.*, 2022). Apart from being edible when used for cooking oil, margarine, and ice creams, it is used in factories to produce detergents, cosmetics, biodiesel, fertilizers, and animal feeds (Lee *et al.*, 2016; Otuba *et al.*, 2022).

Vegetable oil production, World



Source: Food and Agriculture Organization of the United Nations

OurWorldInData.org/food-supply • CC BY

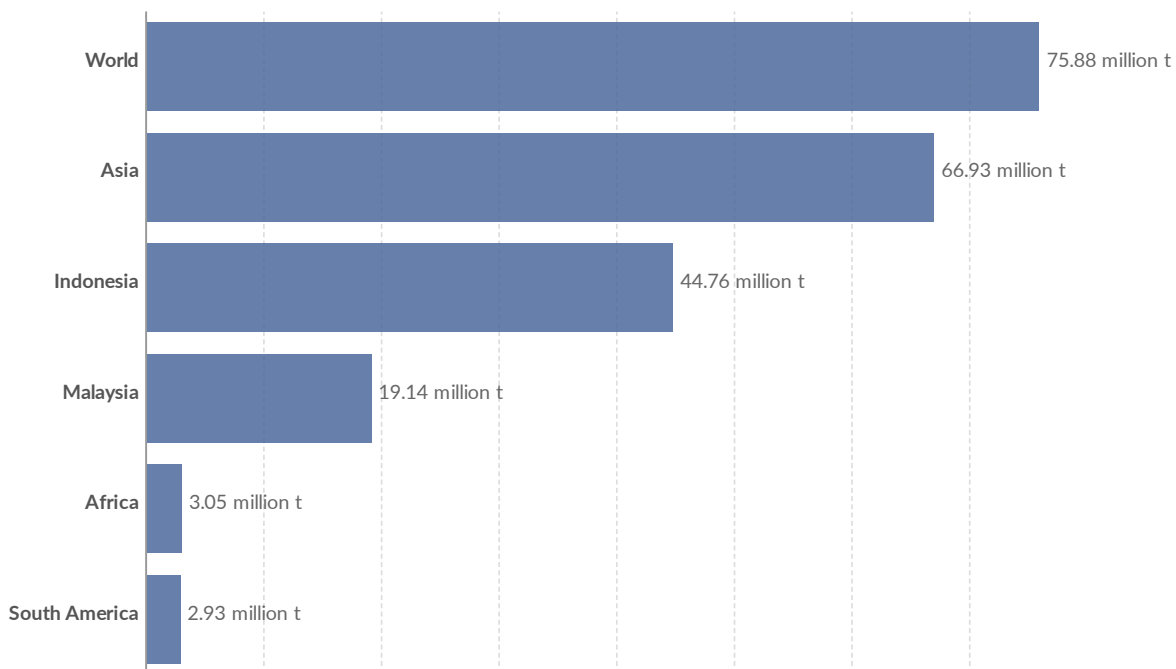
Figure 1.1: World vegetable oil production in tonnes between 1961 and 2020 (Source: Ritchie and Roser, 2020)

Oil palm grows best in areas that receive plenty of rainfall and sunshine and whose temperatures range between 25 to 32 degrees Celsius (Chong *et al.*, 2017). It remains productive for at least 25 years. Indonesia is the world's leading commercial producer of oil palm (**Figure 1.2**), followed by Malaysia (Chong *et al.*, 2017; Shaharun *et al.*, 2020; Otuba *et al.*, 2022). **Figure 1.2** shows that the two countries produced almost three quarters of the global production of oil palm in 2020. Indonesia earned approximately 29 million US dollars from oil palm exports in 2021 and as a result, more players want to dive in and partake of this lucrative oil palm business (Asming *et al.*, 2022). Due to the profitability and ever-growing huge global demand for palm oil which is yet to be satisfied by the current global production output, oil palm growers are intensifying strategies that increase production such as increasing yields on current plantations and the acquisition of more land for the establishment of more plantations (Carlson *et al.*, 2012).

Oil palm production, 2020

Oil palm production is measured in tonnes.

Our World
in Data



Source: Food and Agriculture Organization of the United Nations

OurWorldInData.org/agricultural-production • CC BY

Figure 1.2: Oil palm production in millions of tonnes in 2020 (Source: Ritchie and Roser, 2020)

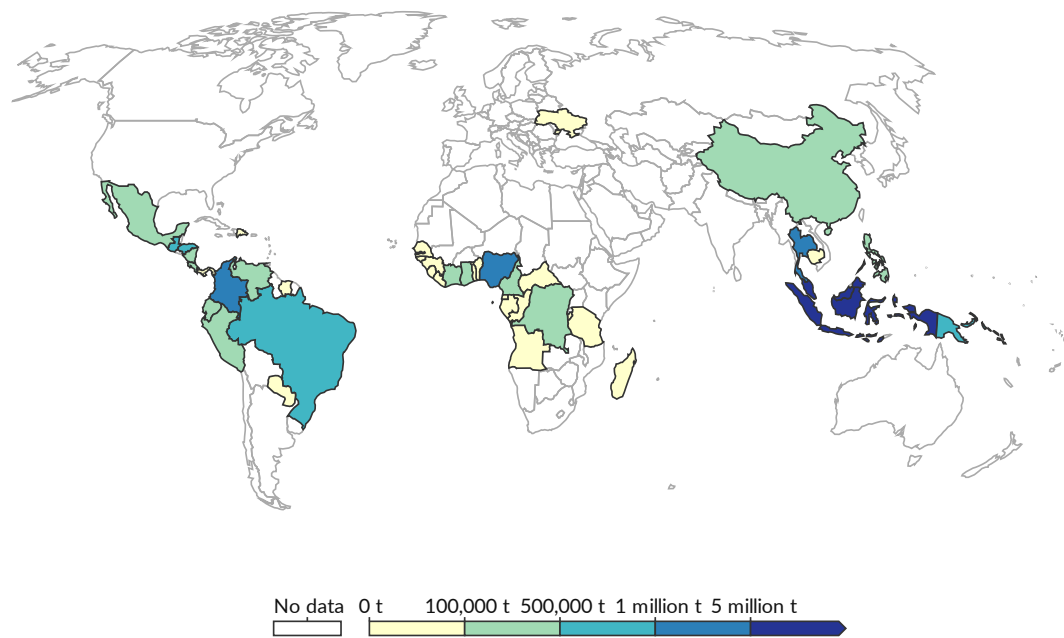
In addition, new players are joining the business by establishing new plantations in other areas of the tropics (**Figure 1.3**) such as Africa, Asia and South America (Lee *et al.*, 2016). Due

to the substantial worldwide market for palm oil, high economic benefits, and the fact that favourable growing conditions exist in the tropics, many tropical countries such as Uganda adopted it as a cash crop (Otuba *et al.*, 2022).

Oil palm production, 2020

Oil palm production is measured in tonnes.

Our World
in Data



Source: Food and Agriculture Organization of the United Nations

OurWorldInData.org/agricultural-production • CC BY

Figure 1.3: Oil palm production in tonnes in 2020 in the tropics (Source: Ritchie and Roser, 2020)

In 2003, the Government of Uganda and a private company Oil Palm Uganda Limited (OPUL) implemented a partnership to grow oil palm commercially in Uganda. The aim of the project was to satisfy the big demand for vegetable oil in Uganda while creating jobs for the citizens on the islands and on the mainland (Otuba *et al.*, 2022; Piacenzar, 2012). According to the Ministry of Agriculture (2019), this involves a four partnership (4P) model that comprises of the Government of Uganda, out growers, Oil Palm Uganda Limited (OPUL), and the International Fund for Agricultural Development (IFAD). The government of Uganda was responsible for acquiring of land and leasing it to OPUL to develop oil palm plantations. The government is responsible for the infrastructural developments such as road construction on the island, electricity supply and operating a ferry service linking Bugala island to the mainland. OPUL is responsible for planting the nucleus oil palm plantation estates. OPUL also

buys fresh oil palm from out growers and operates the processing mills and refineries to process the oil palm bunches (**Figure 1.4**). IFAD funds the out growers to purchase seedlings, fertilisers, and farm equipment such as tractors. The role of the out growers is to grow oil palm on their arable land which they sell to OPUL as fresh oil palm bunches (**Figure 1.5**). As of 2018, there were 2,064 out growers registered under the Kalangala Oil Palm Growers Trust (KOPGT) who receive agronomic and loan extension support. Altogether, OPUL and the out growers have planted approximately 11,348 hectares of oil palm. Many of the out growers were once primarily fishermen but have resorted to oil palm growing for an additional source of income. This has led to increased household income and employment for the citizens having occupations in this sector. In addition, Uganda has drastically cut down on the importation of crude palm oil since the harvest of oil palm rose from 37,802 metric tonnes in the financial year 2017/2018 to 44,221 metric tonnes in 2018/2019 bringing in at least 21.1 billion Uganda shillings annually (Ministry of Agriculture, 2019).



Figure 1.4: Oil palm mill operated by OPUL surrounded by its nucleus oil palm plantations. In the background is Lake Victoria (Source: Ministry of Agriculture, 2019)



Figure 1.5: An out grower poses with freshly harvested oil palm bunches before transporting them to the OPUL mill. In the background are oil palm trees. (Source: Ministry of Agriculture, 2019)

Before the establishment of the oil palm project on Bugala island in 2003, fishing was the primary economic activity carried out on the surrounding Lake Victoria using small wooden boats. The fish were then sold fresh or smoked for preservation and sold to traders from the mainland. Subsistence farming involving food crops such as beans, maize, cassava, bananas, and ground nuts was also being carried out. However, despite all these economic activities, Kalangala district with Bugala island as its most productive island was among the five poorest districts in Uganda with deplorable infrastructure developments that relegated it as a remote and hard-to-reach area. According to the 2016 oil palm impact evaluation report by the Ministry of Agriculture (2019), The development of oil palm plantations on the island has turned this situation around by improving the quality of life of the islanders. The report found that houses constructed using iron sheets rose from 40% in 2002 to 95% in 2016, households using electricity as primary source of lighting rose from 0.1% in 2002 to 56.6% in 2016 and food secure households rose from 16.4% in 2002 to 70.5% in 2016. It was also simulated that an acre of mature oil palm earns an out grower about 2 million Uganda shillings annually.

Table 1 summarises key proceeds from the oil palm project.

Table 1.1: The outcomes from the oil palm investment in Kalangala as of December 2018 (Source: Ministry of Agriculture, 2019)

OUTCOMES	VALUE
1. Registered oil palm farmers (number of farmers)	2,064 (37% female)
2. Oil palm fresh fruit bunches harvested by farmers (Jan 2010 to December 2018)	143,446 tons
3. Gross income earned by smallholder farmers (Jan 2020 to December 2020)	UGX 69.6 billion
4. Monthly gross income earned by the smallholder farmers	UGX 1.9 billion
5. Area under nucleus estate (private sector controlled)	6,500 Ha
6. Area under smallholder estate	4,848 Ha
7. Smallholder establishment and maintenance loans disbursed to farmers	UGX 52 billion
8. Loans repaid by smallholder farmers	UGX 32.4 billion
9. Area under harvest by smallholder farmers (area with mature oil palm trees)	3,602 Ha
10. Average income per acre per year	UGX 2.6 million
11. Average annual income per household	UGX 15.5 million
12. Taxes paid by OPUL to the Government annually (2017)	UGX 180 billion
13. Taxes paid by Private Sector Partner in taxes	UGX 899.44 billion
14. Employment opportunities created at the Palm Oil Mill and Nucleus Estate	3,000 people
15. Employment opportunities created in the smallholder scheme	900 people
16. Farm roads constructed	879 kms
17. Dividends paid by OPUL to the oil palm farmers (KOPGT)	UGX 17.75 billion
18. Monthly With Holding Tax paid by smallholder farmers	UGX 20 million
19. Taxes paid by smallholder farmers on dividends	UGX 500 million

1.2 Research Problem and Rationale

However, despite its economic benefits, oil palm growing has led to vast deforestation in most oil palm growing countries such as Indonesia, Malaysia, and Africa as more gigantic chunks of forested land are cleared to make room for oil palm plantations (Carlson *et al.*, 2012; Shaharun *et al.*, 2020; Lee *et al.*, 2016). Carlson *et al.* (2012) used Landsat imagery-based time series to quantify past and future oil palm plantation expansion impacts on carbon flux, forests, and community land cover in Indonesia Borneo. The study showed a strong positive correlation between oil palm plantation expansion and net carbon emissions attributed to tree cutting and forest burning. According to Lee *et al.* (2016), it has been calculated that the establishment of oil palm plantations was directly to blame for around 57% of the deforestation between 2000 and 2010 in Kalimantan, the Indonesian portion of Borneo. Around 19% of Sumatra's deforestation during that time period occurred within oil palm concessions. The peat ecosystems of Peninsular Malaysia, Borneo, and Sumatra, which serve

as crucial carbon repositories, have been shown to be negatively affected by industrial oil palm farms. Negative consequences of the changing of tropical forests into oil palm plantations include biodiversity loss, greater carbon dioxide emissions, raised temperatures in aquatic habitats, and increased silt buildup in aquatic systems (Lee et al., 2016).

In Uganda, the government degazetted forest land and public land on Bugala island in Lake Victoria in Kalangala district, purchased land from absentee landlords and leased it for 99 years to OPUL for oil palm plantations development. This involved clearing 6500 hectares of land that had tropical forests on them by burning and cutting down the trees (Otuba *et al.*,2022; Piacenzar,2012). In addition, tenants and squatters were forced to lose access to arable land for growing food crops or harvesting forest products like timber and firewood. This caused much uproar from environmentalists, opposition politicians, and local communities who assert that the project led to deforestation, environmental degradation, loss of biodiversity, land grabbing, and forced displacement of local people in favour of OPUL investors (Piacenzar,2012). In addition, more mainlanders have migrated to the island by purchasing land from the indigenous people and established oil palm plantations as out growers. This has led to high prices in value of real estate on the island and may lead to future reduction in arable land available for growing other food crops responsible for food security.

This study investigates the impacts of oil palm plantation development on land cover change of forest land and arable land on Bugala island motivated by the valuable findings and research gaps identified in a previous study carried out by Piacenzar (2012) that utilized field work interviews of families of oil palm growers via the focus group method. There are no previous studies that the author is aware of that have examined the impact of oil palm plantations on land cover change on Bugala island using satellite remote sensing. However, Piacenzar (2012) utilized fieldwork focus group interviews to investigate the impact of oil palm plantation development on how different genders access land and its commercial benefits in a patriarchal society found on Bugala island. Her findings indicated that whereas the men benefit from the increased cash income obtained from their monthly sale of oil palm bunches to OPUL as out-growers or as employees on OPUL plantations, the women do not benefit because their negotiating power is curtailed due to diminished access to both forest and arable land (Piacenzar,2012).

Prior to the introduction of oil palm plantations, there was plenty of arable land available to women to grow food crops like bananas, cassava, maize, and beans for both consumption and sale. In addition, because of the presence of vast areas of forests, they could freely obtain firewood and charcoal that could be sold to fishermen to be used in the smoking and preservation of fish for sale. Forests were also a convenient and cheap major source of medicinal herbs and trees that have been utilised by women for centuries to treat ailments amongst their families and livestock even after the introduction of modern medical facilities on Bugala island. Most of this land that once provided these benefits has been converted to oil palm plantations leading to unprecedeted pressure on arable land (Piacenzar,2012). According to Piacenzar (2012), oil palm plantations occupy close to one-third of Bugala island's land cover leading to an increasing scarcity of forest and arable land that can be utilised by the women.

The overall objective of this study is to evaluate the effects of oil palm plantation development on the land cover and land use change on Bugala island in Uganda using remote sensing techniques and satellite data by establishing how much land cover is under oil palm plantation, forest, and arable land. According to Piacenzar (2012), it is impossible to establish the exact amount of private forest that once covered Bugala Island before the dawn of oil palm plantations on the island since available records only show the 6,462 hectares of protected district forest reserves. In addition, according to the National Forestry Authority Office on Bugala island, there are no resources to map the private forests beyond the district forest reserves to establish how much land was covered by private forest before oil palm plantation developments and how much currently remains after the introduction of oil palm plantations (Piacenzar,2012). A low-cost, easily available, and user-friendly tool is required for forest scientists and managers in economically disadvantaged nations to monitor the development and expansion of industrial oil palm plantations (Lee et al., 2016). This study is very relevant since it will use a cheap approach using satellite remote sensing and machine learning to tackle and answer the questions and concerns raised by Piacenzar (2012). Furthermore, although the oil palm project has dramatically reduced poverty amongst the oil palm out-grower farmers and the plantation workers, it has led to negative repercussions for the islanders such as lack of public land for expansion of public infrastructural developments such as schools, dams, and hospitals (Piacenzar,2012).

This study will utilize satellite remote sensing to identify how much forest, public land, and arable land has been lost to oil palm plantations leading to the disenfranchising of the indigenous population in access to land and forests as reported by Piacenzar (2012).

1.3 Aim and Research Objectives

The primary aim of this research is to conduct a spatial and multi-temporal analysis of the impact of oil palm plantation expansions on the land cover and land use on Bugala island.

To address the primary aim, the investigation will focus on the following objectives:

- To identify the most accurate supervised machine learning classifier for detecting and mapping of oil palm plantations and other land cover on Bugala island.
- To create accurate land cover and land use classification maps for the years 2002, 2016, and 2022 and to subsequently quantify the area and change in area of each land cover class on Bugala island.
- To map and quantify the major land cover transitions induced by oil palm plantation development and expansion on Bugala island between 2002 and 2022.

1.4 Thesis Overview

This thesis is structured into five core chapters. Chapter 1 has introduced and presented the research problem and motivation for this investigation. Chapter 2 will review the contemporary literature concerning accuracy assessment, supervised machine learning algorithms namely; random forest, support vector machines and maximum likelihood and their application in oil palm induced land cover and land use change. Chapter 3 outlines the satellite data acquisition and preprocessing techniques, as well as the methods used to implement the supervised classification, mapping and change detections undertaken. In Chapter 4, the results are presented spot lighting informative oil palm-induced land cover change trends. Chapter 5 then amalgamates these results with suitable literature to discuss the impacts of oil palm expansion and recommended policy change. It also offers a concise recap of the main discoveries in this study, while also offering insights into prospective research directions in response to the ongoing expansion of oil palm cultivation.

2. Literature Review

This chapter summarizes the literature on applications of earth observation imagery for oil palm mapping. It also presents and assesses the machine learning methods used in earth observation to establish how well they work. It also delves into literature on accuracy assessment and change detection. This chapter gives a foundational justification for the research design and the methods utilized.

2.1 Remote Sensing of Oil palm

Remote sensors such as satellites have the capability to detect oil palms as a unique feature on the Earth's surface and as such have been utilised in diverse applications (**Table 2.1**) in oil palm plantation monitoring.

Table 2.1: some applications of remote sensing to oil palm plantation monitoring

	Application	Author(year)	Summary
1	Tree counting using Airborne Imaging Spectrometer for Applications (AISA)	Shafri, Hamdan and Saripan (2011)	a semi-automated approach to count and distinguish oil palms from non-oil palms was achieved by the utilisation of several analytical techniques, including texture examination, spectrum analysis, edge improvements, morphological inspection, and bob analysis.
2	Age estimation using WorldView-2 multispectral satellite data	Chemura van Duren and van Leeuwen (2015)	The use of object-based image analysis (OBIA) was employed to ascertain the crown projection sizes of oil palms. The crown projection sizes were then employed for the purpose of estimating the age of oil palm plants.
3	Estimation of Above Ground Biomass (AGB) and carbon production using SPOT-5 satellite data	Singh, Malhi and Bhagwat (2014)	The Fourier transform was employed to assess the structural characteristics and biomass changes in a tropical forest environment with oil palm plantations.
4	Pests and disease detection using Quickbird satellite data	Santoso et al. (2010)	high resolution imagery was utilised to detect and map Ganoderma disease infested oil palm trees utilising NDVI, spectral reflectance, and additional vegetation indices
5	Yield estimation using Quickbird satellite images	Balasundram, Memarian and Khosla (2013)	Ratio vegetation index derived from Quickbird imagery was correlated with oil palm yield

Earth observation, satellite remote sensing and image classification involving categorising objects based on the class of their land cover facilitates the differentiation of oil palm plantations from surrounding land cover types, including forests, water bodies, and human settlements (Chong et al., 2017). This technology facilitates the delineation of borders and precise assessment of the extent of oil palm cultivation. When used in a temporal study, this technique proves to be of great value in identifying the increase of oil palm cultivation and associated land activities. Optical remote sensing is a method of collecting the sun's radiation within the visible and near-infrared (NIR) spectrum that is reflected off the Earth's surface into the satellite's sensor (Chong et al., 2017).

Various signals are obtained from the reflected solar radiation throughout the electromagnetic spectrum, including red, blue, green, red edge, near-infrared (NIR), and infrared wavelengths. The specific signals detected depend on the capabilities of the sensors used. Various terrain surfaces exhibit varying degrees of intensity throughout the electromagnetic spectrum. Through the examination of reflected energy and the categorization of this energy based on specific spectral signatures, it becomes possible to distinguish various land cover classes (Chong et al., 2017). Optical remote sensing methodology uses two approaches, namely: image-based and phenology-based approaches (Lee et al., 2016). Phenology-based approaches use time-dependent variations in the greenness of vegetation to identify the extent of deforestation resulting from the spread of large-scale oil palm cultivation. Image-based approaches use both spectral signatures and texture information in order to distinguish oil palm plants from their environment (Lee et al., 2016). Land cover classification is often performed by categorizing pixels with identical pixel values, based on the machine learning classifier employed. A pixel-based classification technique is used to assign a distinct class to each pixel across the entire image (Chong et al., 2017). The use of the spectral angle mapper revealed that the near-infrared (NIR) band consistently exhibited the maximum contrast, therefore making it the most effective in distinguishing oil palm crowns from the backdrop (Chong et al., 2017).

2.2 Common machine learning algorithms for image classification

2.2.1 Random Forest Classifier

The Random Forest algorithm invented by Breiman (2001) (**Figure 2.1**) is a widely used machine learning technique that combines many decision trees to make predictions (Lee *et al.*,2016). It is an ensemble based technique that is used as a classifier and regressor. The ensemble model comprises of several decision trees, whereby each tree is trained on a randomly selected portion of the data and a randomly selected subset of the characteristics (Breiman,2001). The ultimate forecast is derived by combining the predictions of individual trees, such as via a voting mechanism for classification tasks (Breiman,2001; Sheykhmousa et al., 2020; Jarayee et al. ,2022).

The operational mechanism of the algorithm is such that it constructs an ensemble of decision trees, often known as a "forest." In the forest, a bootstrapping of the training data and a random selection of characteristics are implemented for each individual tree (Breiman,2001). The growth of each tree occurs autonomously via the recursive division of nodes, using the optimal feature and split criteria (Breiman,2001; Lee *et al.* ,2016). When generating predictions for a novel data point, every individual tree within the ensemble predicts the corresponding class (in the context of classification) or value (in the context of regression) (Sheykhmousa et al., 2020).

The strengths of the algorithm are as follows: The technique of reducing overfitting is achieved by the process of integrating numerous trees. In addition, random forest classifier is capable of processing both categorical and numerical data. The Random Forest algorithm has been widely recognised and used in land cover classification owing to its transparent and comprehensible procedure for making decisions and its ability to provide high-quality classification outcomes (Jarayee et al.,2022; Lee *et al.*,2016; Shaharun *et al.*,2020).

Additionally, the ease with which Random Forest can be implemented in a parallel structure for accelerating the computation of large-scale geographic data has contributed to its appeal in this field (Sheykhmousa et al., 2020).

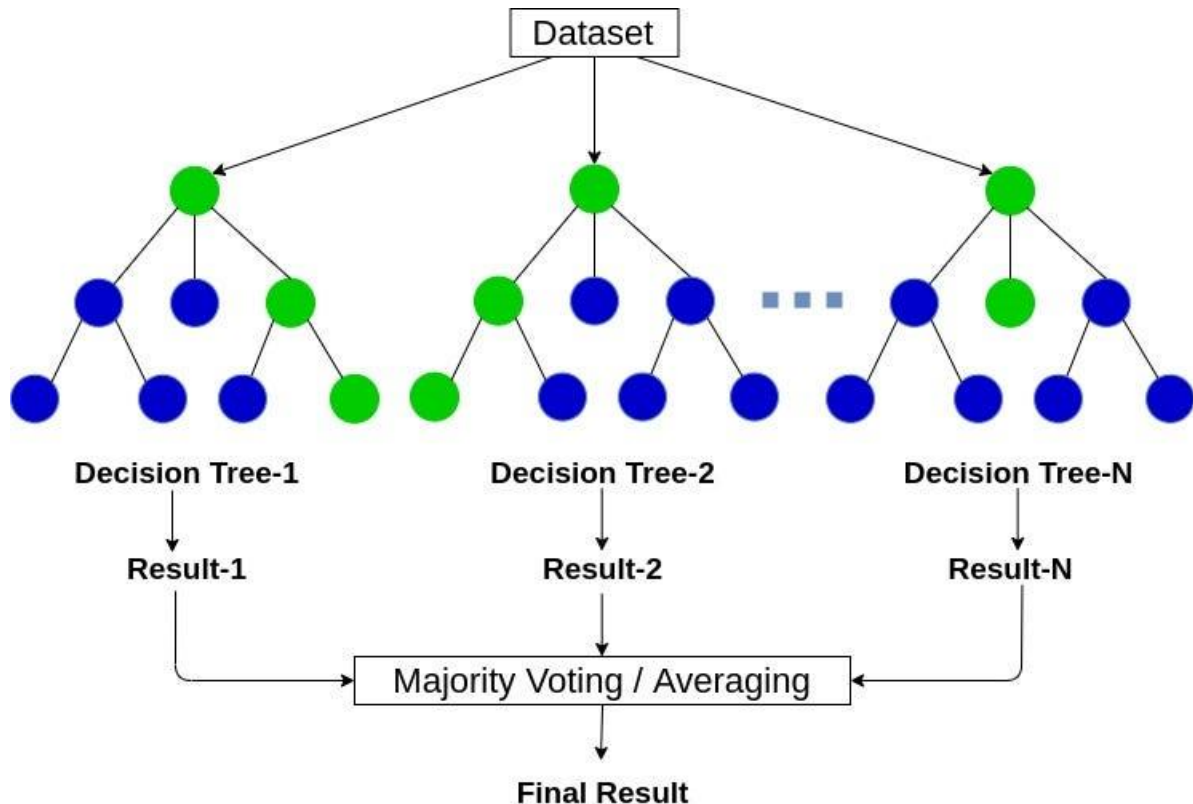


Figure 2.1: Implementation of the Random Forest algorithm (Source: Rastogi, 2020)

Sheykhmousa et al. (2020) identify several additional benefits associated with the Random forests. Firstly, it effectively handles a vast quantity of variables that are entered without the need for variable deletion. Secondly, it is able to reduce the variance in predictions without introducing any significant bias. Thirdly, it is capable of calculating nearness between pairs of instances which can be utilised for identifying outliers. Fourthly, the classifier demonstrates robustness in the presence of outliers and noise. Lastly, it offers computational simplicity compared to alternative tree ensemble methods such as Boosting. However, it becomes computationally intensive, especially with a gigantic number of trees and features (Lee et al., 2016). According to Svetnik et al. (2003), to increase the accuracy of the classifier more trees are utilised and too many trees slow down the algorithm.

2.2.2 Support Vector Machine Classifier

The Support Vector Machine (SVM) by Cortes and Vapnik (1995) is a machine learning algorithm used in both classification and regression tasks (Nunez et al., 2019). It is based on the concept of finding an optimal hyperplane that separates different classes (Jarayee et al.

,2022). The objective is to identify a hyperplane that optimally segregates data points into discrete groups or forecasts numerical values (Cortes and Vapnik ,1995).

According to Sheykhmousa et al. (2020), the operational mechanism of the algorithm is as follows: The Support Vector Machine (SVM) algorithm (**Figure 2.2**) seeks to identify the hyperplane that optimizes the separation between a pair of classes within the training dataset. The data is subjected to a transformation into a space of greater dimensions using a kernel function that is a linear, polynomial, or radial basis function (Cortes and Vapnik ,1995; Noon et al. ,2014). Within the context of a space with several dimensions, the objective is to identify the hyperplane that optimizes the margin while simultaneously minimizing the occurrence of classification errors (Jarayee et al.,2022). Support vectors, which refer to data points that either sit on the margin or inside it, influence the determining of the decision boundary (Nooni et al. ,2014).

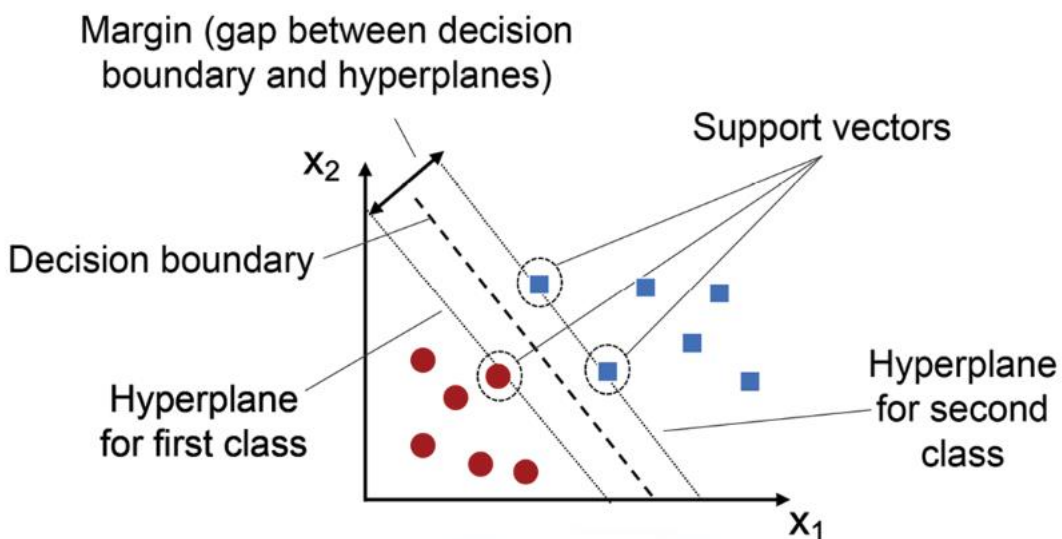


Figure 2.2: Implementation of the Support Vector Machine algorithm (Source: Kumar, 2022)

The merits of the algorithm are; its effective in high-dimensional spaces, works well when there is a clear margin of separation and can handle non-linear classification through kernel functions (Sheykhmousa et al., 2020; Nooni et al. ,2014).

The challenges of the algorithm include; the selection of the kernel and the process of tweaking hyperparameters are both factors that need careful consideration (Nunez et al., 2019; Nooni et al. ,2014). The computational cost is high, particularly when dealing with massive datasets. Furthermore, the task of achieving interpretability might present

difficulties, particularly when dealing with non-linear kernels (Sheykhmousa et al., 2020).

2.2.3 The Maximum Likelihood Classifier

According to Stigler (2007), the Maximum Likelihood estimation was developed by Ronald Fisher in 1922. The Maximum Likelihood Classifier (**Figure 2.3**) is a probabilistic classification technique often used in remote sensing and image classification (Nunez et al., 2019). The process involves the allocation of each individual pixel inside an image to the specific class that yields the highest probability of the observed pixel values, taking into consideration the statistical model associated with that class (Nooni et al., 2014). The operational mechanism of the algorithm is as follows: Every class is represented by a probability distribution, usually in the form of a Gaussian or Normal distribution (Stigler, 2007; Nunez et al., 2019). The method calculates the probability of the pixel values given the distribution of each class for every pixel in the picture. The class label for a pixel is determined by selecting the class with the greatest probability (Nooni et al., 2014).

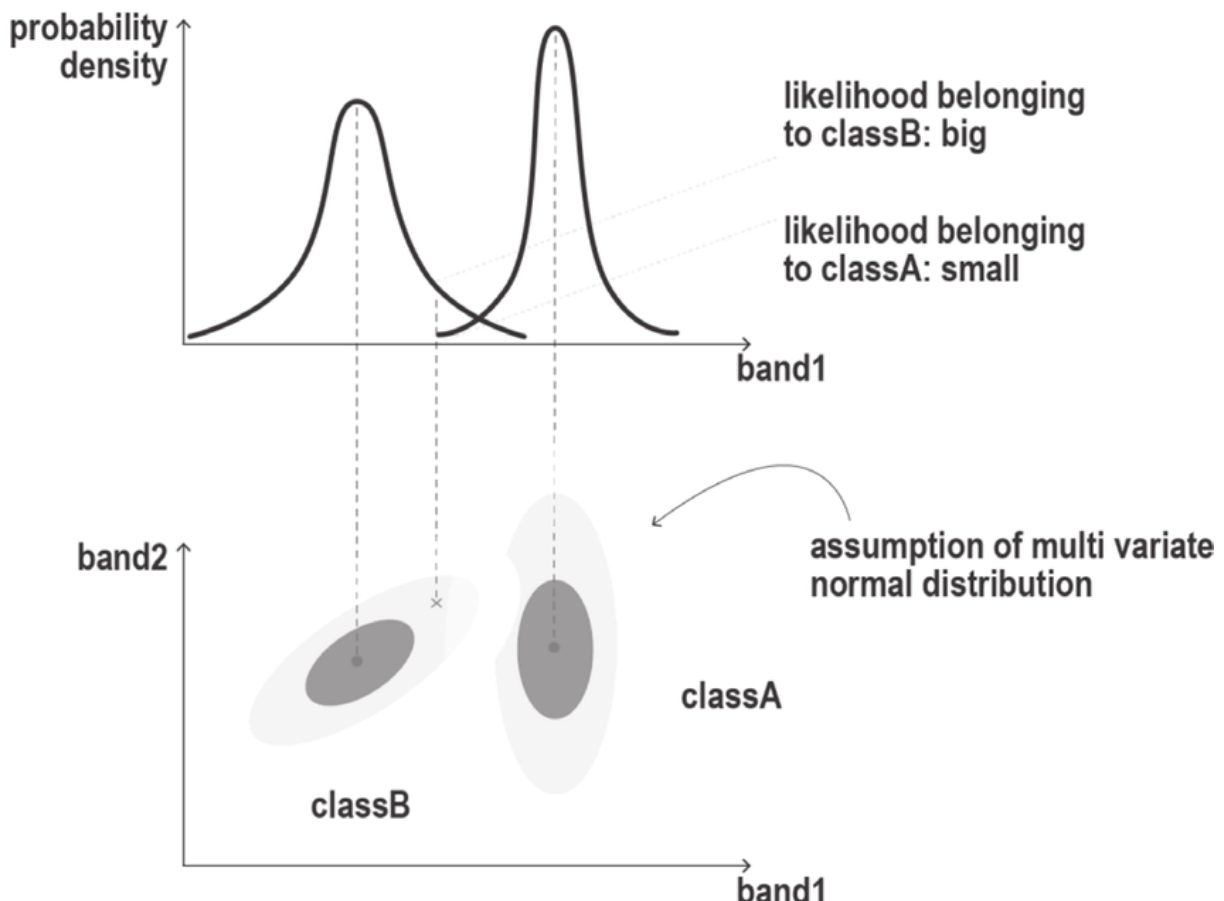


Figure 2.3: The Maximum Likelihood algorithm (Source: Nunez et al., 2019)

The use of prior probabilities, when available, into the Maximum Likelihood algorithm may enhance the accuracy of classification. The algorithm works at a granular level, analyzing each individual pixel, so rendering it well-suited for the categorization of remote sensing images (Nunez et al., 2019). The strengths of the algorithms are as follows; First, the system generates probabilistic predictions for each class. Secondly, this algorithm is appropriate for doing pixel-based picture categorization in the field of remote sensing (Nunez et al., 2019). The limitations of the algorithm are as follows; Firstly, the assumption of data conforming to certain probability distributions, such as the Gaussian distribution, may not always be valid (Nunez et al., 2019). Secondly, the selection of a statistical model and its associated parameters is critical due to its potential impacts on the results and conclusions of a study. Lastly, this method is not appropriate for capturing intricate non-linear connections within the dataset (Nooni et al., 2014).

2.3 Thematic Accuracy Assessment

Maps play a crucial role in quantifying the scope and dispersion of resources, examining the interplay between resources, and determining appropriate sites for certain endeavours, such as development or conservation. Additionally, maps serve as a valuable tool for monitoring changes through time (Congalton and Green, 2019). The evaluation of accuracy plays a crucial role in assessing the quality of a map derived from remotely sensed data. The primary objective of quantitative accuracy evaluation is to identify and quantify map inaccuracies, hence enhancing the use of the map for decision-making purposes (Congalton and Green, 2019). Accuracy assessment is also used to evaluate the effectiveness of classifiers utilised in the process of mapping, in order to choose the most effective method. The level of accuracy shown by a map is determined by two key factors: positional accuracy and thematic accuracy. Positional accuracy pertains to the precision of the spatial placement of features on a map, quantifying the extent to which a given spatial feature deviates from its actual or designated position on the Earth's surface (Congalton and Green, 2019). Thematic accuracy pertains to the categorizations or characteristics assigned to the elements shown on a map and evaluates whether the assigned labels for these elements deviate from the accurate or reference labels (Congalton and Green, 2019).

2.3.1 The Error matrix

The error matrix or confusion matrix is a fundamental tool in accuracy assessment for maps and classification tasks. It helps in quantifying the performance of a classification or prediction model by comparing the predicted class (classified data) labels to the actual class(reference data) labels (Congalton and Green, 2019). It is used to compute overall, producer's and user's accuracies. The overall accuracy is computed by adding up the correctly classified units found on the major diagonal and dividing their sum by the sum of all units(reference points) in the error matrix (Congalton and Green, 2019). It is recorded as a percent. Overall accuracy tells us what percentage of our reference data was indeed correctly mapped. The overall error is the compliment of the overall accuracy i.e overall error = 100% - overall accuracy. To determine the accuracy of specific classes, producer's and user's accuracies are calculated.

Figure 2.4 illustrates an example of calculating these metrics for four land cover class categories of deciduous, conifer, agriculture and shrub.

		Reference Data				row total
		D	C	AG	SB	
Classified Data	D	65	4	22	24	115
	C	6	81	5	8	100
	AG	0	11	85	19	115
	SB	4	7	3	90	104
column total		75	103	115	141	434

Land Cover Categories

D = deciduous

C = conifer

AG = agriculture

SB = shrub

OVERALL ACCURACY = $(65+81+85+90)/434 = 321/434 = 74\%$

PRODUCER'S ACCURACY

D = 65/75 = 87%
C = 81/103 = 79%
AG = 85/115 = 74%
SB = 90/141 = 64%

USER'S ACCURACY

D = 65/115 = 57%
C = 81/100 = 81%
AG = 85/115 = 74%
SB = 90/104 = 87%

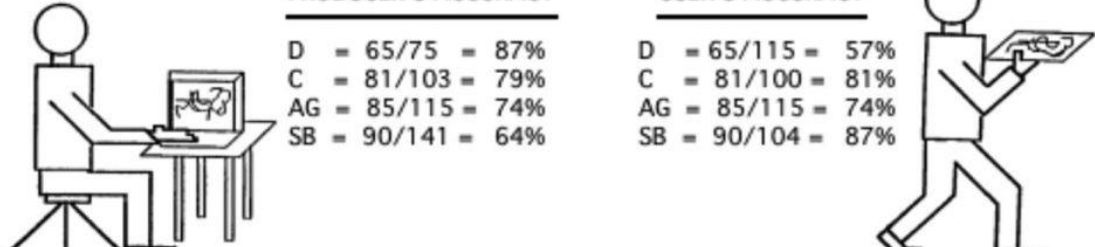


Figure 2.4: Calculation of producer, user and overall accuracies from the error matrix (Source: Congalton and Green ,2019)

Producer accuracy for a particular class tells the map maker the proportion of reference sites that are classified correctly for that class. It's calculated by division of the correctly classified

value from the major diagonal for that class by the column total of reference data for that class. Its recorded as a percent. The omission error is the compliment of the producer accuracy i.e omission error = 100% - producer accuracy (Congalton and Green, 2019).

The user accuracy tells the map user the probability that a particular class shown on a map will actually be found on the ground. Its calculated by division of the correctly classified value from the major diagonal for that class by the row total of classified data for that class. Its recorded as a percent. The commission error is the compliment of the user accuracy i.e commission error = 100% - user accuracy (Congalton and Green, 2019).

2.3.2 The Kappa Coefficient

The Kappa coefficient is obtained from the error matrix and calculated from

$$K = \frac{P_0 - P_e}{1 - P_e}$$

where P_0 is the ratio of units that were classified correctly (overall accuracy) and P_e is the expected ratio of units that were classified correctly by chance (Foody, 2020). Alternatively, according to Cohen (1968), a weighted kappa statistic below can be used

$$\kappa = 1 - \frac{\sum_{i=1}^k \sum_{j=1}^k w_{ij} x_{ij}}{\sum_{i=1}^k \sum_{j=1}^k w_{ij} m_{ij}}$$

where k are the number of codes, w_{ij} are weight factors, x_{ij} are observed frequencies and m_{ij} are expected frequencies. (Cohen, 1968)

According to Foody (2020), Its value lies from -1 to 1 with positive values used for practical applications since negativity implies an agreement level below that due to chance which is hard to interpret. Zero value implies observed agreement is due to chance while positive one value implies perfect agreement (Foody, 2020). **Figure 2.5** shows scales for its interpretation.

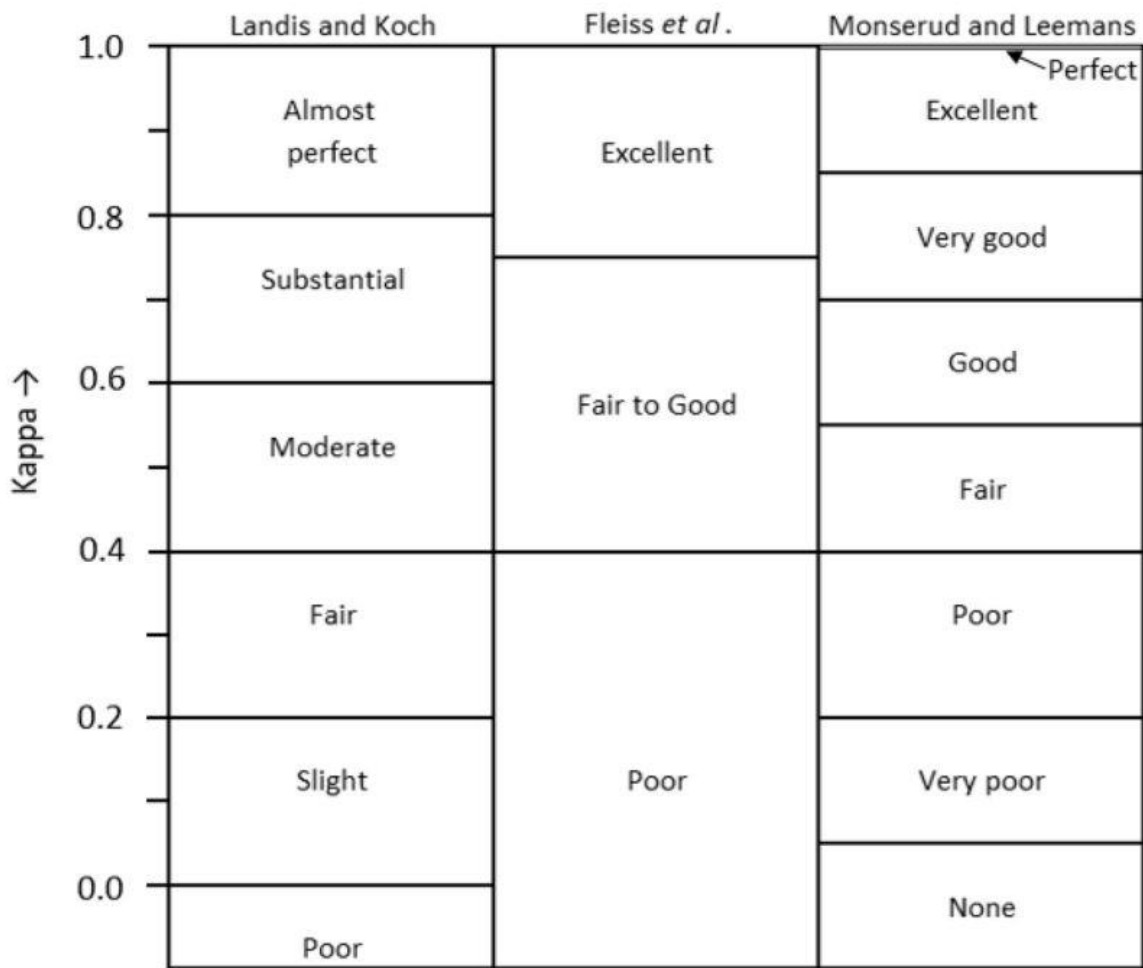


Figure 2.5: Scales used for the interpretation of Kappa coefficient (Source: Foody, 2020)

Congalton and Green (2019) promote the kappa coefficient as an advancement and improvement to overall accuracy by summarizing accuracy over all classes but according to Foody (2020), it is not an index of overall agreement or accuracy as stated by Congalton and Green (2019) but is one of chance agreement or agreement beyond chance. Foody (2020) advocates for the abandonment of the use of kappa for accuracy assessment and proposes use of overall, user and producer accuracy plus the confusion matrix as sufficient.

2.4 Comparison of accuracy of Machine Learning algorithms in oil palm mapping

Nooni et al. (2014) compared Support Vector Machine (SVM) and Maximum Likelihood (ML) classifiers for mapping oil palm in Ghana's Ashanti region. SVM showed superior performance, with overall accuracy of 78.3% and kappa score of 0.73. It attained the highest producer accuracy (100%) and user accuracy (85%) for oil palm. The ML classifier achieved an overall accuracy of 71.7% and a kappa value of 0.65 but had lower accuracies for producers (93.75%)

and users (84.21%). Both classifiers demonstrated a primary constraint in that they fail to reach the frequently accepted standard of overall accuracy evaluation, as outlined in the existing literature (Foody, 2020), which requires a minimum threshold of 80%. The study demonstrated that the spectral characteristics of red, near infrared, and mid-infrared frequency ranges of Landsat 7 ETM + exhibit the highest level of distinguishability for oil palm trees (Chong et al., 2017; Nooni et al., 2014). The observed phenomenon may be attributed to the significant absorption of chlorophyll in the red band area and the pronounced absorption of water in the infrared wavelength region.

Lee et al. (2016) used Landsat 8's 30m resolution satellite image to classify oil palm plantations in Tripa, Aceh, Indonesia. They used supervised machine learning classifiers including Classification and Regression Trees (CART), the Random Forest (RF), and Minimum Distance (MD) to create pixel-based classification maps. The classification classes included forest, immature oil palm, water, mature oil palm, non-oil palm, cloud and non-forest. The CART algorithm had the highest overall accuracy and Kappa coefficients, with an overall accuracy of 93.6% and a kappa coefficient of 0.92. The Minimum Distance classifier was effective in situations where the difference between means was greater than the variability within each class relative to its mean.

Shaharun et al. (2020) mapped oil palm growing in Malaysia utilising Google Earth Engine (GEE) and machine learning classifiers. Landsat 8 images of 30m spatial resolution were processed using the cloud-based Google Earth Engine to obtain oil palm cover classifications using machine learning approaches namely: Support Vector Machines (SVM), Random Forest (RF), and Classification and Regression Tree (CART). Seven classes were used namely; built-up, base soil, other vegetation, oil palm, water, paddy and forest. Random Forest (RF) had the best accuracy for classifying oil palm for the whole peninsula although SVM classified all the seven classes best. Overall accuracy for SVM was 93.16%, RF was 86.5%, and CART was 80.08%. For the oil palm, SVM gave a producer accuracy of 93.52% and user accuracy of 90.01%. RF gave producer accuracy of 86.92% and user accuracy of 82.75%. CART gave producer accuracy of 82.19% and user accuracy of 71.82%. The authors proposed that future research should utilise higher resolution Sentinel- 2 data of 10m resolution to improve the classification accuracy.

Recently, Jarayee et al. (2022) used Sentinel-2 imagery and machine learning algorithms to map oil palm land cover in Pahang state, Malaysia. They compared classification accuracy of

Support Vector Machines (SVM), the Random Forest (RF), and Deep Neural Network (DNN). The DNN achieved 98.63% overall accuracy, while RF and SVM had 98.51% and 95.7% overall accuracy, respectively. The study found that DNN provided greater classification accuracy than Random Forest and SVM.

In summary, it can be observed that deep learning algorithms exhibit the ability to extract intricate patterns and significant features from satellite data, thereby demonstrating superior performance compared to machine learning algorithms like Random Forest and Support Vector Machines (Jarayee et al., 2022; Sheykhmousa et al., 2020). However, a notable drawback of deep learning algorithms is their inherent complexity, characterised by hidden layers or black boxes, which ultimately compromises their interpretability (Sheykhmousa et al., 2020). Furthermore, the implementation of these methods requires a high level of expertise and incurs significant computational costs (Jarayee et al., 2022). Moreover, specialised hardware is required to effectively handle the processing requirements. Lastly, their reliance is heavily contingent upon the accessibility of copious amounts of high-resolution ground truth data (Sheykhmousa et al., 2020; Jarayee et al. ,2022).

2.5 Change Detection of oil palm induced land cover changes

Within the realm of oil palm monitoring, the primary area of interest in change detection-related studies is on the identification of oil palm expansion and its associated consequences (Afaq and Manocha, 2021; Chong *et al.*, 2017). The implementation process involves conducting an examination of the land cover map over an interval of time to ascertain if any land has undergone conversion into oil palm plantations (Afaq and Manocha, 2021). The alterations are visually represented using maps and charts, enabling the identification of forest loss rates, settlement patterns, and the expanse of oil palm plantations. The precision of change detection is contingent upon how accurate the land cover maps are generated by the classification of multi-temporal satellite images (Chong *et al.*, 2017).

In their study, Glinskis and Gutiérrez-Vélez (2019) employed a comprehensive approach that integrated data from optical and radar satellite sensors, along with training data, field conversations, and examination of public records. This approach was utilised to investigate the policy incentives and spatial patterns linked to the increase of oil palm cultivation by both

small-scale farmers and industrial entities in the Ucayali region of Pucallpa in the Peruvian Amazon, which is characterised by rapid transformation. The process of data fusion included the integration of older 2010 Landsat and ALOS/PALSAR imagery with more recent 2016 Sentinel 1 and Sentinel 2 images. The evaluation of the Maximum Likelihood classifier's performance was conducted by analysing the error matrix. The results indicated an overall accuracy of 92% and a Kappa coefficient of 0.88 for the classification process, which used the 2010 Landsat and ALOS/PALSAR datasets. The classification performed on 2016 Sentinel-2 and Sentinel-1 images yielded an overall accuracy of 88% and a Kappa value of 0.82.

Based on their analysis of land cover change using satellite data, it was observed that during the period from 2010 to 2016, smallholders allocated an additional land area of 21,070 hectares for oil palm cultivation compared to industries. Notably, the oil palm expansion by industrial growers primarily took place in old growth forests, accounting for 70% of the total expansion, while smallholders predominantly utilised degraded lands, which constituted 56% of their expansion (Glinskis and Gutiérrez-Vélez, 2019). The research conducted on national laws pertaining to the spread of oil palm cultivation exposed the presence of policy loopholes within Peru's categorization system for determining optimal land use. These loopholes facilitated the conversion of standing forests into extensive agricultural areas for oil palm production, with no supervision from the government. The authors reached the conclusion that effective monitoring and active involvement from the government are necessary in both sectors in order to minimise the loss of old-growth forests and devise effective measures to address the potential environmental consequences of expanding oil palm cultivation (Glinskis and Gutiérrez-Vélez, 2019).

More recently, Arlete Silva, Vieira, and Ferraz (2020) conducted an analysis to characterise the space-time dynamics of Land Use Land Cover changes within an agricultural context of oil palm farming. The study focused on a multi-temporal analysis spanning the years 1991 to 2013, with the aim of understanding the impacts of these changes on the landscape. The researchers conducted a classification of Landsat imagery and performed an analysis of changes in the landscape within an area of 2588.72 km² in the oil palm development zone situated in the Moju region of Brazil. The study revealed that, throughout the specified timeframe, around 47.7% of the main forest underwent conversion for alternative purposes, while the extent of degraded forest had a notable increase of 17%. Additionally, there was an

observed 11% rise in the area occupied by oil palm plantations. During the 22 years, it was seen that 30% of the primary forest underwent conversion into oil palm cultivation. However, it is noteworthy that the rate of primary forest conversion to oil palm saw a mere two percent growth between the years 2005 and 2013 (Arlete Silva, Vieira, and Ferraz ,2020). The results of their study provide evidence in favour of the concept that the continuous deterioration of the environment linked to the production of oil palm contributes to the progressive fragmentation, isolation, and decrease in size of remaining forest patches. The significant reduction of around 50% of the primary forests in the area over a span of just twenty years highlights the pressing need for implementing measures aimed at safeguarding the remaining forests and rehabilitating damaged and secondary forests. These efforts are crucial in order to enhance the total percentage of forests within the landscapes dominated by oil palm plantations.

From the literature above, many studies have been undertaken and documented in Ghana, Indonesia, Malaysia, Peru, Brazil and in other countries on oil palm induced land cover and land use change. However, to the best knowledge of the author, there are no documented studies that have been carried out in Bugala island or Uganda as a country to investigate oil palm induced deforestation, land cover and land use changes utilizing satellite remote sensing. From **Figure 1.3** which is showing oil palm production data in the tropics for 2020 as reported by the United Nations (UN), there is no available data for Uganda even though it has been growing oil palm since 2003. This maiden study is much needed to fill that knowledge and research gap by not only providing data on the status of oil palm development and production on Bugala island in Uganda but by also exploring its impact on forests and other land cover and land use.

3. Methodology

This chapter introduces the study area and the design of the study highlighting the procedure followed for downloading the satellite data, preprocessing, image classification, accuracy assessment and categorical land cover change detection.

3.1 Study Area

Bugala Island is situated between the geographical coordinates of Latitude $0^{\circ}13'$ South Longitude $32^{\circ}3'$ East and Latitude $0^{\circ}33'$ South Longitude $32^{\circ}21'$ East, specifically located in the Kalangala district of Uganda (**Figure 3.1**). With a land area of 275 square kilometers, it is the biggest among the 84 islands of the Ssese Islands archipelago. Bugala Island, located in Lake Victoria, Uganda, has a tropical climate characterised by average temperatures that fluctuate between 22°C and 28°C .

The island has two distinct periods of precipitation, from March to May and September to November, characterised by heavy rainfall that contributes to the development of lush green landscapes. In contrast, the dry seasons, occurring from December to February and June to August, are distinguished by reduced levels of precipitation. Bugala Island is characterised by a mostly tropical rainforest land cover, which includes palm trees and indigenous vegetation. The island exhibits agricultural pursuits, including the production of oil palm, bananas, maize, and cassava, as well as a flourishing fishing sector, which may be attributed to its advantageous location inside Lake Victoria.

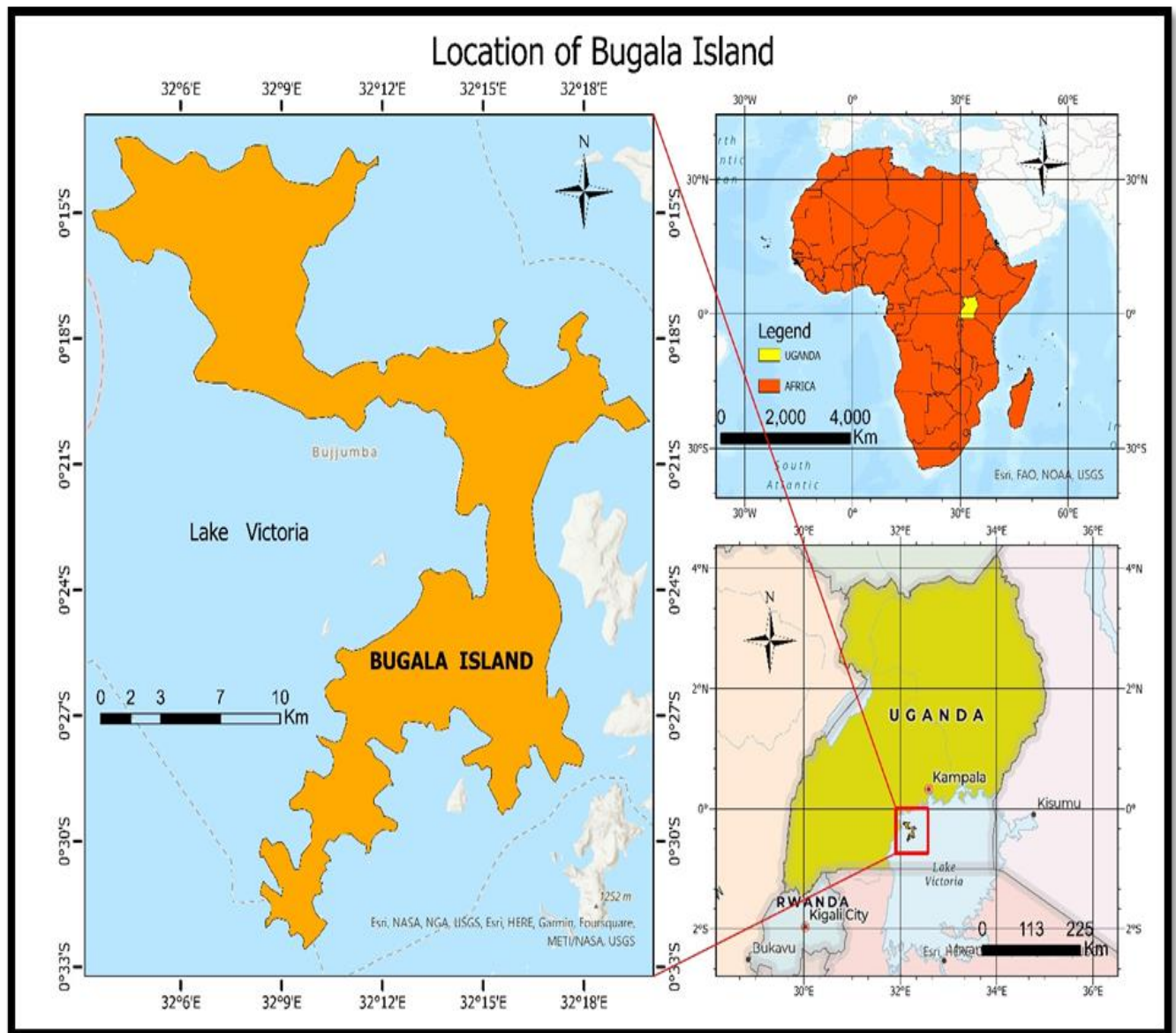


Figure 3.1: Location of Bugala island on Lake Victoria inside Uganda which is in Africa.

3.2 Study Design

The design of the study is shown in **Figure 3.2** and consists of four steps including image pre-processing, image classification, accuracy assessment and change detection.

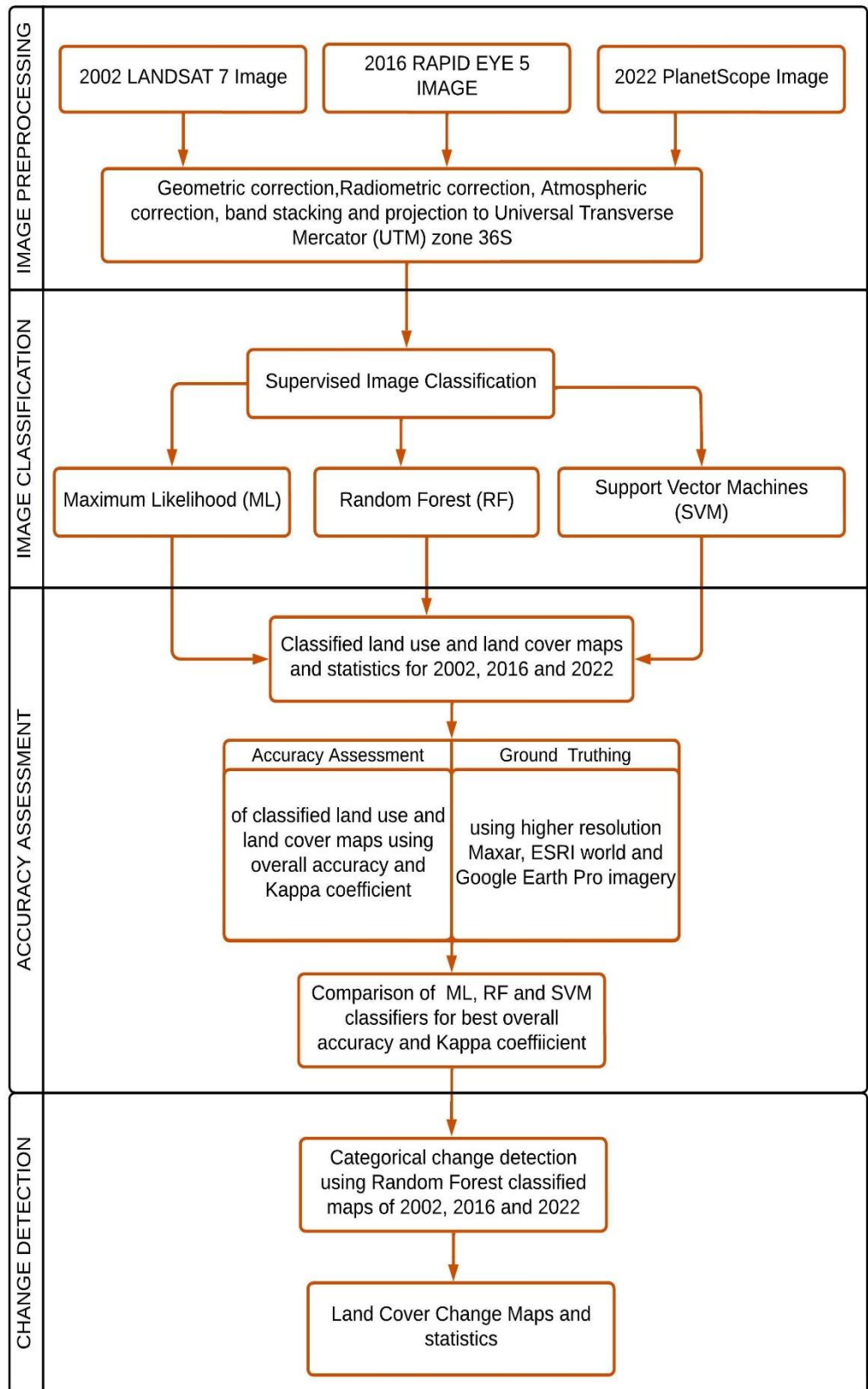


Figure 3.2: Methodology flow chart for the study design

3.3 Data Acquisition and Pre-processing

A shape file of the study area was first downloaded from <https://geojson.io/>. A cloud free 2002 Landsat 7 image (**Figure 4.1**) was downloaded as a TIFF file from the United States Geological Survey's earth explorer at <https://earthexplorer.usgs.gov/> using the shape file of the study area. The image was clipped, and band stacked or composited using Quantum Geographical Information System (QGIS) software. The shapefile was then uploaded to Planet Labs' explorer at <https://www.planet.com/explorer/> and used to search and download cloud free GeoTIFF files of the 2016 Rapid Eye 5 image (**Figure 4.2**) and the 2022 PlanetScope image (**Figure 4.3**). Before downloading, the files were clipped to the area extent of the shape file, composited(stacked) and downloaded as surface reflectance ortho tile Geo TIFF files. Ortho tile products from Planet Labs are images that have undergone geometric, radiometric, and atmospheric corrections using Planet's internal algorithms. **Table 3.1** shows the characteristics of the satellites and imagery used.

Table 3.1: Characteristics of Landsat 7, Rapid Eye 5 and PlanetScope imagery (Source: Planet Labs, 2022; USGS, 2023)

IMAGE DATE	SATELLITE	SPATIAL RESOLUTION	TEMPORAL RESOLUTION	SPECTRAL RESOLUTION	IMAGE CHARACTERISTICS
1 January 2002	Landsat 7	30m	16 days	-Blue (0.45-0.52) μ m -Green (0.52-0.60) μ m -Red (0.63-0.69) μ m -Near Infra-Red (0.77-0.90) μ m -Shortwave Infrared 1(1.55-1.75) μ m -Thermal (10.40-12.50) μ m -Shortwave Infrared 2(2.09-2.35) μ m -Panchromatic (0.52-0.90) μ m	-Level 2 Tier 1 -Meets geometric and radiometric quality -Atmospherically corrected -Surface reflectance
25 December 2016	Rapid Eye 5	5m	5.5 days	-Blue (0.44-0.51) μ m -Green (0.52-0.59) μ m -Red (0.63-0.68) μ m -Red Edge (0.69-0.73) μ m -Near Infra-Red (0.76-0.85) μ m	-Ortho tile analytic -surface reflectance -geometrically, radiometrically, and atmospherically corrected
4 October 2022	PlanetScope	3m	1 day	-Blue (455-515) nm -Green (500-590) nm -Red (590-670) nm -Near Infra-Red (780-860) nm	-Ortho tile analytic -surface reflectance -geometrically, radiometrically, and atmospherically corrected

All three images were projected to Universal Transverse Mercator (UTM) zone 36S projected coordinate system with World Geodetic System (WGS) 1984 datum. Planet Labs' Geometric correction algorithm catered for correction of effects due to sensor by using sensor model and sensor telemetry. Co-registration of bands was conducted, and attitude telemetry and ephemeris data used to rectify effects due to space craft (Planet Labs,2022). Further ortho rectification was done using ground control points and fine Digital Elevation Models at a posting of 30m to 90m.

Radiometric correction involved using calibration coefficients to convert to radiometric values which were then scaled by a factor of 100 so that the error due to quantization is minimized. Atmospheric correction involved using the Moderate Resolution Imaging Spectroradiometer (MODIS) near real time data and the 6SV2.1 code for radiative transfer to convert to values of surface reflectance. A factor of 10,000 was used to scale the values of reflectance to minimize the quantization error (Planet Labs,2022).

3.4 Image Classification

Considering the aforementioned difficulties associated with deep learning algorithms (Sheykhmousa et al., 2020; Jarayee et al. ,2022), this study will use machine learning techniques, including Support Vector Machines, Random Forest, and Maximum Likelihood. The conclusion is based on the observation that these algorithms possess a reasonably straightforward implementation process and are capable of effectively addressing learning problems even when provided with a limited training dataset. Furthermore, they can provide outcomes that are comparable in quality and accuracy to those achieved by deep learning algorithms (Sheykhmousa et al., 2020). In addition, deep learning approaches exhibit increased computational complexity and lesser interpretability in comparison to the aforementioned methods. Specifically, Random Forest has superior average accuracy and less volatility in the context of land cover and land use applications, as compared to Support Vector Machines. When dealing with low spatial resolution imagery, the Random Forest approach routinely outperforms Support Vector Machines in terms of achieving superior accuracy (Sheykhmousa et al., 2020). However, it was shown that support vector machines exhibited higher average accuracy compared to Random Forest when classifying datasets with a larger number of characteristics (Sheykhmousa et al., 2020). The efficacy of the Support Vector Machine classifier lies on its ability to effectively address the challenges posed by high

dimensionality and a scarcity of training samples. This study aims to compare several classifiers discussed in the literature to choose the most appropriate one for addressing the research topic under investigation. Hence, Image classification using machine learning classifiers namely; random forest, maximum likelihood and support vector machines was carried out using the classification tools found in ArcMap 10.8.2. Six land cover classes were used namely; water, forest, oil palm, settlement, wetland and arable land.

3.4.1 Collection of Training samples

The raster or TIFF file of the image to be classified was loaded into ArcMap 10.8.2 and using the “training sample manager” tool, training samples in the form of polygons were created for each class using random sampling. The number of polygons for water were 33, 138 for forest, 411 for oil palm, 56 for settlement, 21 for wetland and 105 for Arable land. Ground truthing using ESRI world imagery and Google Earth imagery was also used to ascertain the land cover classes. The training samples were then saved as a shape file.

3.4.2 Training of machine learning classifiers

Using the “Train classifier” tool in ArcMap 10.8.2, the machine learning classifier was then trained by loading the saved shape file that contains the training samples and setting the parameters of the classifier. For the random forest classifier, default settings were used namely; maximum tree depth as 30, the maximum number of trees as 50 with maximum number of samples per class as 1000. Segment attributes used were color and mean. For the support vector machine classifier, maximum number of samples per class was 500 with segment attributes as color and mean. A classifier definition file was created for each machine learning classifier and saved.

3.4.3 Classifying of Raster

Using the classifier definition file that was saved together with the image file or raster, the “classify raster” tool in ArcMap was used to classify the raster into the 6 land cover classes and the classified raster saved as a TIFF file. Each of the 3 images was classified by all three machine learning algorithms generating 3 classified TIFFs for Random Forest, Support vector machine and maximum likelihood. This led to a final total of 9 classified TIFF files. From these TIFF files, classification maps were made and statistics of the areas of each class were extracted for 2002, 2016 and 2022.

3.5 Accuracy Assessment

The classified image or raster was loaded into ArcGIS PRO 3.1. Using higher resolution Maxar, Google Earth and ESRI world imagery as ground truth or reference data, the “create accuracy assessment points” tool was engaged to select 300 reference points using equalized stratified random sampling. This meant that 50 reference points were picked from each of the 6 land cover classes making the approach unbiased and representative of each class (Congalton and Green, 2019). By referencing and comparing with the higher resolution imagery, each reference point was labelled with its true land cover class. Subsequently, the aforementioned reference points were juxtaposed with the classified data at the same location using the “compute confusion matrix” tool to produce a confusion or error matrix. Confusion matrices were created for each of the 9 classified TIFF rasters resulting into a total of 9 confusion matrices. These matrices provided statistics such as user accuracies, producer accuracies, overall accuracies, and kappa coefficients. By comparing the values of overall accuracy and kappa coefficients for the 2002, 2016 and 2022 classified maps, the machine learning classifier with the highest score was identified to be Random Forest and hence, going forward, all change detection analysis was conducted only on Random Forest classifier generated maps or categorical raster datasets.

3.6 Change detection

Categorical change detection was carried out using the “change detection wizard” in ArcGIS Pro 3.1. By using image differencing, a pair of categorical random forest classified land cover maps namely; 2002 with 2016, 2016 with 2022, and 2002 with 2022 were ‘subtracted’ to highlight areas where the land cover had changed between these years. Filtering methods used included displaying “changed only” areas or both “changed only” and “no change” areas in a single output. To symbolise classes that had changed, the transition class colour method used was “to colour” meaning the colour of the changed pixel became the colour of its terminal class. No smoothing neighbourhood was done. The final output were change maps that showed areas where changes had taken place and the statistics of change areas were reported and visualised via maps, tables, charts, and graphs.

4. Results

This chapter presents the processed satellite imagery and detailed results organised for each of the three objectives set.

4.1 Satellite Imagery

The pre-processed satellite imagery used are shown in **Figure 4.1**, **Figure 4.2** and **Figure 4.3**.

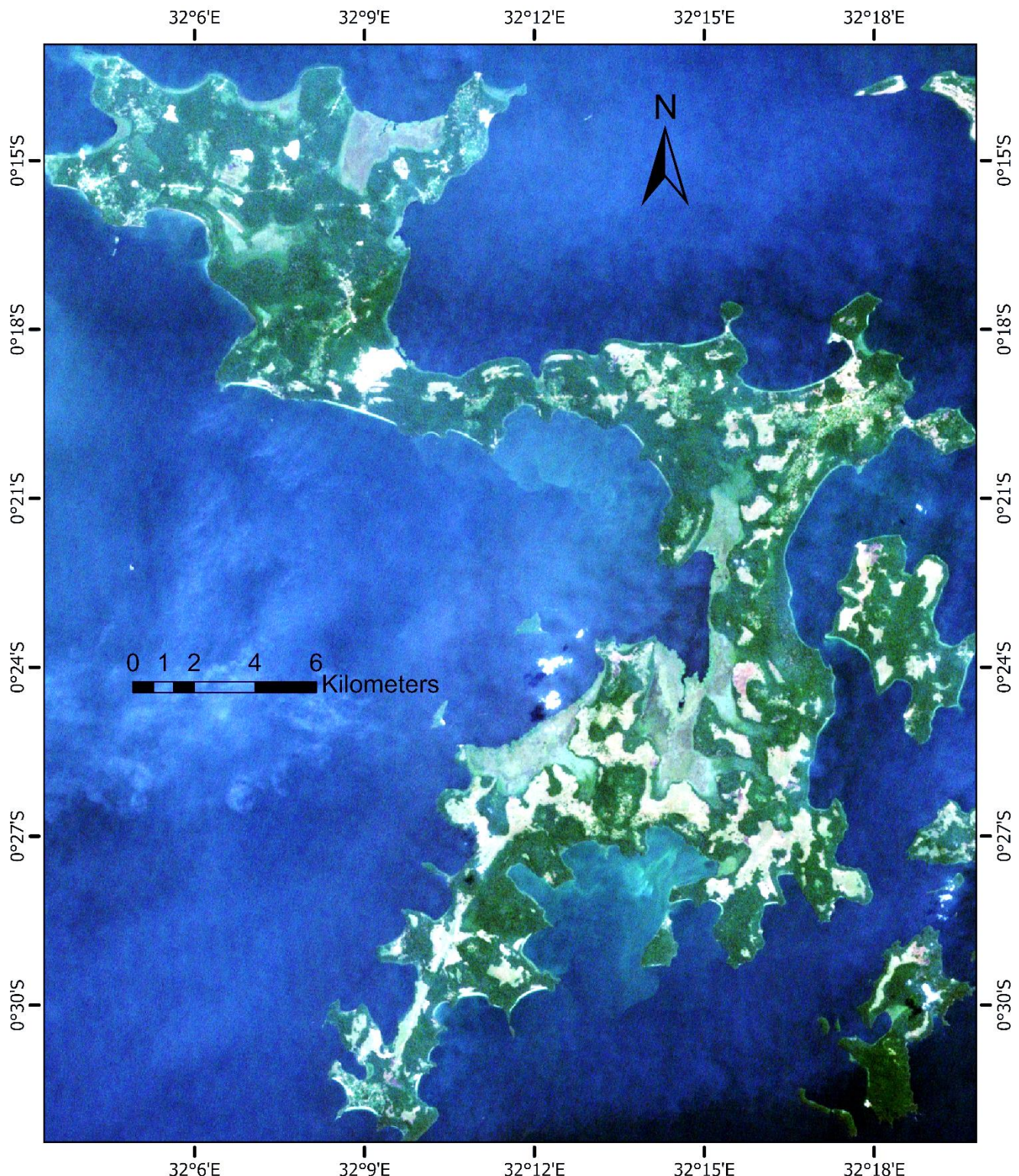


Figure 4.1: 2002 Landsat 7 true colour image of Bugala island. (Source: USGS, 2023)

2016 Rapid Eye 5 image of Bugala island

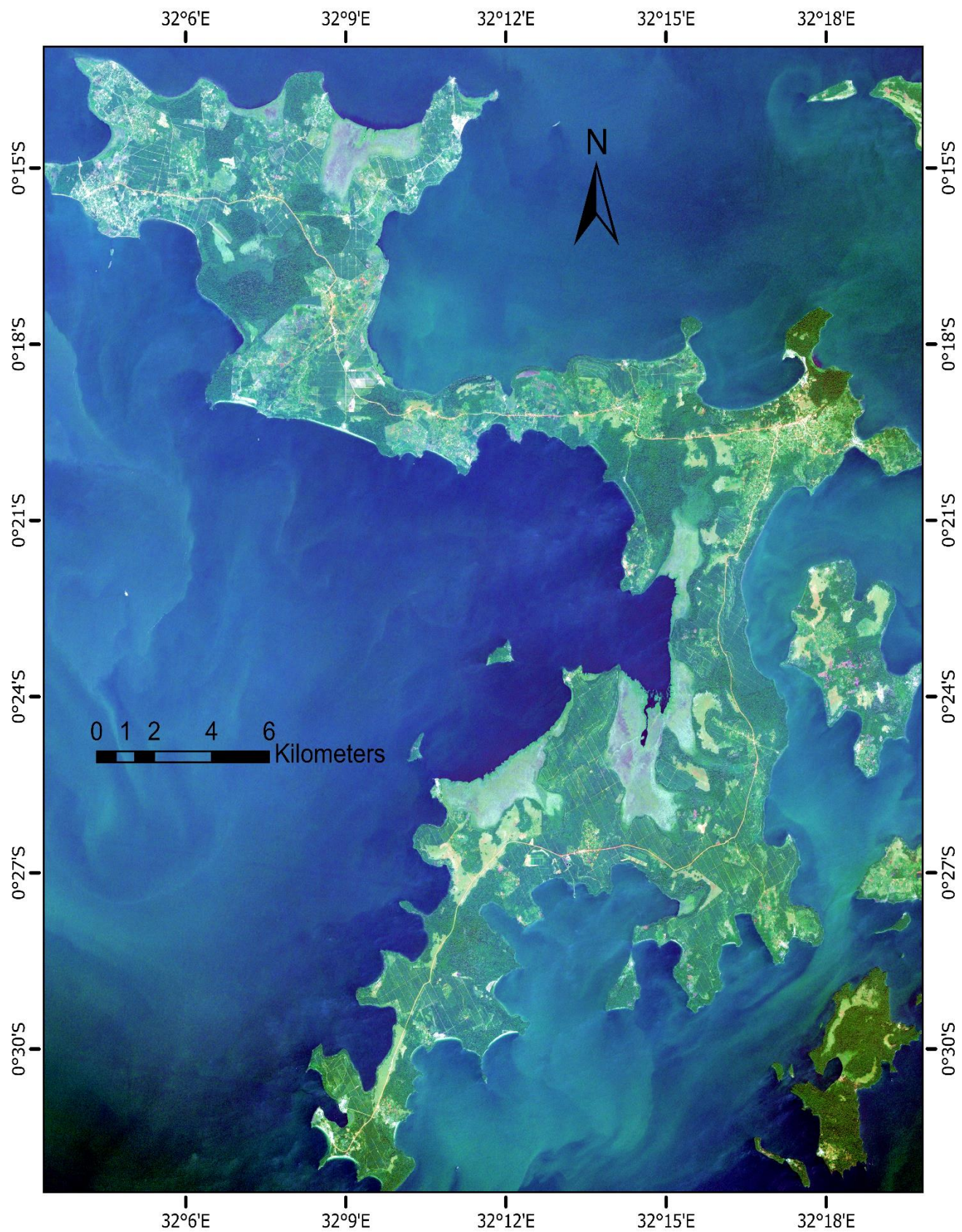


Figure 4.2: 2016 Rapid Eye 5 true colour image of Bugala island. (Source: Planet Labs, 2022)

2022 PlanetScope image of Bugala island

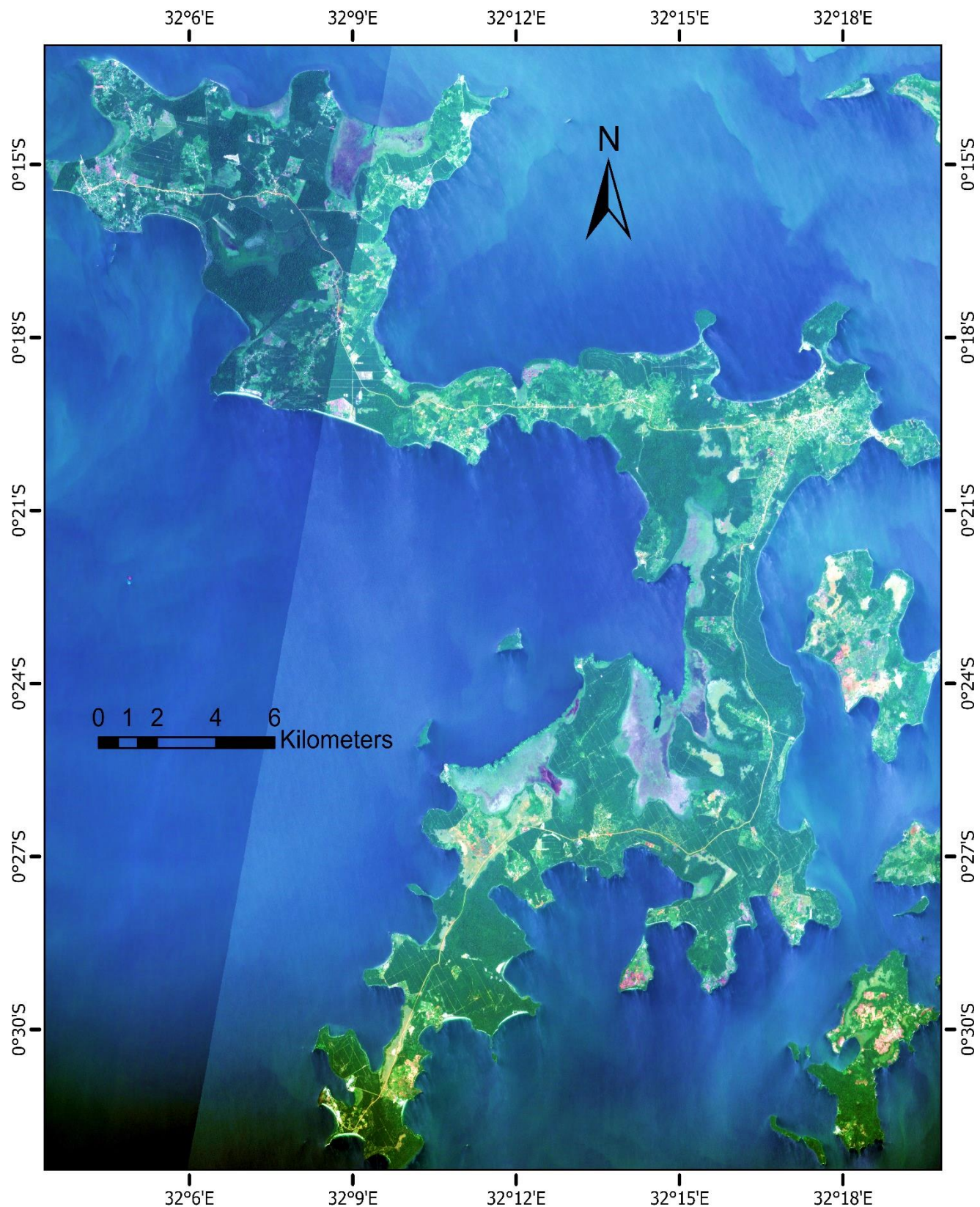


Figure 4.3: 2022 PlanetScope true colour image of Bugala island. (Source: Planet Labs, 2022)

4.2 Objective1: Identification of the most accurate machine learning classifier

4.2.1 Summary of all Accuracy Assessment

The summary results below (**Table 4.1**) of the image classification procedure outlined in **section 3.4** and the accompanying accuracy assessment procedure outlined in **section 3.5** show that the Random Forest classifier was the best classifier with 94%, 86% and 83% overall accuracy for the 2002, 2016 and 2022 image classification. It also recorded the highest kappa coefficients for all classified images namely; 0.92, 0.83 and 0.80 for the 2002, 2016 and 2022 images. Detailed confusion matrices and classified maps generated using the Support Vector Machine and Maximum Likelihood classifiers are in **Appendices A, B, C and D**. Going forward the most accurate results of the Random Forest classifier are interpreted and utilised in the subsequent change detection analysis.

Table 4.1: Summary of Accuracy assessment results for the three classifiers on all the 3 images

MACHINE LEARNING CLASSIFIER	OVERALL ACCURACY OF 2002 MAP	OVERALL ACCURACY OF 2016 MAP	OVERALL ACCURACY OF 2022 MAP	2002 KAPPA	2016 KAPPA	2022 KAPPA
RANDOM FOREST (RF)	0.94	0.86	0.83	0.92	0.83	0.80
SUPPORT VECTOR MACHINE (SVM)	0.85	0.84	0.75	0.81	0.81	0.70
MAXIMUM LIKELIHOOD (ML)	0.76	0.83	0.74	0.70	0.79	0.69

4.2.2 Random Forest Classification and Accuracy Assessment of the 2002 image

From **Table 4.2**, the overall accuracy was 94% resulting in an overall error of 6%. This means that 94% of all the reference data was correctly mapped. The Kappa coefficient of 0.94 was excellent or almost perfect implying that the classification was significantly better than random (Foody,2020). Forest and Water classes had the best user accuracy of 100% and zero commission error implying that the probability of finding these classified map classes on the ground was 1. These were followed by Arable land (92%), Settlement (90%) and wetland (86%) having commission errors as 8%, 10% and 14% respectively.

Settlement class had the highest producer accuracy of 100% with zero omission error meaning all reference sites for the settlement class were classified correctly. This was

followed by wetland (96%), water (94%), arable land (92%) and forest (88%) having omission errors as 4%, 6%, 8% and 12% respectively.

Table 4.2: Random Forest based confusion matrix of classified map from 2002 image.

ID	Class	FOREST	WATER	WETLAND	SETTLEMENT	ARABLE LAND	Total	User Accuracy	Kappa
1	FOREST	50	0	0	0	0	50	1.00	
2	WATER	0	50	0	0	0	50	1.00	
3	WETLAND	3	1	43	0	3	50	0.86	
4	SETTLEMENT	1	2	1	45	1	50	0.90	
5	ARABLE LAND	3	0	1	0	46	50	0.92	
6	Total	57	53	45	45	50	250		
7	Producer Accuracy	0.88	0.94	0.96	1.00	0.92		0.94	
8	Kappa								0.92

Figure 4.4 shows the areas of each land cover class as extracted from the map showing the distribution of the land cover classes in 2002 on Bugala island (Figure 4.5). 55% of Bugala island was covered in tropical forest in 2002 before the introduction of oil palm. Forest covered approximately 173 km². Settlements, Wetlands and Arable land occupied 24.2 km², 61.8 km² and 53.2 km² respectively. This was a time prior to oil palm introduction.

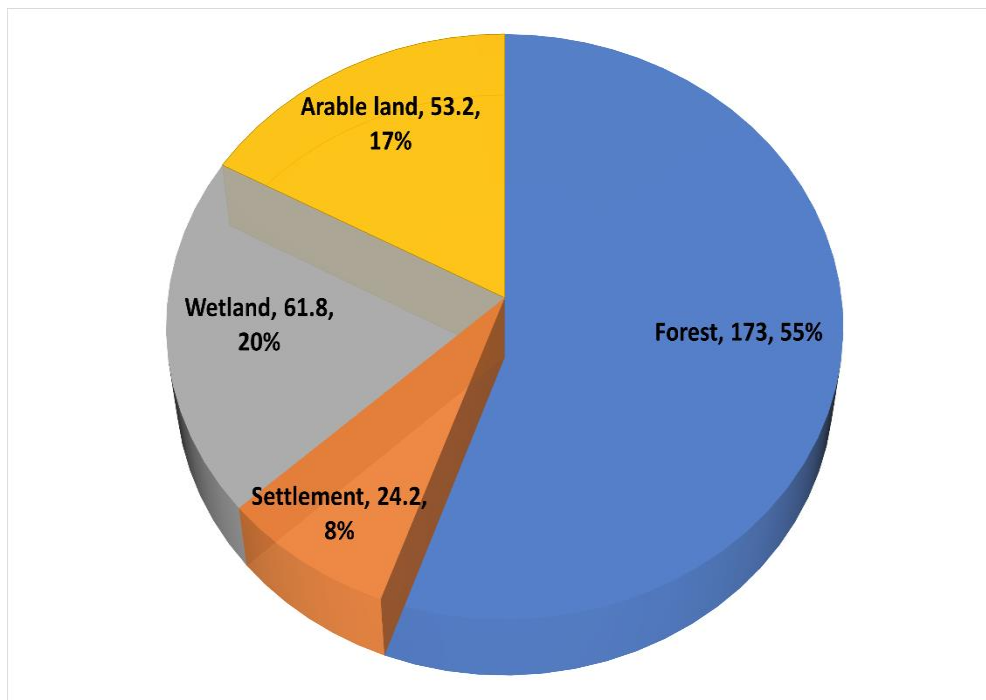


Figure 4.4: Random Forest classifier generated areas of land cover classes for 2002 in km² and percentages

2002 Land Cover by Random Forest Classification

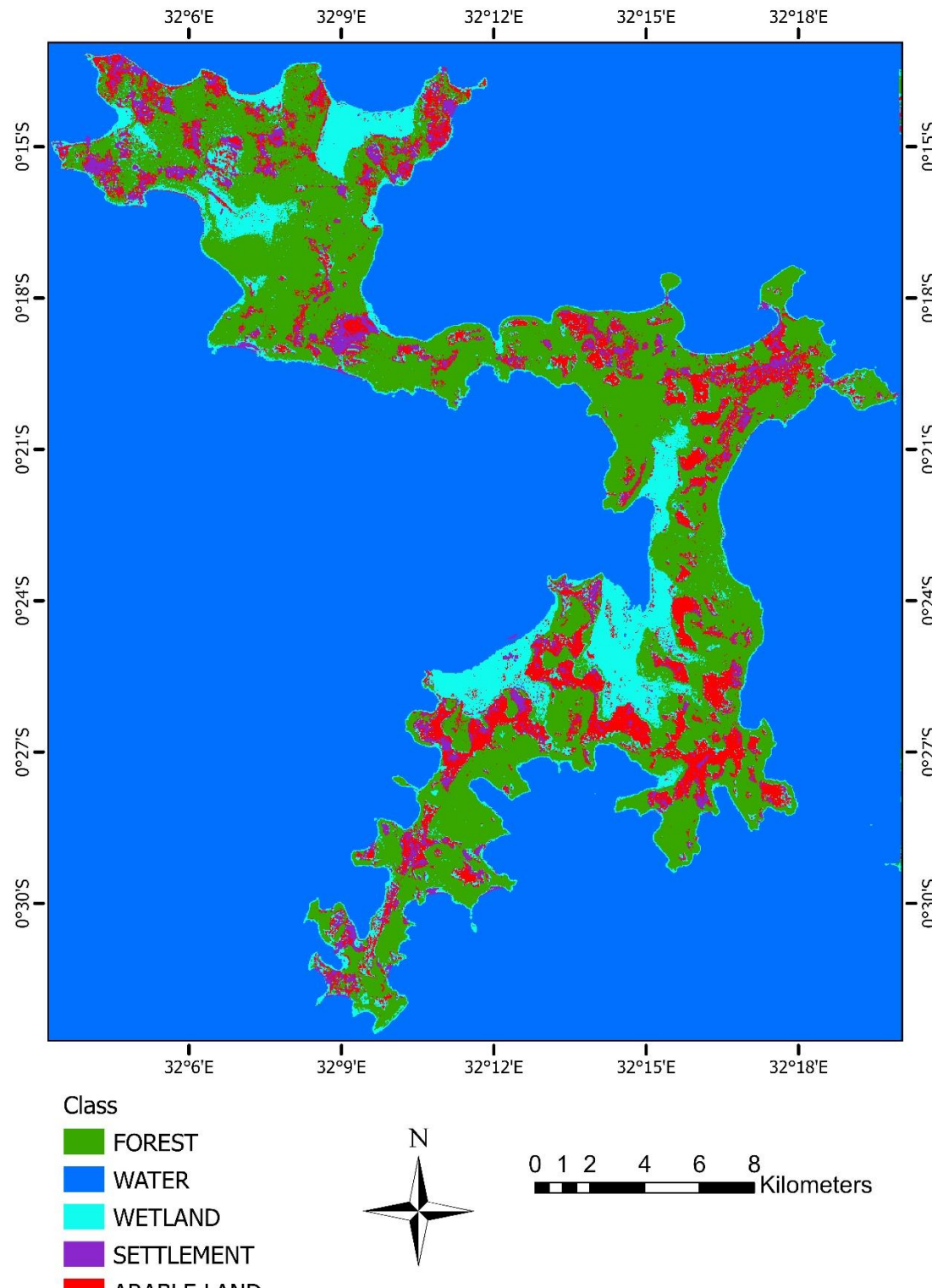


Figure 4.5: Random Forest classified land cover map from the 2002 Landsat 7 image

4.2.3 Random Forest Classification and Accuracy Assessment of the 2016 image

Table 4.3 shows that 86% of the reference data was mapped correctly with an overall accuracy of 86% and an overall error of 14%. The Kappa coefficient of 0.83 was very good or almost perfect. Water class had both the highest user and producer accuracy at 100%. From the producer accuracies, 80% of forest, 83% of Oil palm, 95% of settlement, 90% of wetlands and 72% of arable land reference data was classified correctly. However, the probability that a particular class shown on the map will actually be found on the ground was 0.86 for forest, 1 for water, 0.8 for oil palm, 0.84 for settlement, 0.70 for wetland and 0.94 for arable land.

Table 4.3: Random Forest based confusion matrix of the classified map from 2016 image.

ID	Class	FOREST	WATER	OIL PALM	SETTLEMENT	WETLAND	ARABLE LAND	Total	User Accuracy	Kappa
0	FOREST	43	0	7	0	0	0	50	0.86	
1	WATER	0	50	0	0	0	0	50	1.00	
2	OIL PALM	9	0	40	0	1	0	50	0.80	
3	SETTLEMENT	1	0	0	42	2	5	50	0.84	
4	WETLAND	0	0	0	2	35	13	50	0.70	
5	ARABLE LAND	1	0	1	0	1	47	50	0.94	
6	Total	54	50	48	44	39	65	300		
7	Producer Accuracy	0.80	1.00	0.83	0.95	0.90	0.72		0.86	
8	Kappa									0.83

Figure 4.6 shows the distribution of the land cover classes in 2016 on Bugala island with the extracted area of each land cover class shown in **Figure 4.7**. The forest cover area had reduced from 173 km² (55%) in 2002 to 104.4 km² (34%) in 2016 since part of it had been cleared to introduce oil palm plantations. Oil palm plantations occupied 73.4 km² (24%) of the land cover while arable land, wetlands and settlements occupied 75.7km²(25%), 38.5km²(13%), and 11.9km²(4%) respectively of the land cover.

2016 Land Cover by Random Forest Classification

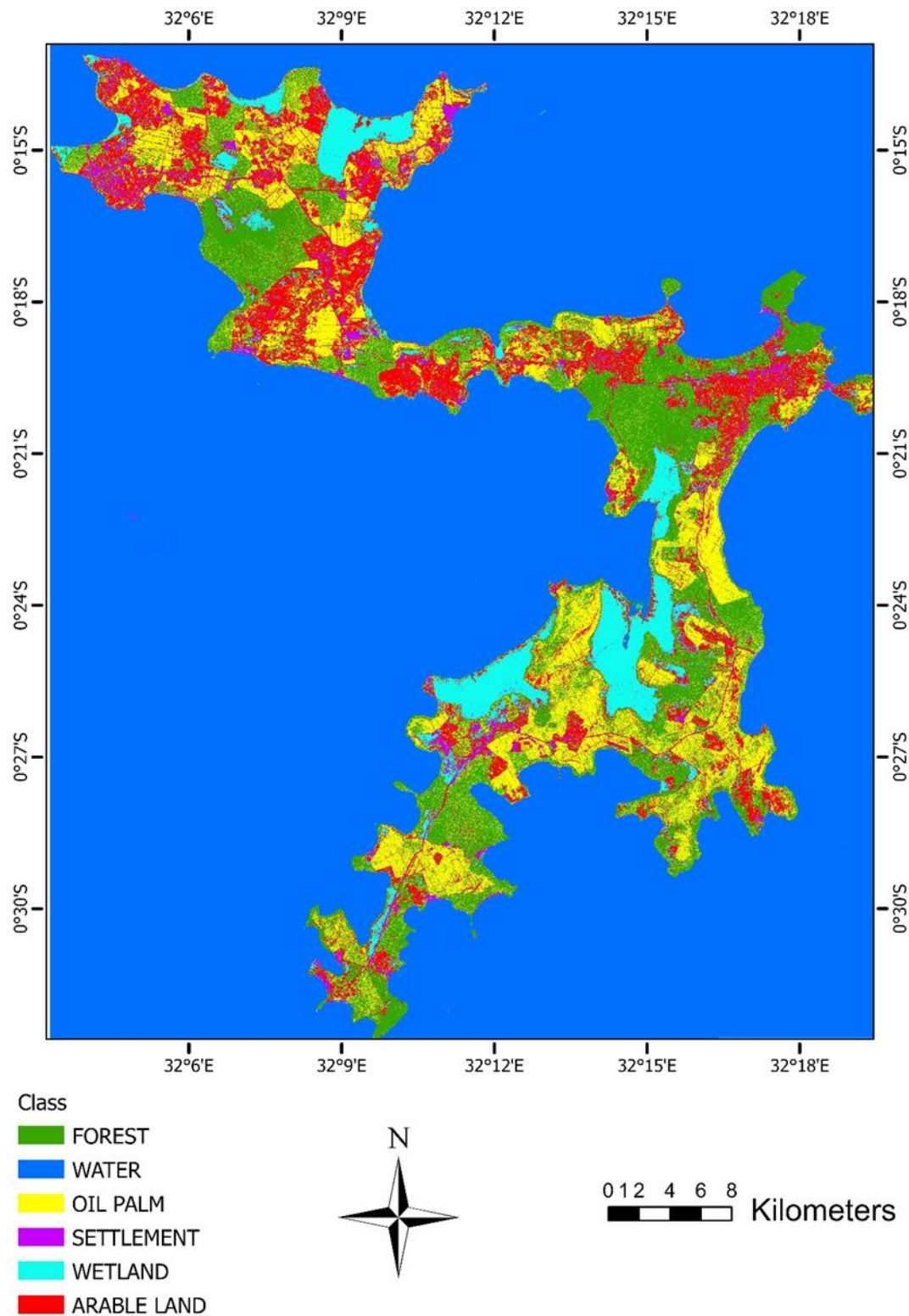


Figure 4.6: Random Forest classified land cover map from the 2016 Rapid Eye 5 image

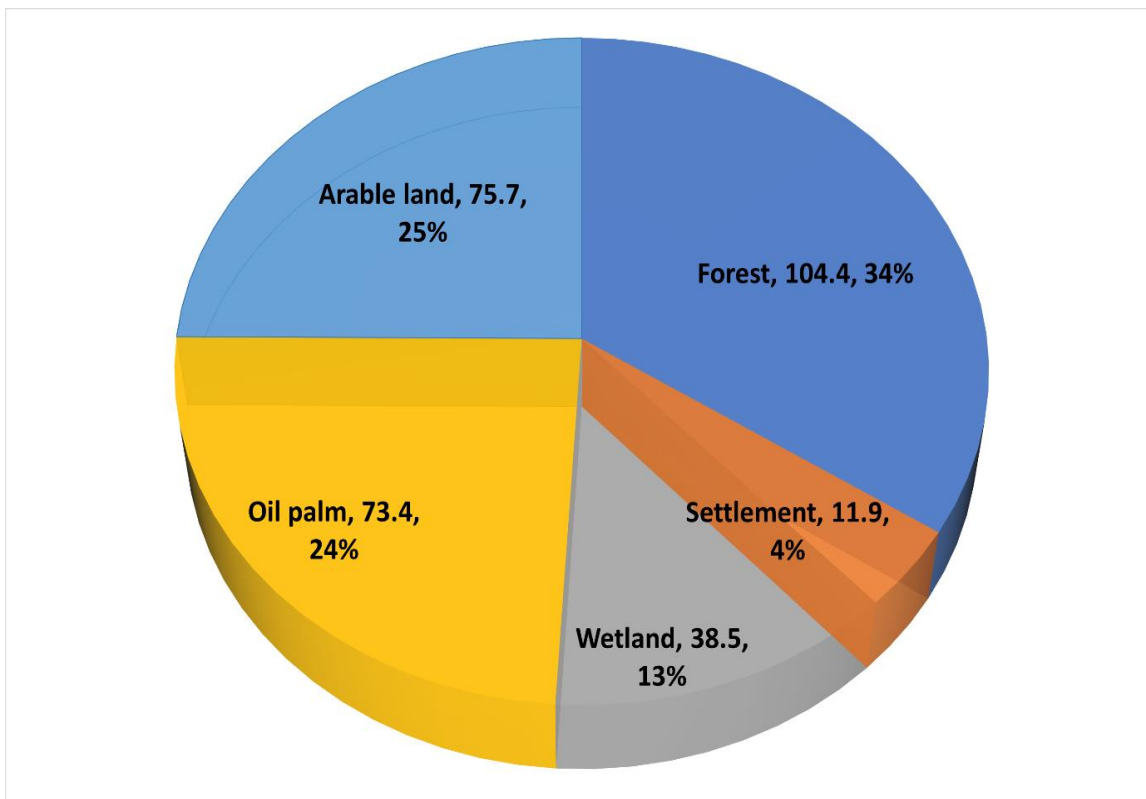


Figure 4.7: Random Forest classifier generated areas of land cover classes for 2016 in km² and percentages

4.2.4 Random Forest Classification and Accuracy Assessment of the 2022 image

Table 4.4 shows that 83% of the reference data was mapped correctly with overall accuracy of 83% and an overall error of 17%. Kappa coefficient of 0.8 was very good or almost perfect. Water class had the highest user accuracy at 100% followed by arable land at 94%. From the producer accuracies, 93% of water, 72% of forest, 76% of Oil palm, 98% of settlement, 95% of wetlands and 71% of arable land reference data was classified correctly. However, the probability that a particular class shown on the map will actually be found on the ground was 0.78 for forest, 1 for water, 0.7 for oil palm, 0.78 for settlement, 0.76 for wetland and 0.94 for arable land.

Table 4.4: Random Forest based confusion matrix of the classified map from 2022 image.

ID	Class	WATER	FOREST	OIL PALM	SETTLEMENT	WETLAND	ARABLE LAND	Total	User Accuracy	Kappa
0	WATER	50	0	0	0	0	0	50	1.00	
1	FOREST	0	39	11	0	0	0	50	0.78	
2	OIL PALM	0	15	35	0	0	0	50	0.70	
3	SETTLEMENT	3	0	0	39	0	8	50	0.78	
4	WETLAND	1	0	0	0	38	11	50	0.76	
5	ARABLE LAND	0	0	0	1	2	47	50	0.94	
6	Total	54	54	46	40	40	66	300		
7	Producer Accuracy	0.93	0.72	0.76	0.98	0.95	0.71		0.83	
8	Kappa									0.80

Figure 4.8 shows the areas of each land cover class as extracted from the map showing the distribution of the land cover classes in 2022 on Bugala island (Figure 4.9). The forest cover area had reduced further from 104.4 km² (34%) in 2016 to 98.8 km² (33%) in 2022. Oil palm plantations occupied 91.2 km² (30%) of the land cover while arable land, wetlands and settlements occupied 66.1km²(22%), 39.9km²(13%), and 7.6km²(2%) respectively of the land cover.

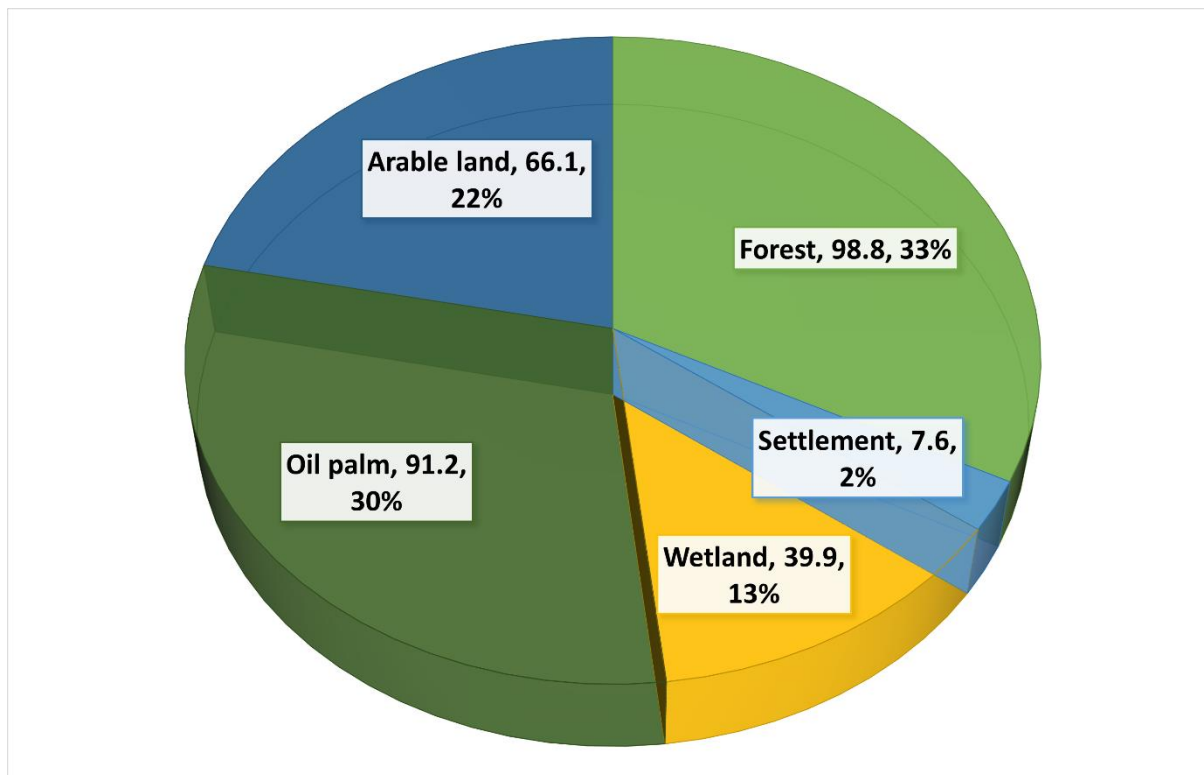


Figure 4.8: Random Forest classifier generated areas of land cover classes for 2022 in km² and percentages

2022 Land Cover by Random Forest Classification

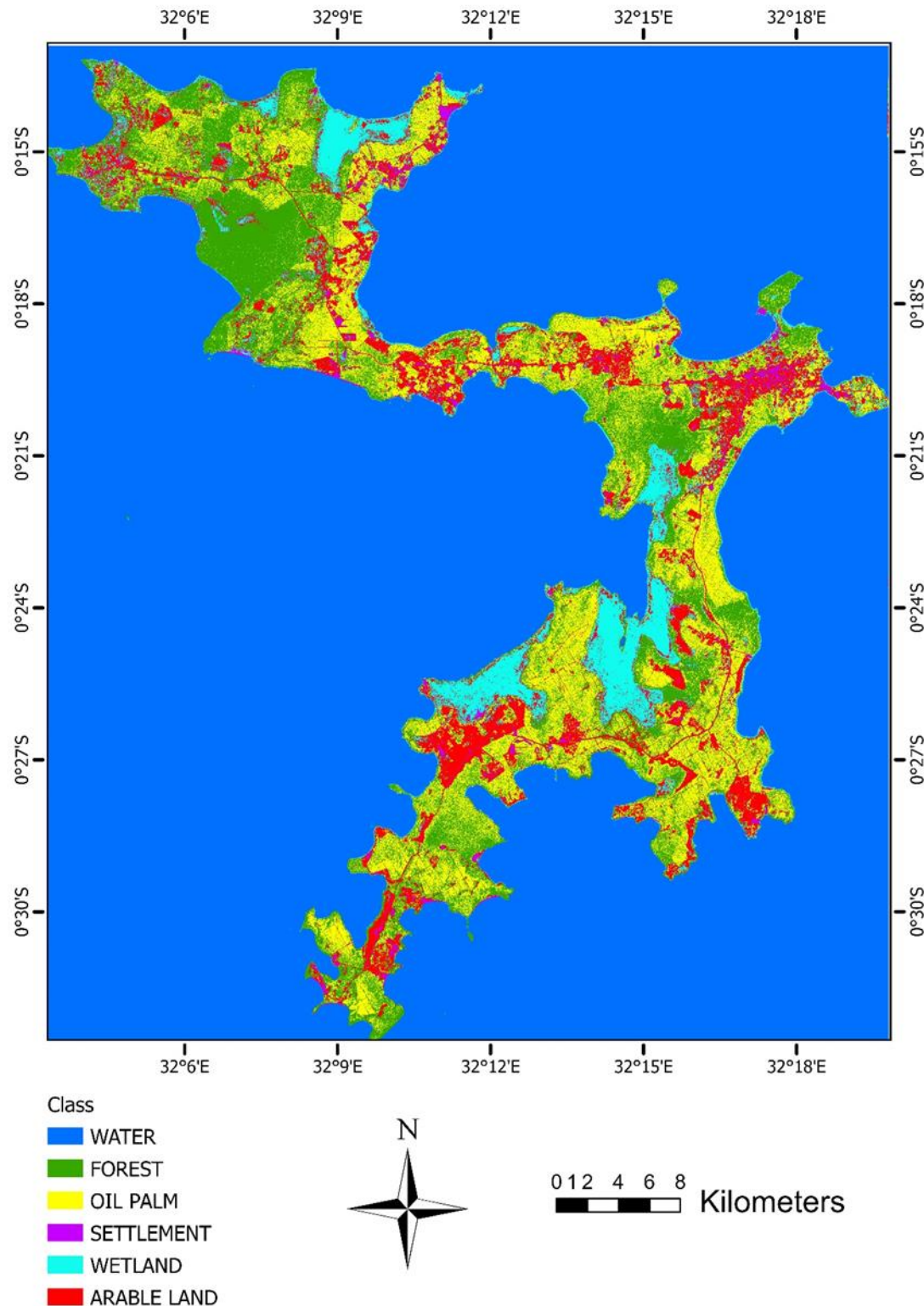


Figure 4.9: Random Forest classified land cover map from the 2022 PlanetScope image

4.3 Objective 2: Land cover areas and changes by class between 2002 and 2022

Table 4.5 shows the Random Forest derived areas of each land cover class and the corresponding changes in area for 2002, 2016 and 2022. The areas of each land cover class are visualized in Figure 4.10 while the analyzed changes in area per class are visualized in Figure 4.11 and Figure 4.12

Table 4.5: Random Forest classifier derived class area changes between 2002 and 2022

no	CLASS	2002 Area/km ²	2016 Area/km ²	2022 Area/km ²	2002-2016 Change/km ²	2016-2022 Change/km ²	2002-2022 Change/km ²
1	FOREST	173.0	104.4	98.8	-68.5	-5.7	-74.2
2	WATER	806.4	806.7	807	0.3	0.3	0.6
3	OIL PALM	0.0	73.4	91.2	73.4	17.7	91.2
4	SETTLEMENT	24.2	11.9	7.6	-12.3	-4.3	-16.6
5	WETLAND	61.8	38.5	39.9	-23.4	1.4	21.9
6	ARABLE LAND	53.2	75.7	66.1	22.4	-9.6	12.9

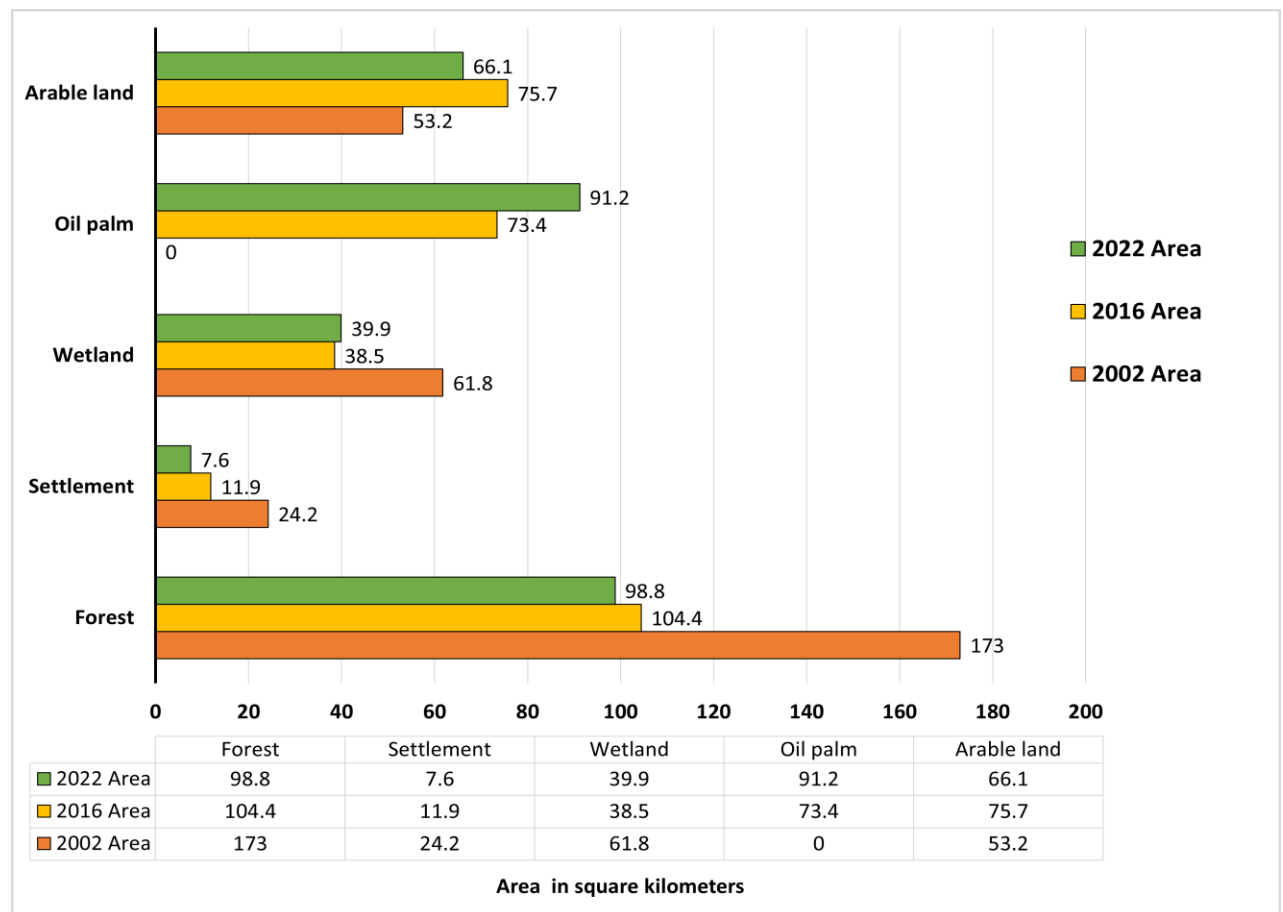


Figure 4.10: Land cover class areas per class on Bugala island for 2002, 2016 and 2022

Results show (**Figure 4.11**) that between 2002 and 2016, the forested area decreased by 68.5 km² while the area under oil palm plantations grew from zero to 73.4 km² as that for arable land grew by 22.4 km². The explanation for this is that forested land was cleared, and oil palm plantations introduced. In addition, arable land increased by 22.4 km² originating from cleared previously forested land. However, the area of settlements reduced by 12.3 km² and this was attributed to forced displacement of illegal tenants whose land was allocated to OPUL for establishment of oil palm plantations. Area of wetland increased by 23.4 km² due to conversion of previously forested wetlands into oil palm plantations but also due to low user accuracy of 0.7 for wetland class in 2016 map (**Table 4.3**)

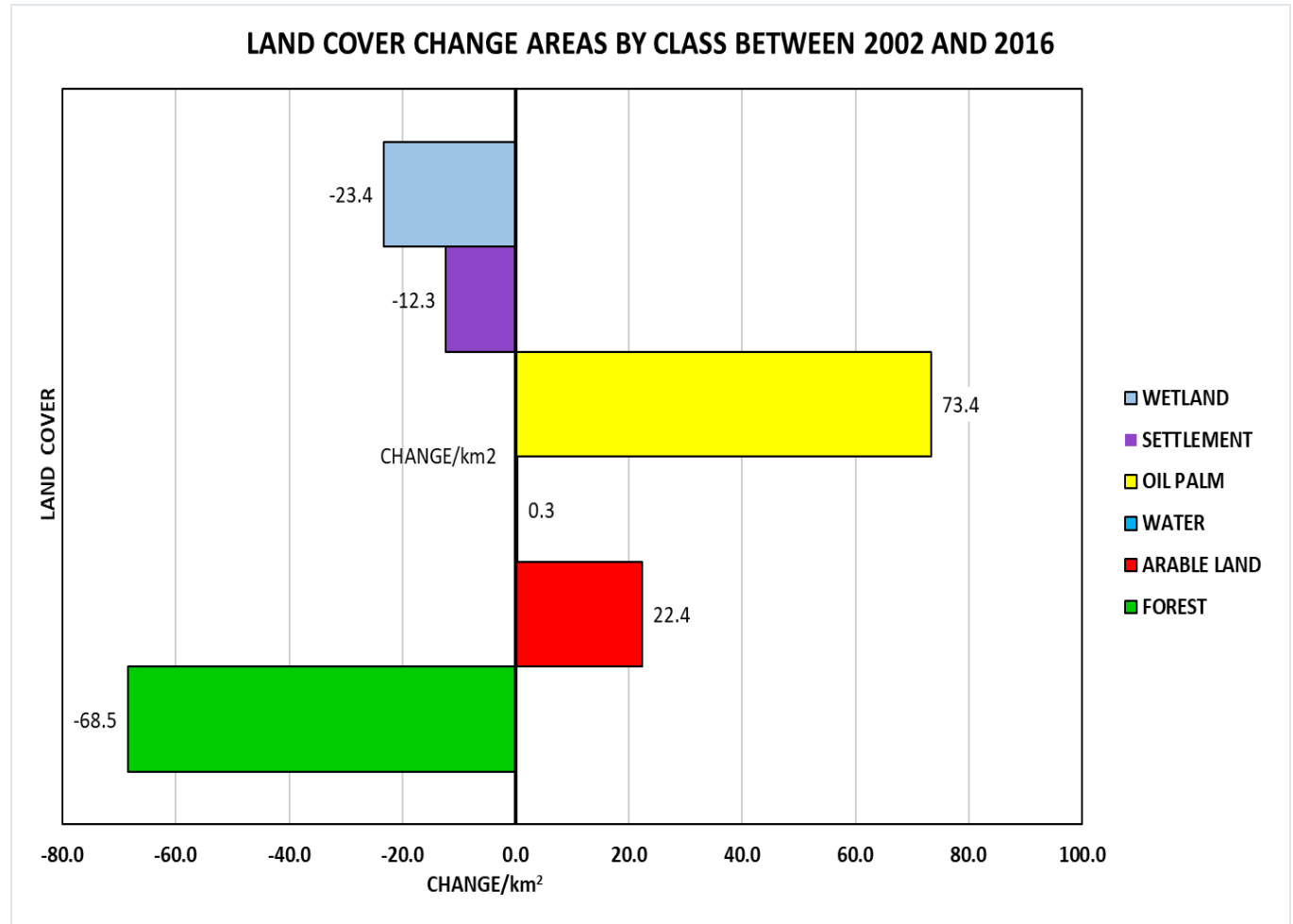


Figure 4.11: Land cover change areas by class between 2002 and 2016

Figure 4.12 shows that between 2016 and 2022, the forested area decreased further by 5.7 km² while the area under oil palm plantation increased by 17.7 km². This is because more forests were converted into oil palm plantations by out growers. Arable land and settlement

areas decreased by 9.6 km² and 4.3 km² respectively and the explanation is that some out growers converted some of their arable land into oil palm plantations while government continued to displace illegal tenants from their settlements with the settlements being converted into oil palm plantations. However, the area of wetland and water increased by 1.4 km² and 0.3 km² respectively. The explanation is that user accuracies for wetland were 0.70 (**Table 4.3**) and 0.76(**Table 4.4**) for 2016 and 2022 respectively causing some commission errors and misclassification. In addition, the Lake Victoria water level rose from 12metres on 1st October 2019 to a record breaking 13.32metres on 30 May 2020 due to intense and prolonged rainfall (Ministry of Water and Environment, 2020).

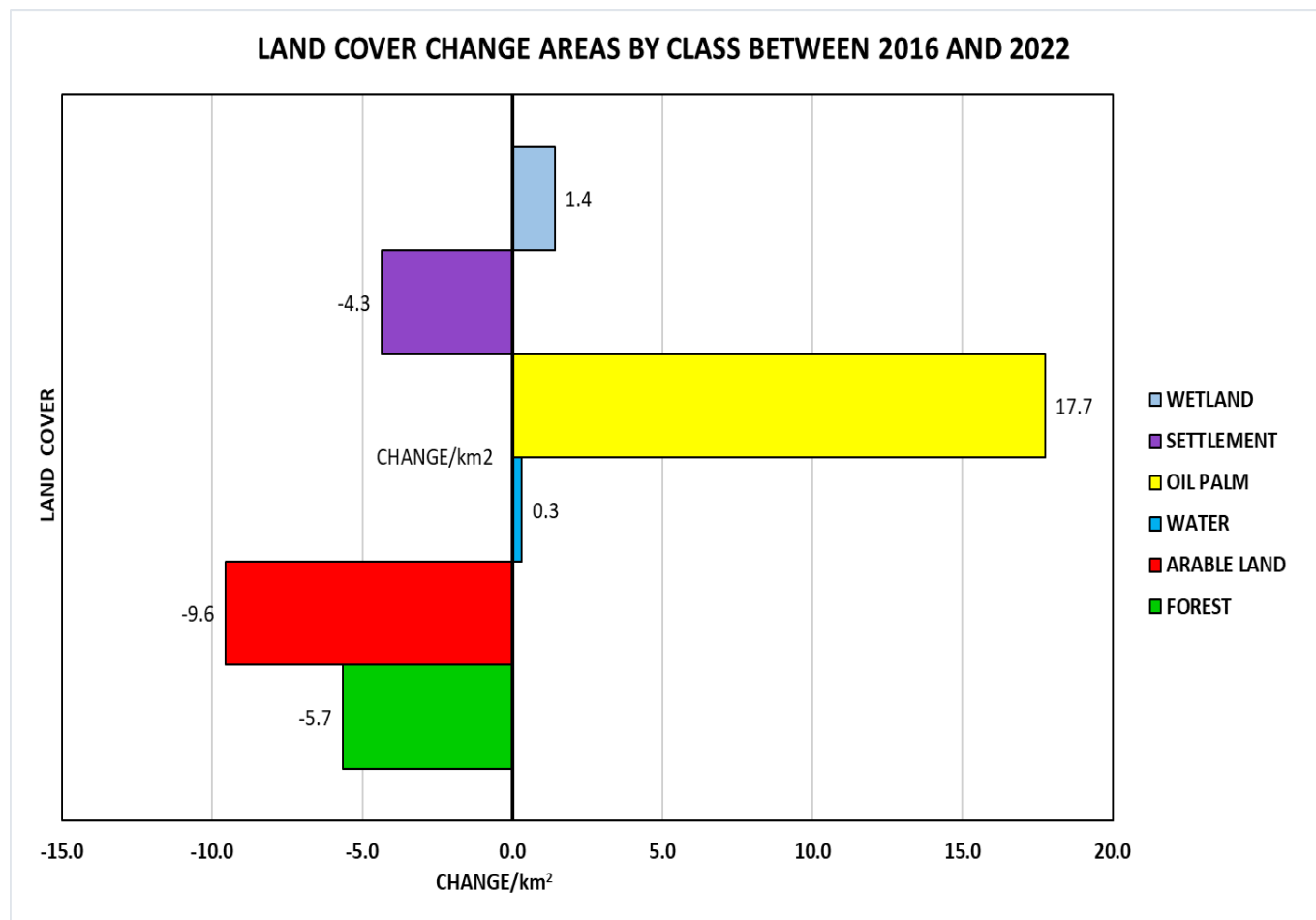


Figure 4.12: Land cover change areas by class between 2016 and 2022

4.4 Objective 3: Oil palm induced Land cover class transitions

4.4.1 Land cover class transitions between 2002 and 2016 (14-year period)

From 2002 to 2016, some areas experienced a change in land cover class while others remained unchanged. **Figure 4.13** shows the distribution of the transitions that occurred from 2002 to 2016 while **Table 4.6** provides the areas of these transitions in a transition matrix. From the results, between 2002 and 2016, 50.1 km² of forest changed to oil palm while 36.7 km² of forest changed into arable land. 6km² of wetland changed to oil palm while 9.2km² became arable land. An additional 13.8km² of wetland changed to forests. In addition, between 2002 and 2016, 12.6km² of arable land changed to oil palm while 8.4km² of arable land became forest. 9.2 km² of settlement became arable land.

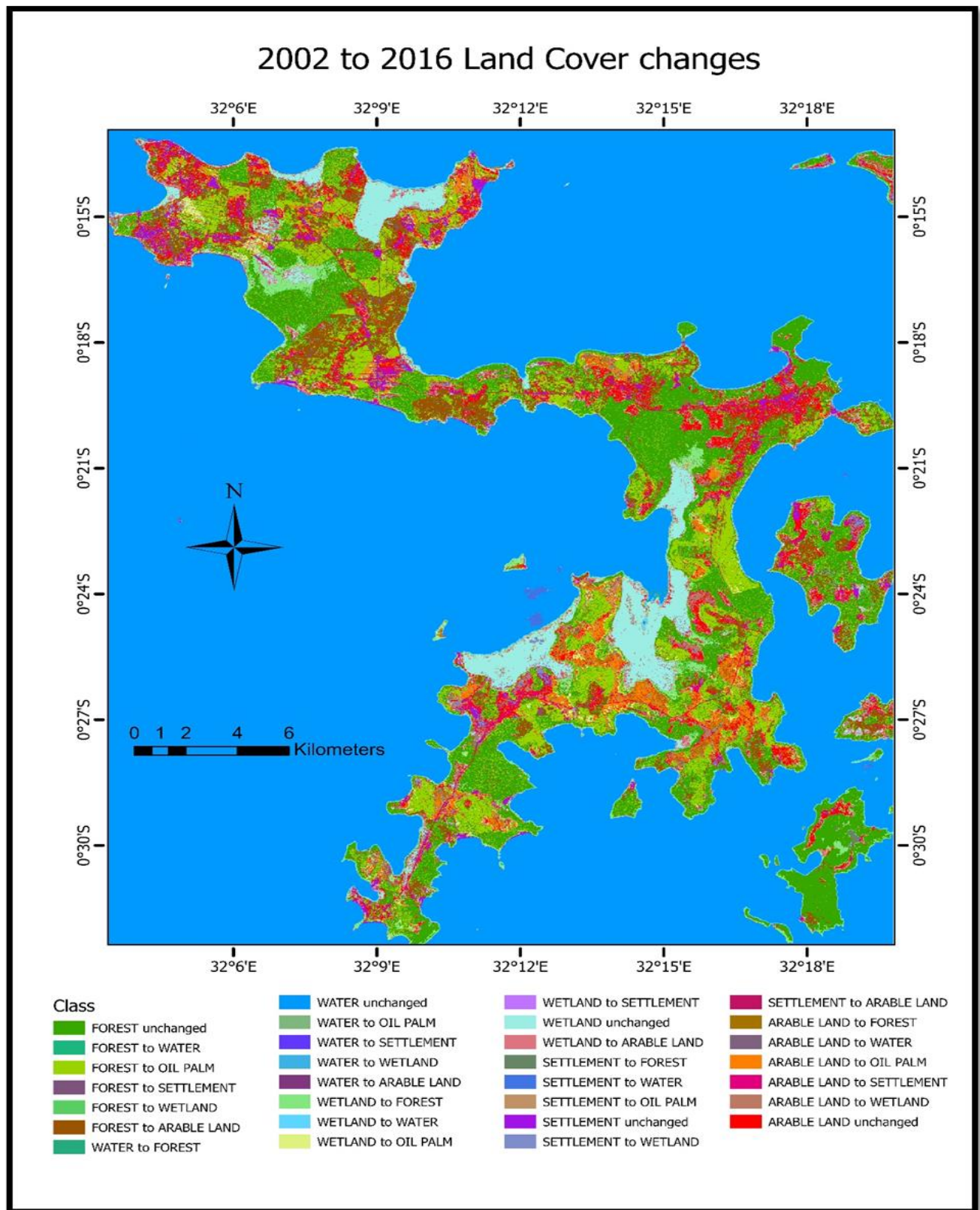


Figure 4.13: Map showing land cover transitions between 2002 and 2016.

Table 4.6: Area transition matrix from 2002 to 2016

OID_	2002\2016	WATER/km ²	%	FOREST/km ²	%	OIL PALM/km ²	%	SETTLEMENT/km ²	%	WETLAND/km ²	%	ARABLE LAND/km ²	%
0	WATER	798.7	99.0	0.6	0.6	0.1	0.1	0.5	4.2	0.4	1.0	0.1	0.1
1	FOREST	0.6	0.1	78.6	75.3	50.1	68.5	2.7	22.5	3.2	8.3	36.7	48.5
2	SETTLEMENT	0.9	0.1	3	2.9	4.3	5.9	3.7	30.8	2.9	7.6	9.2	12.2
3	WETLAND	6.2	0.8	13.8	13.2	6	8.2	1.4	11.7	24.6	64.1	9.2	12.2
4	ARABLE LAND	0.2	0.0	8.4	8.0	12.6	17.2	3.7	30.8	7.3	19.0	20.5	27.1
5	Total	806.6	100	104.4	100	73.1	100	12	100	38.4	100	75.7	100

4.4.2 Land cover class transitions between 2016 and 2022 (6-year period)

Figure 4.14 shows the distribution of the transitions that occurred from 2016 to 2022 while Table 4.7 provides the areas of these transitions in a transition matrix. From the results, 30.6km² of forest changed to oil palm while 13.1 km² of forest changed to arable land. 11km² of wetland changed to arable land. 17.4 km² of arable land changed to forest while 17.1km² of arable land changed to oil palm. 5.2km² of settlement changed to arable land. 22.9km² of oil palm changed to forest while 6.2km² of oil palm changed to arable land.

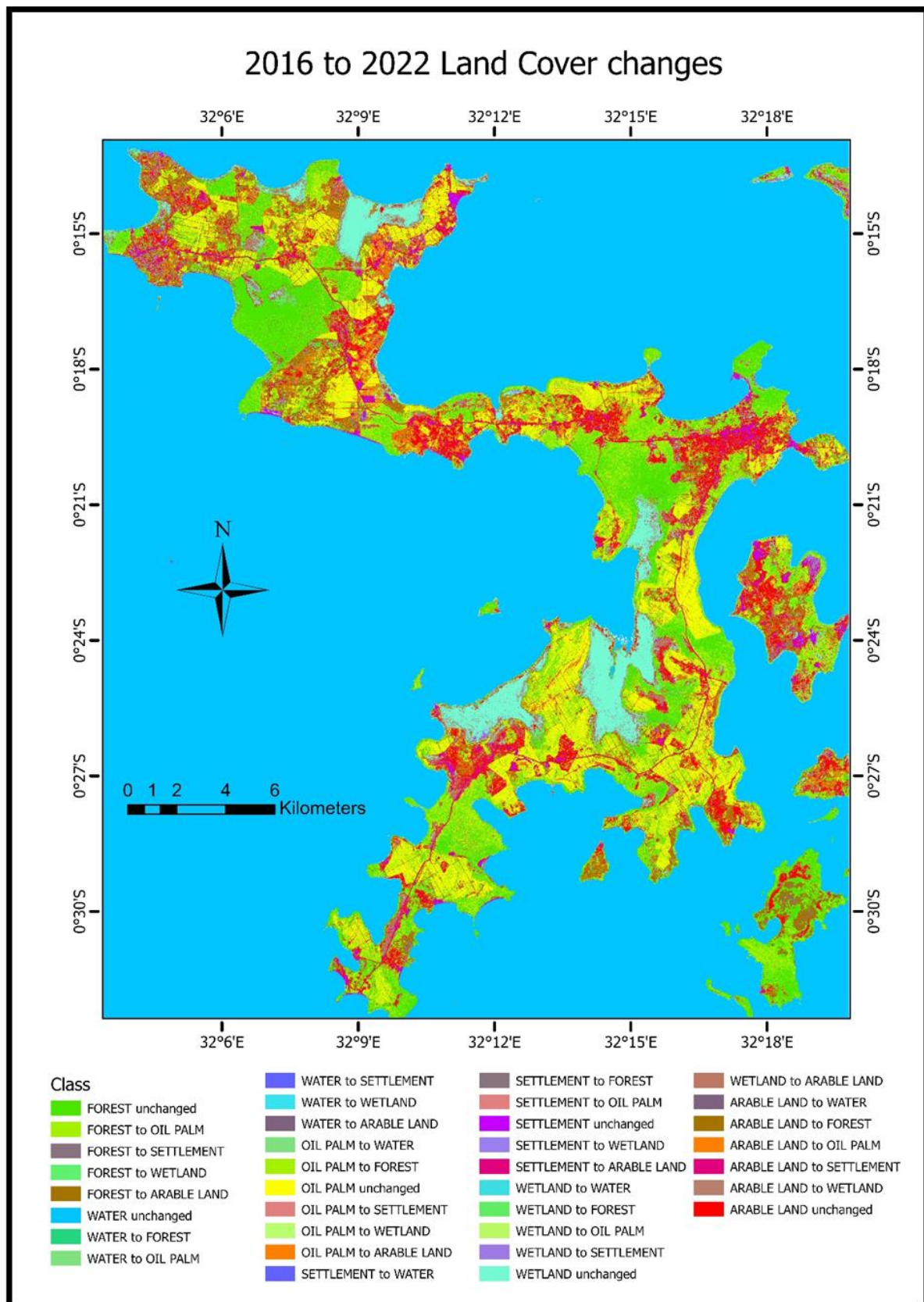


Figure 4.14: Map showing land cover transitions between 2016 and 2022

Table 4.7: Area transition matrix from 2016 to 2022

OID_	2016\2022	WATER/km ²	%	FOREST/km ²	%	OIL PALM/km ²	%	SETTLEMENT/km ²	%	WETLAND/km ²	%	ARABLE LAND/km ²	%
0	WATER	804.2	99.7	0.9	0.9	0	0.0	0	0.0	1.4	3.5	0.1	0.2
1	FOREST	0	0.0	54.7	55.0	30.6	33.6	0.8	10.5	5.3	13.3	13.1	19.8
2	OIL PALM	0.1	0.0	22.9	23.0	41.7	45.8	0.3	3.9	2.2	5.5	6.2	9.4
3	SETTLEMENT	0.9	0.1	0.8	0.8	0.5	0.5	3.2	42.1	1.4	3.5	5.2	7.9
4	WETLAND	0.9	0.1	2.8	2.8	1.2	1.3	0.8	10.5	21.8	54.6	11	16.6
5	ARABLE LAND	0.3	0.0	17.4	17.5	17.1	18.8	2.5	32.9	7.8	19.5	30.6	46.2
6	Total	806.4	100	99.5	100	91.1	100	7.6	100	39.9	100	66.2	100

Figure 4.15 is a Sankey diagram showing the sizes of the area transitions from 2002 through 2016 and up to 2022. The sizes of the flows and the nodes are proportional to the area size of the classes.

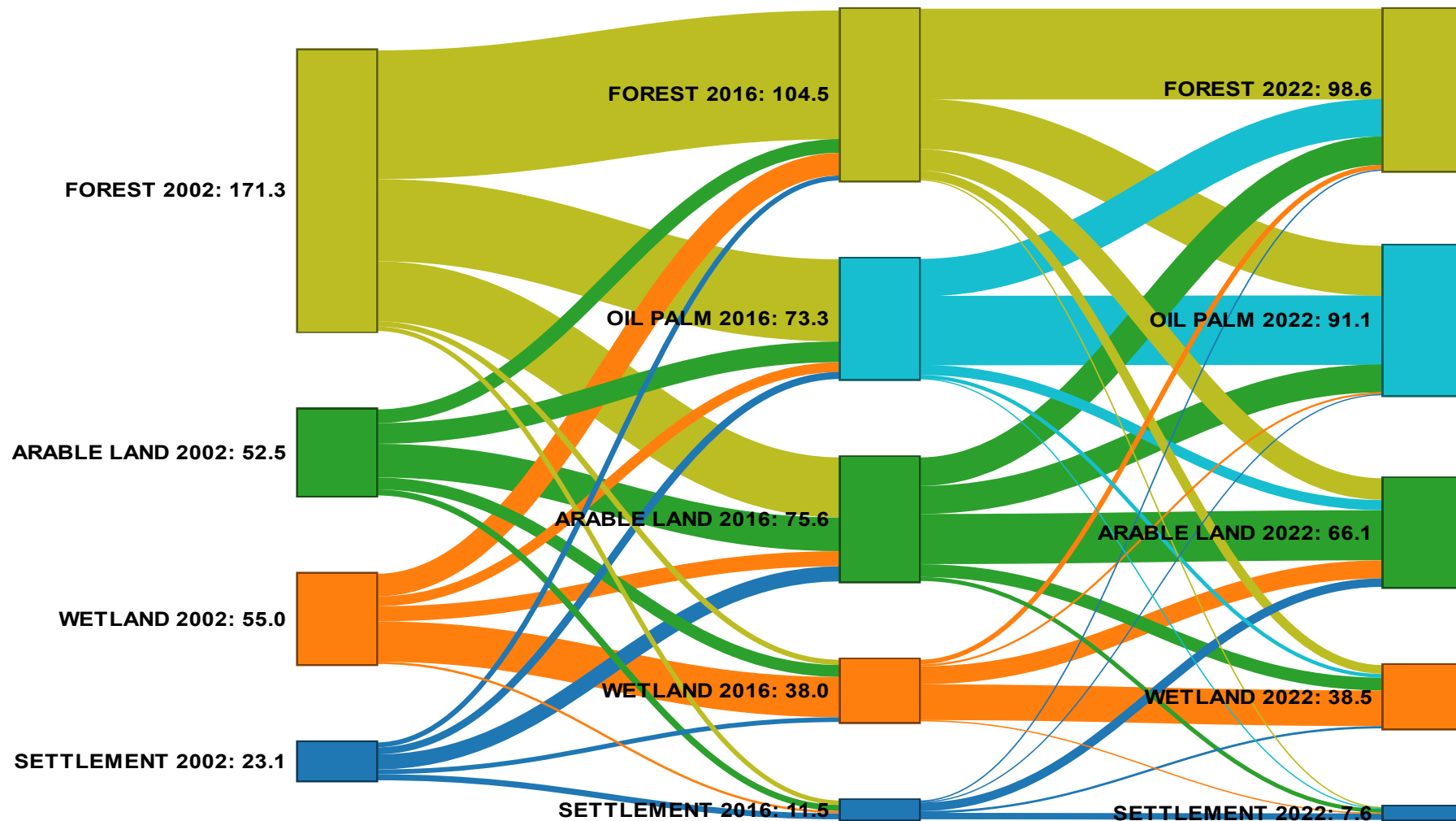


Figure 4.15: Sankey diagram to visualize class area transitions between classes from 2002, through 2016 and up to 2022.

4.4.3 Overall Land cover class transitions between 2002 and 2022(20-year period)

Figure 4.16 below shows the distribution of areas that changed from forests to other land cover classes between 2002 and 2022.

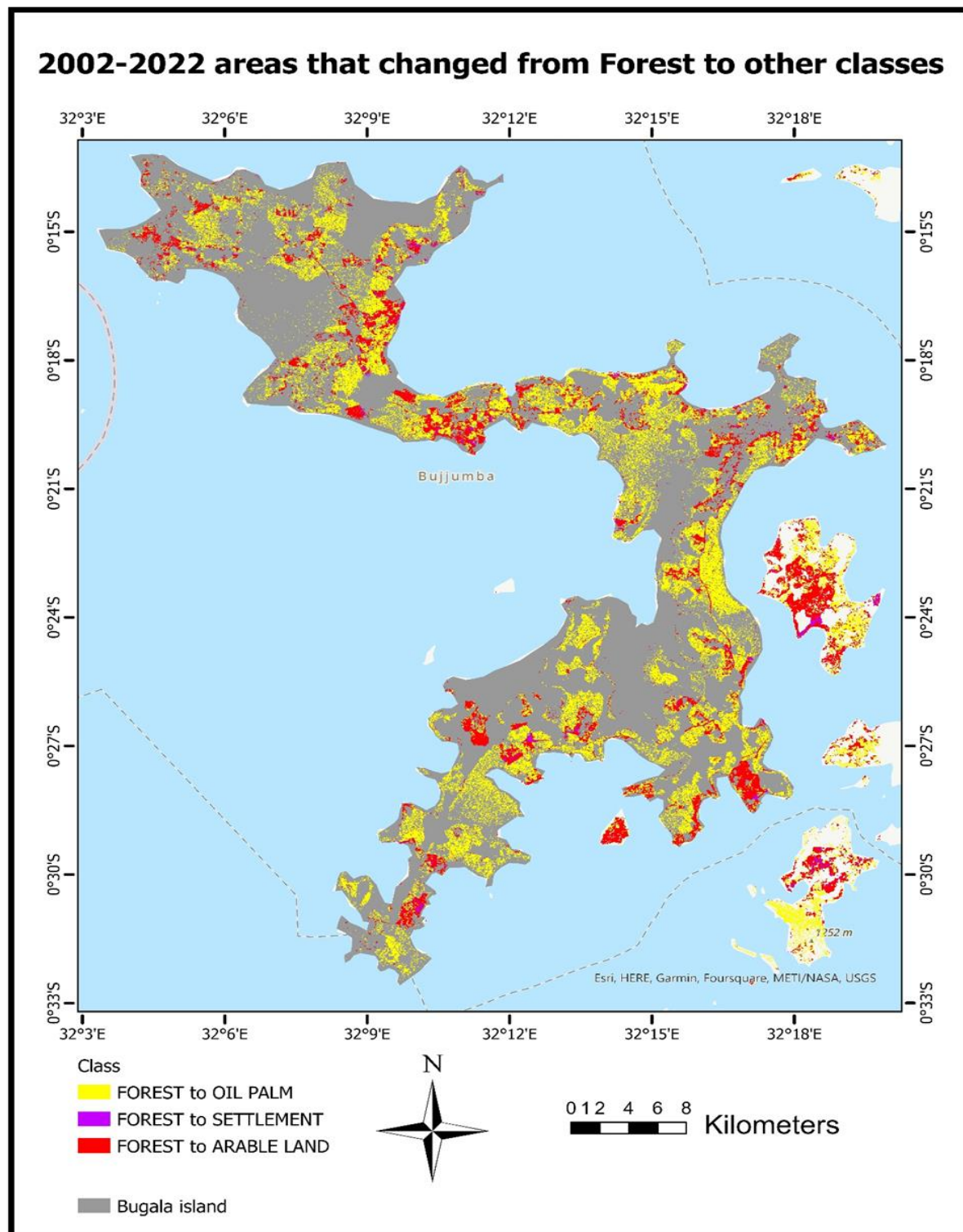


Figure 4.16: Map of areas that changed from Forest to other classes between 2002 and 2022.

Figure 4.16 above shows the distribution of areas that changed from forests to other land cover classes between 2002 and 2022 while **Table 4.8** and **Figure 4.17** below show the areas of these transition classes. The results show that between 2002 and 2022, approximately 64.6km² of forests on Bugala island were cleared and replaced with Oil palm plantations. A further 2km² of forests were cleared and settlements introduced while an additional 29.5km² were cleared and converted into arable land for growing food crops.

Since forests occupied 173km² of land on bugala island in 2002(**Table 4.5**), this means that $(64.6/173) \% = 37.3\%$ of forests have been cleared and replaced by oil palm plantations between 2002 and 2022. It also follows that $(29.5/173) \% = 17\%$ of forests were converted into arable land between 2002 and 2022. In addition, $(2/173) \% = 1.2\%$ of Forests converted into settlements.

Table 4.8: Changed areas from forest to other classes.

ID	Class	Area/m ²	Area/km ²
1	FOREST to OIL PALM	64,556,184	64.6
2	FOREST to SETTLEMENT	1,951,965	2.0
3	FOREST to ARABLE LAND	29,516,260	29.5

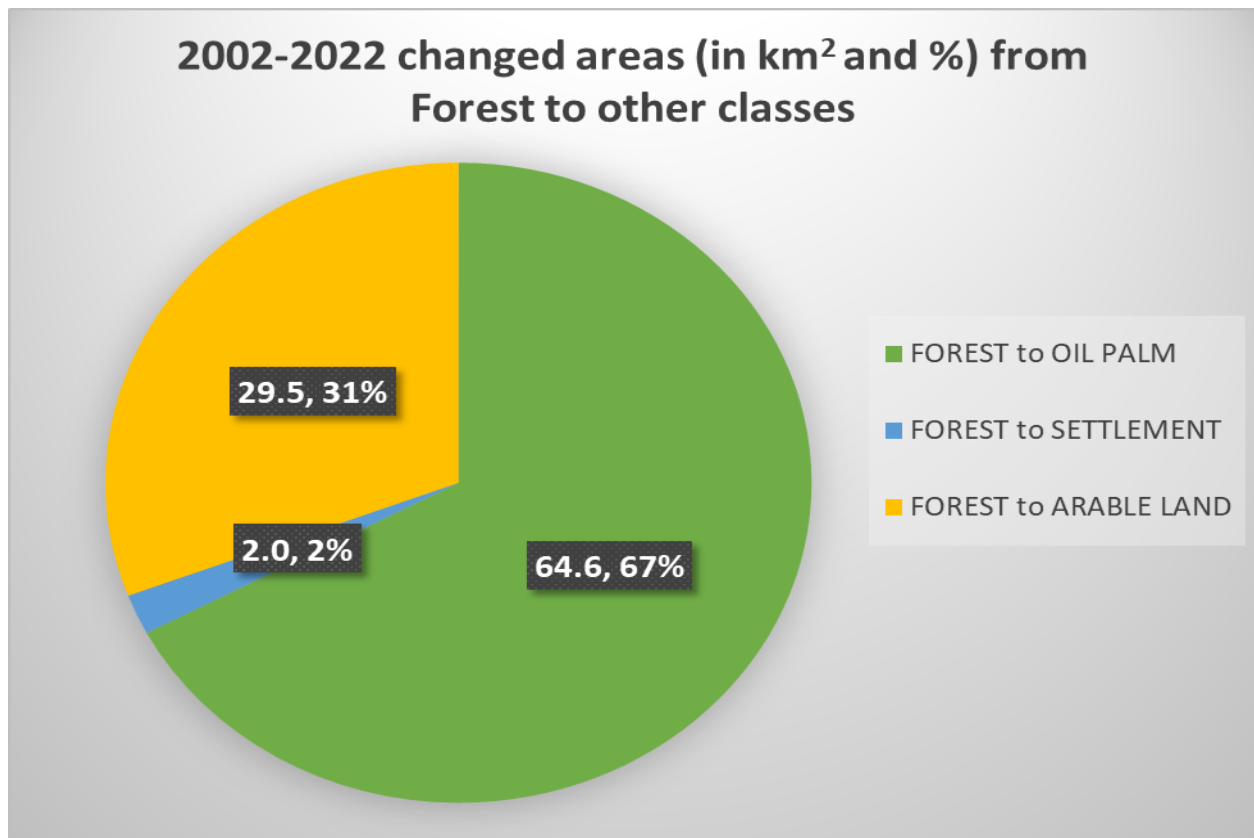


Figure 4.17: Areas that changed from Forest to other classes between 2002 and 2022.

Figure 4.18 below shows the distribution of areas that changed from Arable land to other land cover classes between 2002 and 2022.

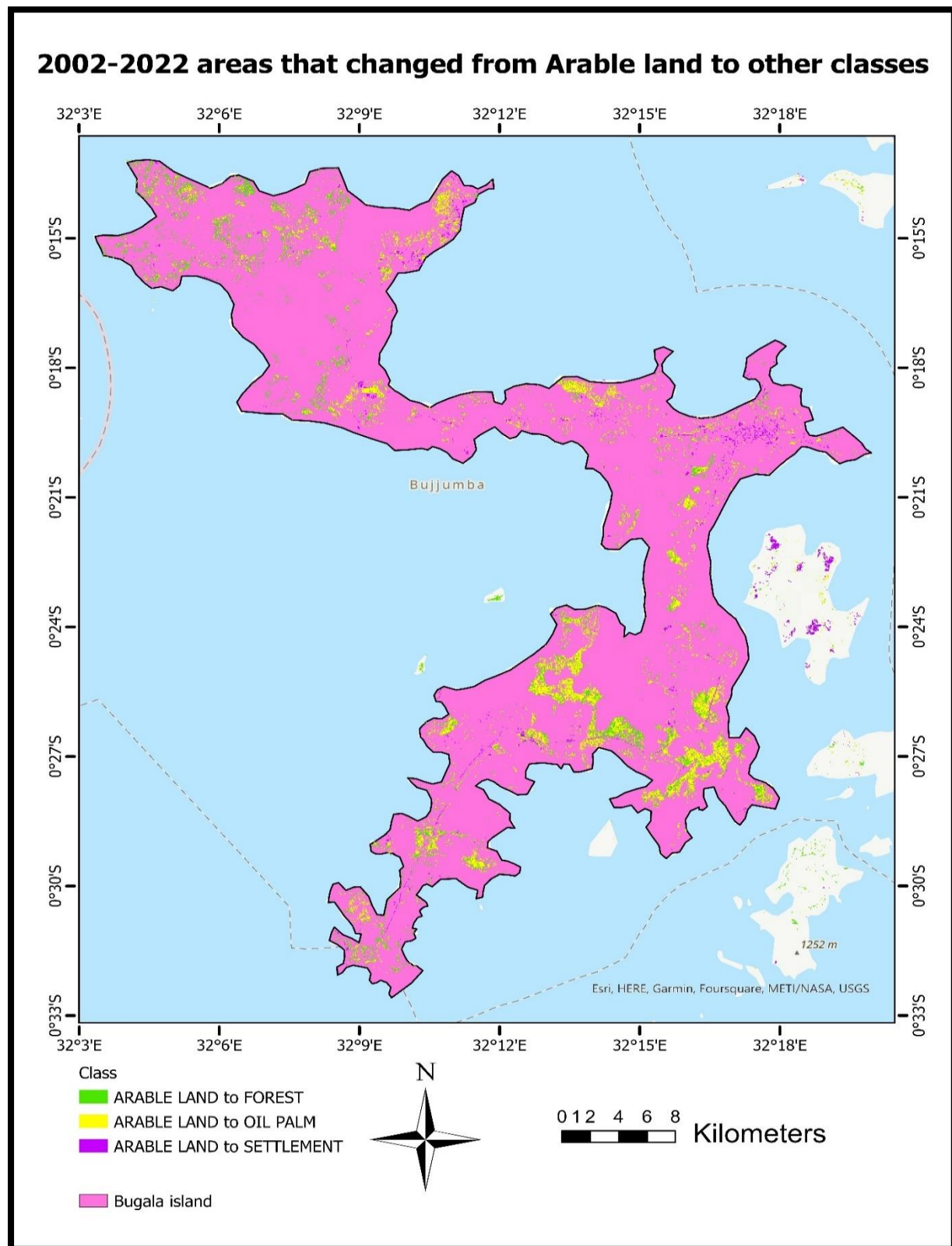


Figure 4.18: Map of areas that changed from Arable land to other classes between 2002 and 2022.

Figure 4.18 above shows the distribution of areas that changed from Arable land to other land cover classes between 2002 and 2022 while **Table 4.9** and **Figure 4.19** below show the areas of these transition classes. The results show that between 2002 and 2022, approximately 15.4km² of arable land on Bugala island were converted to oil palm plantations. A further 2.3km² of arable land were converted to settlements while an additional 10.3km² were converted into forests.

Since arable land occupied 53.2km² of land on bugala island in 2002(**Table 4.5**), this means that $(15.4/53.2) \% = 28.9\%$ of arable land converted into oil palm plantations between 2002 and 2022. It also follows that $(2.3/53.2) \% = 4.3\%$ of arable land converted into settlements between 2002 and 2022. In addition, $(10.3/53.2) \% = 19.4\%$ of arable converted into forests.

Table 4.9: Changed areas from Arable land to other classes.

ID	Class	Area/m ²	Area/km ²
0	ARABLE LAND to FOREST	10,345,952	10.3
1	ARABLE LAND to OIL PALM	15,351,913	15.4
2	ARABLE LAND to SETTLEMENT	2,269,789	2.3

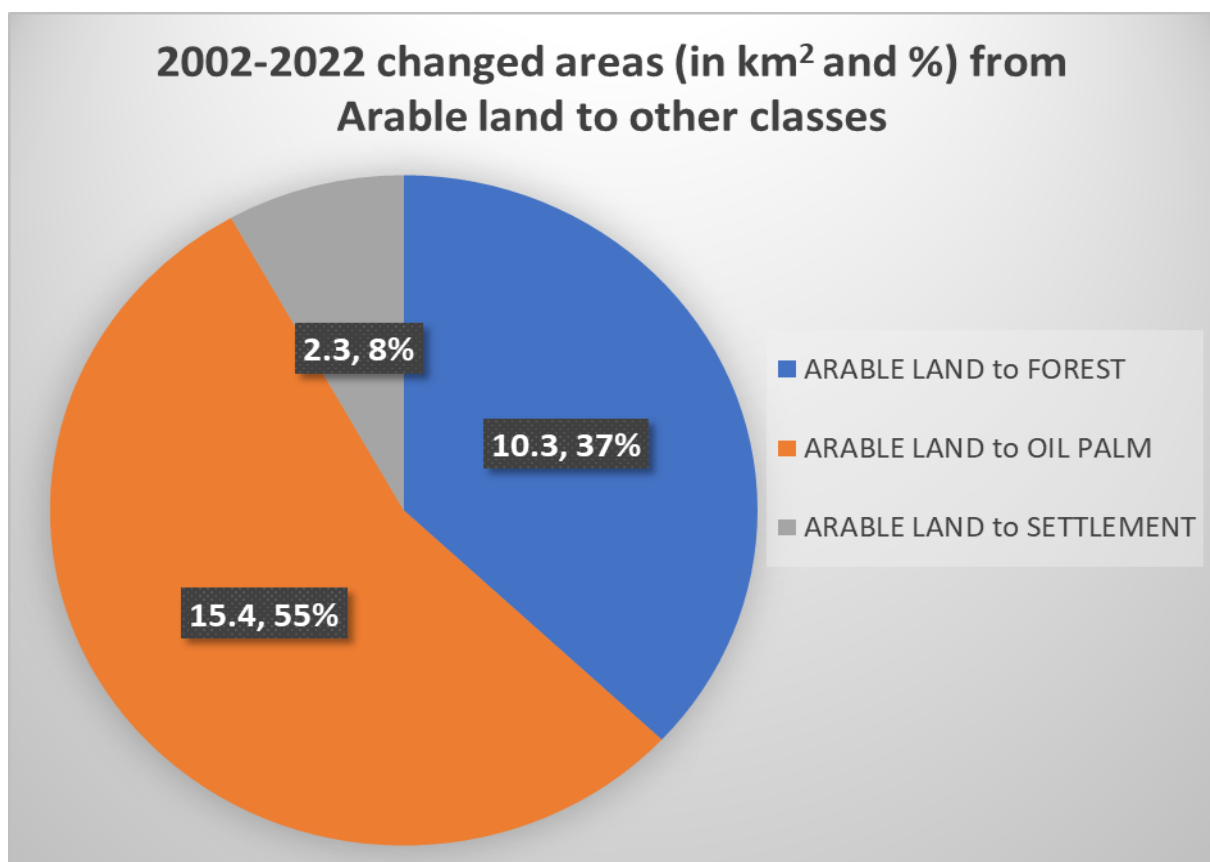


Figure 4.19: Areas that changed from Arable land to other classes between 2002 and 2022.

Figure 4.20 below shows the distribution of areas that changed from settlements to other land cover classes between 2002 and 2022.

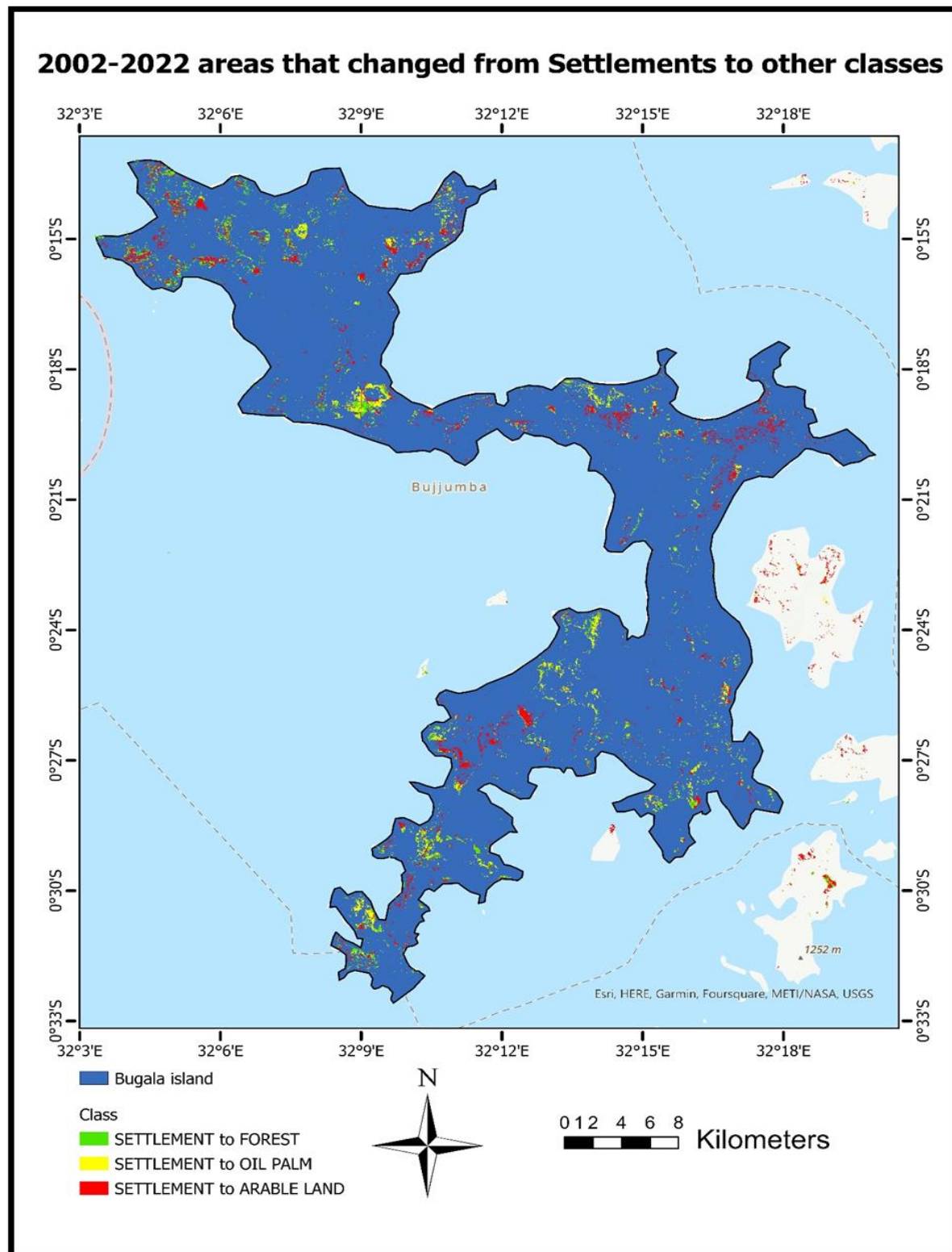


Figure 4.20: Map of areas that changed from Settlements to other classes between 2002 and 2022.

Figure 4.20 above shows the distribution of areas that changed from settlements to other land cover classes between 2002 and 2022 while **Table 4.10** and **Figure 4.21** below show the areas of these transition classes. The results show that between 2002 and 2022, approximately 5.7km^2 of settlements on Bugala island transformed to Oil palm plantations. A further 7.9km^2 of settlements were converted to arable land while an additional 4.4km^2 converted into forests.

Since settlements occupied 24.2km^2 of land on bugala island in 2002(**Table 4.5**), this means that $(5.7/24.2) \% = 23.6\%$ of settlements have been converted into oil palm plantations between 2002 and 2022. It also follows that $(7.9/24.2) \% = 32.6\%$ of settlements were converted into arable land between 2002 and 2022. In addition, $(4.4/24.2) \% = 18.2\%$ of settlements have been converted into forests.

Table 4.10: Changed areas from Settlements to other classes.

ID	Class	Area/m ²	Area/km ²
0	SETTLEMENT to FOREST	4,407,226	4.4
1	SETTLEMENT to OIL PALM	5,746,951	5.7
2	SETTLEMENT to ARABLE LAND	7,874,484	7.9

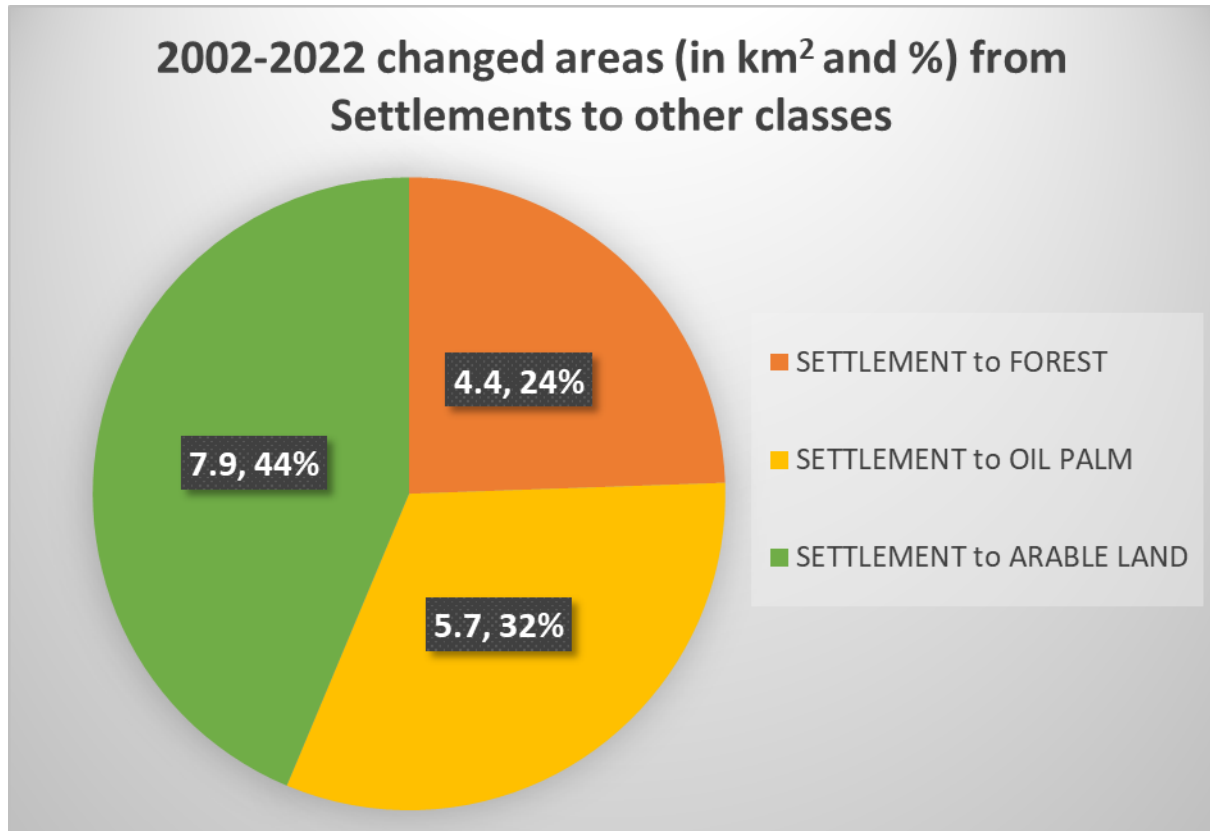


Figure 4.21: Areas that changed from Settlements to other classes between 2002 and 2022.

5. Discussion

5.1 Summary of the findings.

5.1.1 Objective 1: Identification of the most accurate machine learning classifier

The results presented in **Table 4.1** show that the Random Forest machine learning classifier outperformed the Support vector machines and the Maximum Likelihood classifier and hence despite having classified the three images using all three classifiers, only the higher accuracy maps (**Figure 4.5**, **Figure 4.6** and **Figure 4.9**) generated using the Random Forest classifier were used for all subsequent area extractions and change detection analysis. The Random Forest classifier had the highest overall accuracy of 0.94 for the 2002 map, 0.86 for the 2016 map and 0.83 for the 2022 map. It also had the highest Kappa coefficients of 0.92 for the 2002 map, 0.83 for the 2016 map and 0.80 for the 2022 map.

5.1.2 Objective 2: Quantification of the areas of land cover classes in 2002, 2016 and 2022

From **Table 4.5**, forests covered 173km²(55%) of the total land cover of Bugala island before the establishment of oil palm in 2003. Between 2002 and 2016, approximately 68.5km² (**Figure 4.11**) of forested land were deforested reducing forest cover to 104.4km². This deforestation was carried out by both OPUL and the out growers for the establishment of oil palm plantations and arable land for producing food for their employees. This led to a rapid rise in the area under oil palm plantations and arable land by 73.4km² and 22.4km² (**Figure 4.11**) respectively by 2016. Between 2002 and 2016, area under settlements decreased by 12.3km² (**Figure 4.11**) from 24.2km² in 2002 to 11.9km² in 2016 and this was attributed to on-going eviction of illegal tenants by the government whose land was given to OPUL for oil palm expansions. Between 2016 and 2022, deforestation continued with a further loss of 5.7km² (**Figure 4.12**) of forests to oil palm plantations. Because of the high, increasing, and stable oil palm buying prices offered by OPUL to out growers between 2008 and 2018(**Table 1.1**), many out growers decided to allocate more of their arable land for oil palm plantations by abandoning the traditional and less profitable food crops such as beans and maize. This action resulted in arable land decreasing by 9.6km² (**Figure 4.12**) from 75.7km² in 2016 to 66.1km² in 2022 (**Table 4.5**). The result is that oil palm plantations increased by 17.7km² (**Figure 4.12**)

from 73.4km² in 2016 to 91.2km² in 2022(**Table 4.5**). Eviction of illegal tenants by the government continued between 2016 and 2022 leading to further decrease of settlements by 4.3km² (**Figure 4.12**) from 11.9km² in 2016 to 7.6km² in 2022(**Table 4.5**).

Overall, we note from **Table 4.5** that between 2002 and 2022, Oil palm plantations have increased to 91.2km² at the expense of forests that have reduced by 74.2km²(43%). The desire by the government to allocate more land to OPUL for oil palm plantations led to reduction in settlements by 16.6km² through eviction of illegal tenants. Overall, arable land increased by 12.9km² at the expense of forests. Most of this increase in the area of arable land occurred between 2002 and 2016 but between 2016 and 2022, a trend of decreasing arable land emerged driven by out growers allocating more of their arable land to oil palm plantation development which is more lucrative than traditional cash crops like maize and beans.

5.1.3 Objective 3: Quantification of the major land cover transitions between 2002 and 2022

Between 2002 and 2022, 64.6km² of forest were converted into oil palm plantations while 2km² of forest became settlements. An additional 29.5km² of forest was converted into arable land. 15.4km² of arable land were converted into oil palm plantations while 10.3km² of arable land transited into forests. An additional 2.3km² of arable land was converted into settlements. 5.7km² of settlements were converted into oil palm plantations. 7.9km² of settlements became arable land while 4.4km² of settlement transited into forest.

5.2 Comparison with published literature

Studies like ours involving oil palm induced land cover changes characterised by conversion of forest to oil palm plantations have been carried out in Malaysia and Indonesia. According to a recent estimation conducted by Koh and Wilcove (2008), it has been shown that a minimum of 50% of the oil palm increase in both nations over the period of 1990 to 2005 has resulted in the depletion of natural rainforest areas. According to Wicke et al. (2011), the land allocated for cultivation of oil palm in Indonesia rose from 0.1 million hectares in 1975 to 5.5 million hectares at the expense of 40 million hectares of forest cover which resulted in decrease of forested area by 30%. In Malaysia, land for oil palm cultivation expanded from 0.7million hectares in 1975 to 4million hectares in 2005 leading to destruction of 4.6 million

hectares of forest constituting a 20% decrease in forest cover. Arable land in Malaysia decreased in the 1990s due to its conversion to oil palm plantations (Wicke et al.,2011). According to Abdullah and Nakagoshi (2007), the growth of palm oil production in Malaysia has mostly taken place on deforested land and previous coconut and rubber plantations. The detailed finding by Glinskis and Gutiérrez-Vélez (2019) in Peru and Arlete Silva, Vieira, and Ferraz (2020) in Brazil that were presented in **section 2.5** also concur with the findings in **section 5.1** emphasizing the trend of oil palm induced deforestation and conversion of previously arable land into oil palm plantations as key land use and land cover changes that accompany oil palm development. The findings from this study are in agreement with those from already published literature (Abdullah and Nakagoshi,2007; Glinskis and Gutiérrez-Vélez ,2019; Arlete Silva, Vieira, and Ferraz ,2020; Wicke et al.,2011; Koh and Wilcove,2008) which indicate that in most oil palm growing countries, oil palm plantation development has been conducted on forested land and its expansion continues and will continue on forested land unless stopped. In addition, due to the high prices and increasing demand globally for palm oil, there will always be desire to acquire more land for oil palm expansion and arable land and forested land will always be targeted unless mitigative efforts and land use policies are imposed and enforced by governments globally.

5.3 Contributions of the study

The study has proved the robustness of the Random Forest classifier for high accuracy mapping of land cover as already stated by Sheykhmousa et al.(2020) and other authors. The study has provided comprehensive and accurate data on the extent and nature of land cover and land use changes attributed to oil palm cultivation and expansion. The study provides empirical evidence to conservation and environmental monitoring agencies of the environmental impacts of unregulated oil palm cultivation and expansion thereby guiding future policy implementation and interventions to arrest oil palm induced deforestation. The study has also provided part of the missing statistics on oil palm production in Uganda (**Figure 1.3**) and has generated scientific knowledge on the temporal and spatial patterns of land conversion, aiding in the understanding of how oil palm induced land cover changes have evolved over time on Bugala island. It has established causality and correlation between oil palm cultivation and changes in land cover and land use especially deforestation, evictions from land and diminishing arable land.

5.4 Policy recommendations of the study

This study has shown that the cultivation of oil palm results in significant alterations to land cover and land use, which in turn have notable social and environmental consequences. These include biodiversity loss especially of flora and fauna in forests (Fitzherbert et al., 2008), the release of greenhouse gases due to the burning of forest biomass during deforestation, the degradation of soil via monoculture of oil palm, the occurrence of forest fires and associated respiratory ailments, evictions as well as disputes connected to land ownership and human rights (Koh and Wilcove ,2008).

The government of Uganda should incorporate RSPO standards into their national regulations and mandate adherence to those RSPO standards. The Roundtable on Sustainable Palm Oil (RSPO) is an establishment that was formed in 2004 as a non-profit organisation with the objective of advocating for the global sustainable production and use of palm oil (Geibler, 2013). The primary focus of the Roundtable on Sustainable Palm Oil (RSPO) is to advance the promotion of palm oil production, procurement, and utilisation that adheres to clearly defined sustainability standards. This entails mitigating the environmental and social consequences linked to the growth of palm oil such as oil palm induced deforestation and conversion of arable land and peatlands to oil palm plantations (Geibler, 2013). The RSPO is responsible for the establishment and maintenance of a comprehensive framework of criteria and standards that govern the production of sustainable palm oil. The aforementioned requirements include several dimensions, including environmental stewardship, social equity, adherence to legal regulations, and economic sustainability. The RSPO offers a certification system that enables palm oil producers to showcase their adherence to sustainability requirements.

The government of Uganda should increase funding to the National Environmental Management Authority (NEMA) to boost monitoring (Glinskis and Gutiérrez-Vélez, 2019) and conservation of the remaining forest by declaring them as protected forest reserves. In addition, there is need to shift the expansion of oil palm from natural forest to fallow and degraded land that exhibits little environmental value and will therefore release less carbon dioxide emissions (Fitzherbert et al., 2008; Xin, Sun and Hansen, 2022). Increased conversion of arable land to oil palm plantations by out growers is likely to lead to future food shortage

on the island. Strict land use and land tenure policies should be legalised that foster sustainable oil palm development but also ensure food security on the island.

5.5 Gaps and recommendations for further research

The study primarily used optical satellite remote sensing data which is prone to effects of cloud cover that are prevalent in the tropics where this study was done. Presence of clouds despite being removable using cloud masks affects data quality. A multi sensor data fusion approach involving microwave remote sensed radar data from Sentinel-1 and ALOS PALSAR is recommended for future work since it improves the results of classification by effectively distinguishing oil palm trees from forests (Chong et al., 2017). It is also useful in estimating tree age. Radar data is good in the tropics since it penetrates clouds and is all weather. In addition, the fusion of LiDAR (light detection and ranging) data provides very high spatial resolution and three-dimensional information such as canopy height and can provide terrain elevation (Chong et al., 2017). LiDAR can be applicable in analysis of oil palm diseases and the automated counting of palm trees.

In addition, since the demand for palm oil is increasing, there is need to identify fallow land using remote sensing where oil palm plantations can be set up or expanded (Xin, Sun and Hansen, 2022). Future research could study satellite imagery to establish indicators that can be used for automated identification of fallow or degraded land suitable for oil palm plantation development (Chong et al., 2017).

Forest cover pertains to the physical presence of forest vegetation on a given geographical area, regardless of its official classification as forested or non-forested. The term "forest" in this context is interpreted as referring to forest cover, since it is considered to provide a more accurate representation of the land's current condition compared to forest land. Nevertheless, it is important to bear in mind that the idea of forest cover by itself is insufficient for accurately assessing the condition or level of preservation of a forest. This consideration should be taken into account when understanding the findings. This study did not go deeper to identify degradation due to selective logging in the forested areas and never distinguished between various forest types such as montane, low land, peatland and mangrove and to show how oil palm induced land use change affected each type individually. Future further research should monitor the oil palm induced land use and land cover change

s for each of these forest categories. The study did not also distinguish between the oil palm by age or maturity and variety or species yet the plantations on Bugala island contain oil palm at different stages of maturity with some young, youthful and old. Further future studies should quantify the areas of oil palm by both oil palm maturity and variety for deeper analysis by utilisation of radar and LiDAR remote sensing.

5.6 Conclusion

The study has proven the versatility and superior accuracy of random forest classifier over Support Vector Machine and maximum likelihood classifier in mapping oil palm induced land cover changes and transitions on Bugala island. The study has exposed the on going negative effects of uncontrolled and unregulated oil palm expansion such as rapid oil palm induced deforestation which leads to biodiversity loss on Bugala island and reduction in arable land. The study advocates for increased monitoring of forested land (Glinskis and Gutiérrez-Vélez, 2019) on the island and gazetting it into protected reserves. It further recommends shifting oil palm expansions to fallow lands (Xin, Sun and Hansen, 2022) and the adoption of the RSPO regulatory framework for the oil palm industry in Uganda.

6. References

- Abdullah, S.A. and Nakagoshi, N. (2007). 'Forest fragmentation and its correlation to human land use change in the state of Selangor, peninsular Malaysia', *Forest Ecology and Management*, 241(1-3), pp.39–48, doi: 10.1016/j.foreco.2006.12.016
- Afaq, Y. and Manocha, A. (2021). 'Analysis on change detection techniques for remote sensing applications: A review', *Ecological Informatics*, p.101310, doi: 10.1016/j.ecoinf.2021.101310.
- Arlete Silva, de A., Vieira, I.C.G. and Ferraz, S.F.B. (2020). 'Long-term assessment of oil palm expansion and landscape change in the eastern Brazilian Amazon', *Land Use Policy*, 90, p.104321, doi: 10.1016/j.landusepol.2019.104321.
- Asming, M.A., Ibrahim, A.M. and Abir, I.M. (2022) 'Processing and classification of landsat and Sentinel images for Oil Palm Plantation Detection', *Remote Sensing Applications: Society and Environment*, 26(100747), doi: 10.1016/j.rsase.2022.100747.
- Balasundram, S. K., Memarian, H. and Khosla, R. (2013). 'Estimating Oil Palm Yields Using Vegetation Indices Derived from QuickBird', *Life Science Journal* ,10 (4), pp.851– 860
- Breiman, L. (2001). 'Random Forests', *Machine Learning*, 45(1), pp.5–32, doi: 10.1023/a:1010933404324.
- Carlson, K. M., Curran, L. M., Ratnasari, D., Pittman, A. M., Soares-Filho, B. S., Asner, G. P. and Rodrigues, H. O. (2012) 'Committed carbon emissions, deforestation, and community land conversion from oil palm plantation expansion in West Kalimantan, Indonesia', *Proceedings of the National Academy of Sciences*, 109(19), pp.7559-7564, doi: 10.1073/pnas.1200452109.
- Chemura, A., van Duren, I. and van Leeuwen, L.M. (2015) 'Determination of the age of oil palm from crown projection area detected from WorldView-2 multispectral remote sensing data: The case of Ejisu-Juaben district, Ghana', *ISPRS Journal of Photogrammetry and Remote Sensing*, 100, pp.118–127, doi: 10.1016/j.isprsjprs.2014.07.013.

Cheng, Y., Xu, Y., Kasturi, K. and Peng, G. (2017) 'Mapping oil palm extent in Malaysia using ALOS-2 Palsar-2 Data', *International Journal of Remote Sensing*, 39(2), pp. 432–452, doi: 10.1080/01431161.2017.1387309.

Chong, K.L., Kasturi, D. K., Pohl, C. and Tan, P.K. (2017) 'A review of remote sensing applications for Oil Palm Studies', *Geo-spatial Information Science*, 20(2), pp. 184–200, doi: 10.1080/10095020.2017.1337317.

Cohen, J. (1968). 'Weighted kappa: Nominal scale agreement provision for scaled disagreement or partial credit', *Psychological Bulletin*, 70(4), pp. 213–220, doi: 10.1037/h0026256.

Congalton, R.G. and Green, K. (2019). *Assessing the Accuracy of Remotely Sensed Data*. CRC Press.

Cortes, C. and Vapnik, V. (1995) 'Support-vector networks', *Machine Learning*, 20(3), pp. 273–297, doi: 10.1007/bf00994018.

Fitzherbert, E., Struebig, M., Morel, A., Danielsen, F., Bruhl, C., Donald, P. and Phalan, B. (2008) 'How will oil palm expansion affect biodiversity?', *Trends in Ecology & Evolution*, 23(10), pp. 538–545, doi: 10.1016/j.tree.2008.06.012.

Foody, G.M. (2020) 'Explaining the unsuitability of the kappa coefficient in the assessment and comparison of the accuracy of thematic maps obtained by image classification', *Remote Sensing of Environment*, 239, p. 111630, doi: 10.1016/j.rse.2019.111630.

Geibler, J. von (2013) 'Market-based governance for sustainability in value chains: conditions for successful standard setting in the palm oil sector', *Journal of Cleaner Production*, 56, pp. 39–53, doi: 10.1016/j.jclepro.2012.08.027.

Glinskis, E.A. and Gutiérrez-Vélez, V.H. (2019) 'Quantifying and understanding land cover changes by large and small oil palm expansion regimes in the Peruvian Amazon', *Land Use Policy*, 80, pp. 95–106, doi: 10.1016/j.landusepol.2018.09.032.

Jarayee, A.N., Mohd, Z., Ang, Y., Lee, Y.P., Shahrul Azman Bakar, Haryati Abidin, Lim, H.S. and Abdullah, R. (2022) 'Oil Palm Plantation Land Cover and Age Mapping Using Sentinel-2 Satellite Imagery and Machine Learning Algorithms', *IOP conference series*, 1051(1), pp.012024–012024, doi: 10.1088/1755-1315/1051/1/012024.

Koh, L.P. and Wilcove, D.S. (2008) 'Is oil palm agriculture really destroying tropical biodiversity?', *Conservation Letters*, 1(2), pp.60–64, doi:10.1111/j.1755-263x.2008.00011.x.

Kumar, A. (2022) Support Vector Machine (SVM) Python Example. [online] *Data Analytics*. Available at: <https://vitalflux.com/classification-model-svm-classifier-python-example/>.

Kusiima, S.K., Egeru, A., Namaalwa, J., Byakagaba, P., Mfitumukiza, D. and Mukwaya, P. (2022) 'Anthropogenic induced land use/cover change dynamics of Budongo-Bugoma landscape in the Albertine Region, Uganda', *The Egyptian Journal of Remote Sensing and Space Science*, 25(3), pp. 639–649, doi: 10.1016/j.ejrs.2022.05.001.

Lee, J.S., Wich, S., Widayati, A. and Lian, P.K. (2016) 'Detecting industrial oil palm plantations on Landsat images with Google Earth Engine', *Remote Sensing Applications: Society and Environment*, 4, pp. 219–224, doi: 10.1016/j.rsase.2016.11.003.

Ministry of Water and Environment (2020). *Statement on the Rising water levels of Lake Victoria and the Nile System*, Uganda Media Centre, Available at: <https://www.mediacentre.go.ug/media/statement-rising-water-levels-lake-victoria-and-nile-system#:~:text=The%20current%20rise%20in%20Lake> [Accessed 30 Sep. 2023].

Ministry of Agriculture (2019) *National Oil Palm Project*, Available at <https://www.agriculture.go.ug/wp-content/uploads/2021/04/PALM-OIL-ISSUE-COMPRESSED-1.pdf>

Nooni, I.K., Duker, A.A., I.C. van Duren, L. Addae-Wireko and Osei, M. (2014) 'Support vector machine to map oil palm in a heterogeneous environment', *International Journal of Remote Sensing*, 35(13), pp.4778–4794, doi: 10.1080/01431161.2014.930201.

Núñez, J.M., Medina, S., Ávila, G. and Montejano, J. (2019) 'High-Resolution Satellite Imagery Classification for Urban Form Detection', *Satellite Information Classification and Interpretation*, doi:10.5772/intechopen.82729.

Oliphant, A. J., Thenkabail, P. S., Teluguntla, P., Xiong, J., Gumma, M. K., Congalton, R. G., and Yadav, K. (2019) 'Mapping cropland extent of southeast and Northeast Asia using multi-year time-series landsat 30-M data using a random forest classifier on the Google Earth Engine Cloud', *International Journal of Applied Earth Observation and Geoinformation*, 81, pp.110-124, doi: 10.1016/j.jag.2018.11.014

Otuba, M.A., Masika, B.F., Asiimwe, A. and Ddamulira, G. (2022) 'Challenges and Opportunities of Oil Palm Production in Uganda', *Palm Oil - Current Status and Updates*. IntechOpen, doi: 10.5772/intechopen.108008, Available at: <https://www.intechopen.com/online-first/84209>

Piacenzar, C. (2012) 'Negotiating gendered property relations over land: oil palm expansion in Kalangala district, Uganda', *International Conference on Global Land Grabbing II. Cornell University, Ithaca, Land Deal Politics Initiative*. Available at <https://cornell-landproject.org/download/landgrab2012papers/Piacenzar.pdf>

Planet Labs (2022). *Planet imagery product specifications*. [online] Available at: https://assets.planet.com/docs/Planet_Combined_Imagery_Product_Specs_letter_screen.pdf?_gl=1 [Accessed 17 Sep. 2023].

Rastogi, R. (2020). *Random Forest Classification and it's Mathematical Implementation*. [online] Analytics Vidhya. Available at: <https://medium.com/analytics-vidhya/random-forest-classification-and-its-mathematical-implementation-1895a7bb743e>.

Ritchie, H. and Roser, M. (2020). Palm Oil. [online] Our World in Data. Available at: <https://ourworldindata.org/palm-oil>.

Santoso, H., Gunawan, T., Jatmiko, R.H., Darmosarkoro, W. and Minasny, B. (2010) 'Mapping and identifying basal stem rot disease in oil palms in North Sumatra with QuickBird imagery', *Precision Agriculture*, 12(2), pp.233–248, doi:10.1007/s11119-010-9172-7.

Shafri, H.Z.M., Hamdan, N. and Saripan, M.I. (2011) 'Semi-automatic detection and counting of oil palm trees from high spatial resolution airborne imagery', *International Journal of Remote Sensing*, 32(8), pp.2095–2115, doi:10.1080/01431161003662928.

Shaharum, N.S., Shafri, M.Z., Ghani, W.A., Samsatli, S., Mustafa, M.A. and Badonnisa, Y. (2020) 'Oil palm mapping over Peninsular Malaysia using Google Earth engine and machine learning algorithms', *Remote Sensing Applications: Society and Environment*, 17(100287), doi: 10.1016/j.rsase.2020.100287.

Sheykhmousa, M., Mahdianpari, M., Ghanbari, H., Mohammadimanesh, F., Ghamisi, P. and Homayouni, S. (2020) 'Support Vector Machine Versus Random Forest for Remote Sensing Image Classification: A Meta-Analysis and Systematic Review', *IEEE Journal of Selected Topics in Applied Earth Observations and Remote Sensing*, 13, pp.6308–6325, doi:10.1109/jstars.2020.3026724.

Singh, M., Malhi, Y. and Bhagwat, S.A. (2014) 'Biomass estimation of mixed forest landscape using a Fourier transform texture-based approach on very-high-resolution optical satellite imagery', *International Journal of Remote Sensing*, 35(9), pp.3331–3349, doi:10.1080/01431161.2014.903441.

Stigler, S.M. (2007) 'The Epic Story of Maximum Likelihood' *Statistical Science*, 22(4), doi: 10.1214/07-sts249.

Svetnik, V., Liaw, A., Tong, C., Culberson, J.C., Sheridan, R.P. and Feuston, B.P. (2003) 'Random Forest: A Classification and Regression Tool for Compound Classification and QSAR Modeling', *Journal of Chemical Information and Computer Sciences*, 43(6), pp.1947–1958, doi:10.1021/ci034160g.

USGS (2023) *Landsat 7*, United States Geological Survey, Available at: <https://www.usgs.gov/landsat-missions/landsat-7>.

Wicke, B., Sikkema, R., Dornburg, V. and Faaij, A. (2011) 'Exploring land use changes and the role of palm oil production in Indonesia and Malaysia', *Land Use Policy*, 28(1), pp.193–206, doi:10.1016/j.landusepol.2010.06.001.

Xin, Y., Sun, L. and Hansen, M.C. (2022) 'Oil palm reconciliation in Indonesia: Balancing rising demand and environmental conservation towards 2050', *Journal of Cleaner Production*, 380, p.135087, doi: 10.1016/j.jclepro.2022.135087.

7. Appendices

Appendix A : Support Vector Machine (SVM) confusion matrices

2002 SVM CONFUSION MATRIX

ID	Class	FOREST	WATER	WETLAND	SETTLEMENT	ARABLE LAND	Total	User Accuracy	Kappa
1	FOREST	50	0	2	2	0	54	0.93	
2	WATER	0	51	2	0	0	53	0.96	
3	WETLAND	2	0	38	3	4	47	0.81	
4	SETTLEMENT	0	2	1	29	2	34	0.85	
5	ARABLE LAND	5	0	2	11	44	62	0.71	
6	Total	57	53	45	45	50	250		
7	Producer Accuracy	0.88	0.96	0.84	0.64	0.88		0.85	
8	Kappa								0.81

2016 SVM CONFUSION MATRIX

ID	Class	FOREST	WATER	OIL PALM	SETTLEMENT	WETLAND	ARABLE LAND	Total	User Accuracy	Kappa
0	FOREST	41	0	6	0	0	0	47	0.87	
1	WATER	1	50	0	0	0	0	51	0.98	
2	OIL PALM	10	0	39	0	0	2	51	0.76	
3	SETTLEMENT	1	0	0	40	1	4	46	0.87	
4	WETLAND	0	0	0	1	35	11	47	0.74	
5	ARABLE LAND	1	0	3	3	3	48	58	0.83	
6	Total	54	50	48	44	39	65	300		
7	Producer Accuracy	0.76	1.00	0.81	0.91	0.90	0.74		0.84	
8	Kappa									0.81

2022 SVM CONFUSION MATRIX

ID	Class	WATER	FOREST	OIL PALM	SETTLEMENT	WETLAND	ARABLE LAND	Total	User Accuracy	Kappa
0	WATER	50	0	0	0	0	0	50	1.00	
1	FOREST	0	32	13	0	0	0	45	0.71	
2	OIL PALM	0	19	33	0	0	2	54	0.61	
3	SETTLEMENT	4	0	0	38	1	9	52	0.73	
4	WETLAND	0	0	0	0	34	16	50	0.68	
5	ARABLE LAND	0	3	0	2	5	39	49	0.80	
6	Total	54	54	46	40	40	66	300		
7	Producer Accuracy	0.93	0.59	0.72	0.95	0.85	0.59		0.75	
8	Kappa									0.70

Appendix B : Maximum Likelihood (ML) confusion matrices

2002 ML CONFUSION MATRIX

ID	Class	FOREST	WATER	WETLAND	SETTLEMENT	ARABLE LAND	Total	User Accuracy	Kappa
1	FOREST	49	0	3	2	4	58	0.84	
2	WATER	0	49	0	0	0	49	1.00	
3	WETLAND	0	1	34	3	4	42	0.81	
4	SETTLEMENT	1	3	2	20	3	29	0.69	
5	ARABLE LAND	7	0	6	20	39	72	0.54	
6	Total	57	53	45	45	50	250		
7	Producer Accuracy	0.86	0.92	0.76	0.44	0.78		0.76	
8	Kappa								0.70

2016 ML CONFUSION MATRIX

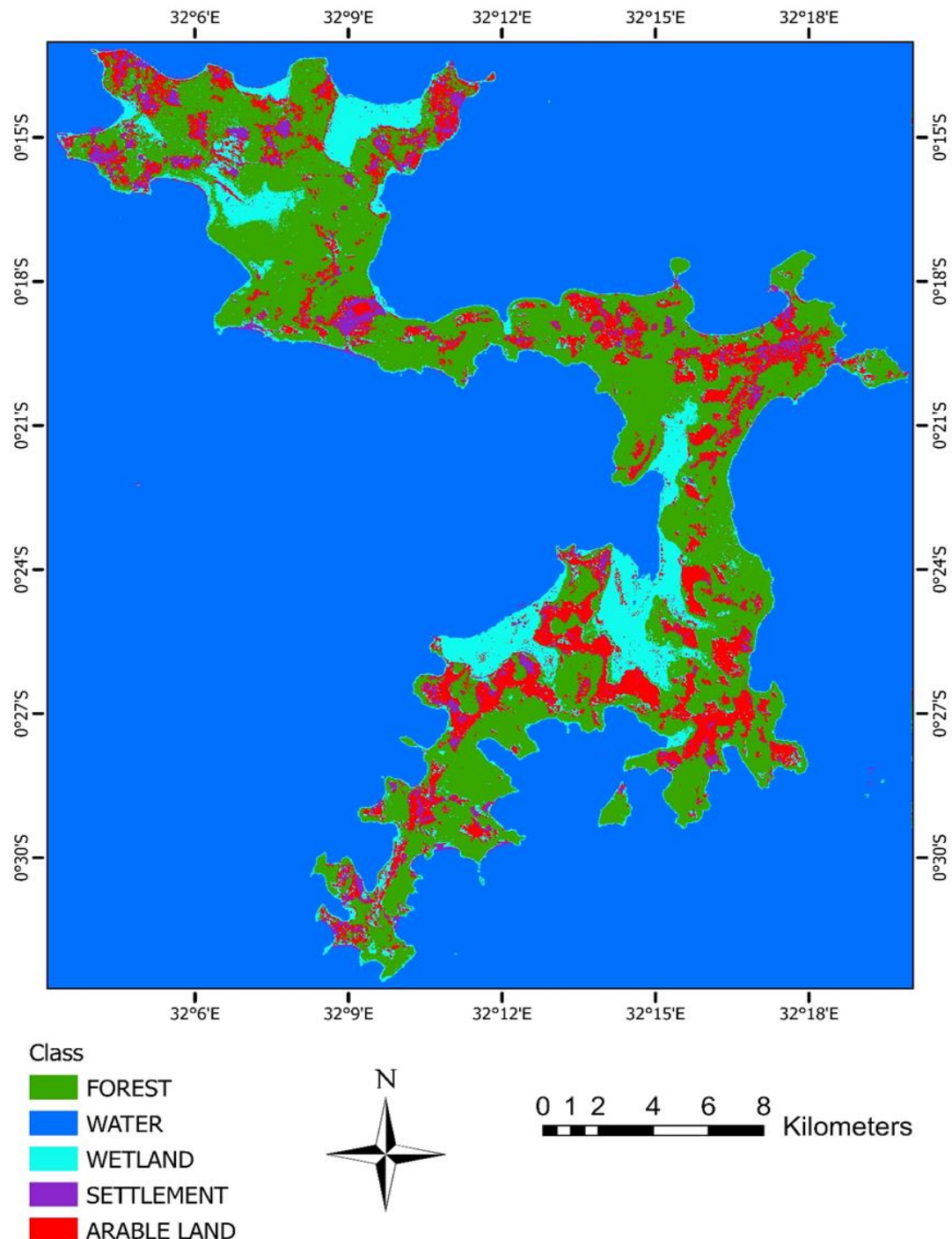
ID	Class	FOREST	WATER	OIL PALM	SETTLEMENT	WETLAND	ARABLE LAND	Total	User Accuracy	Kappa
0	FOREST	41	0	8	0	1	0	50	0.82	
1	WATER	0	49	0	0	0	0	49	1.00	
2	OIL PALM	10	0	38	0	0	3	51	0.75	
3	SETTLEMENT	2	1	0	38	2	4	47	0.81	
4	WETLAND	0	0	0	1	33	9	43	0.77	
5	ARABLE LAND	1	0	2	5	3	49	60	0.82	
6	Total	54	50	48	44	39	65	300		
7	Producer Accuracy	0.76	0.98	0.79	0.86	0.85	0.75		0.83	
8	Kappa									0.79

2022 ML CONFUSION MATRIX

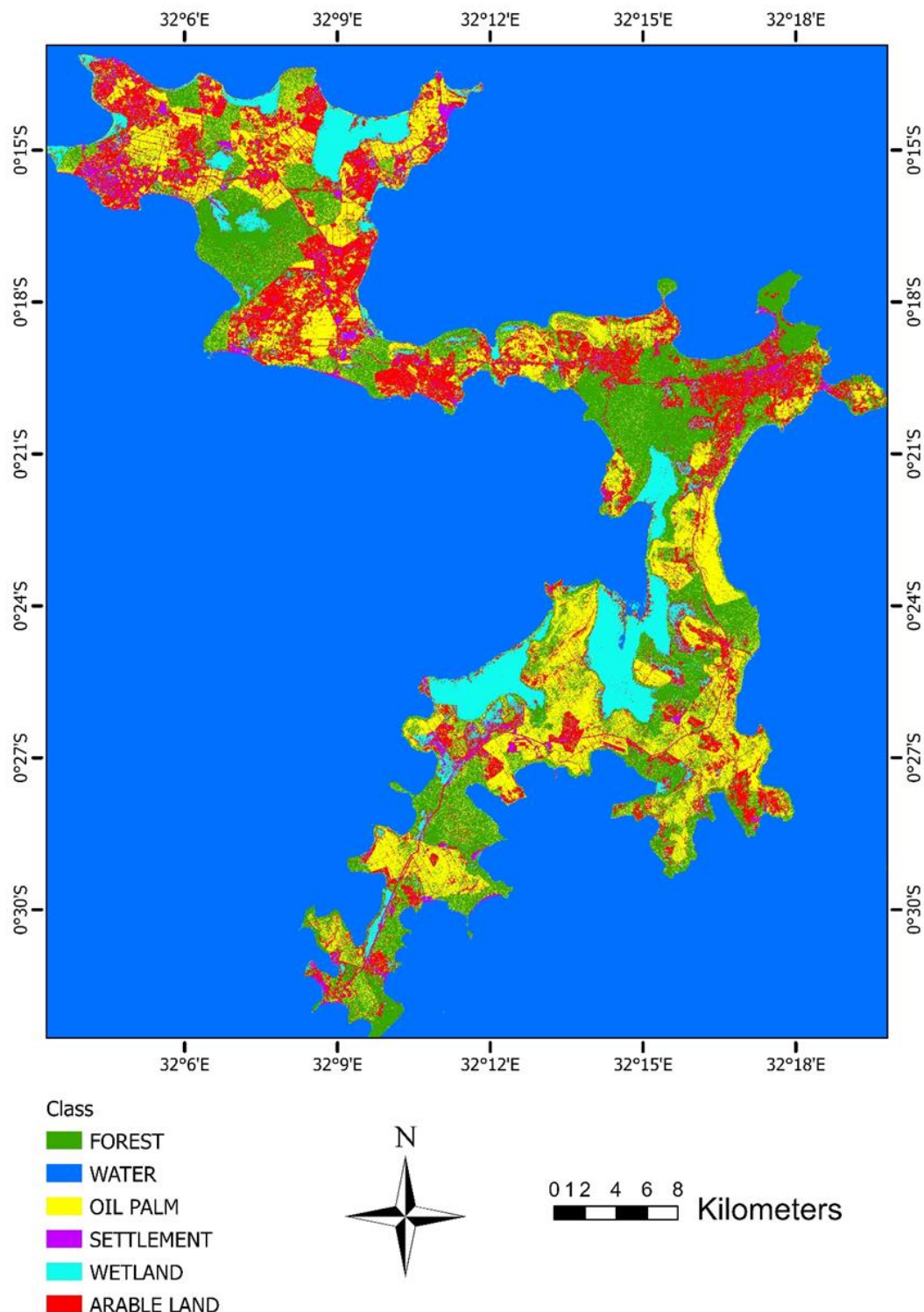
ID	Class	WATER	FOREST	OIL PALM	SETTLEMENT	WETLAND	ARABLE LAND	Total	User Accuracy	Kappa
0	WATER	49	0	0	0	0	0	49	1.00	
1	FOREST	0	29	12	0	0	1	42	0.69	
2	OIL PALM	0	21	33	0	0	1	55	0.60	
3	SETTLEMENT	5	1	1	33	0	8	48	0.69	
4	WETLAND	0	0	0	1	32	10	43	0.74	
5	ARABLE LAND	0	3	0	6	8	46	63	0.73	
6	Total	54	54	46	40	40	66	300		
7	Producer Accuracy	0.91	0.54	0.72	0.83	0.80	0.70		0.74	
8	Kappa									0.69

Appendix C : Support Vector Machine (SVM) classified maps

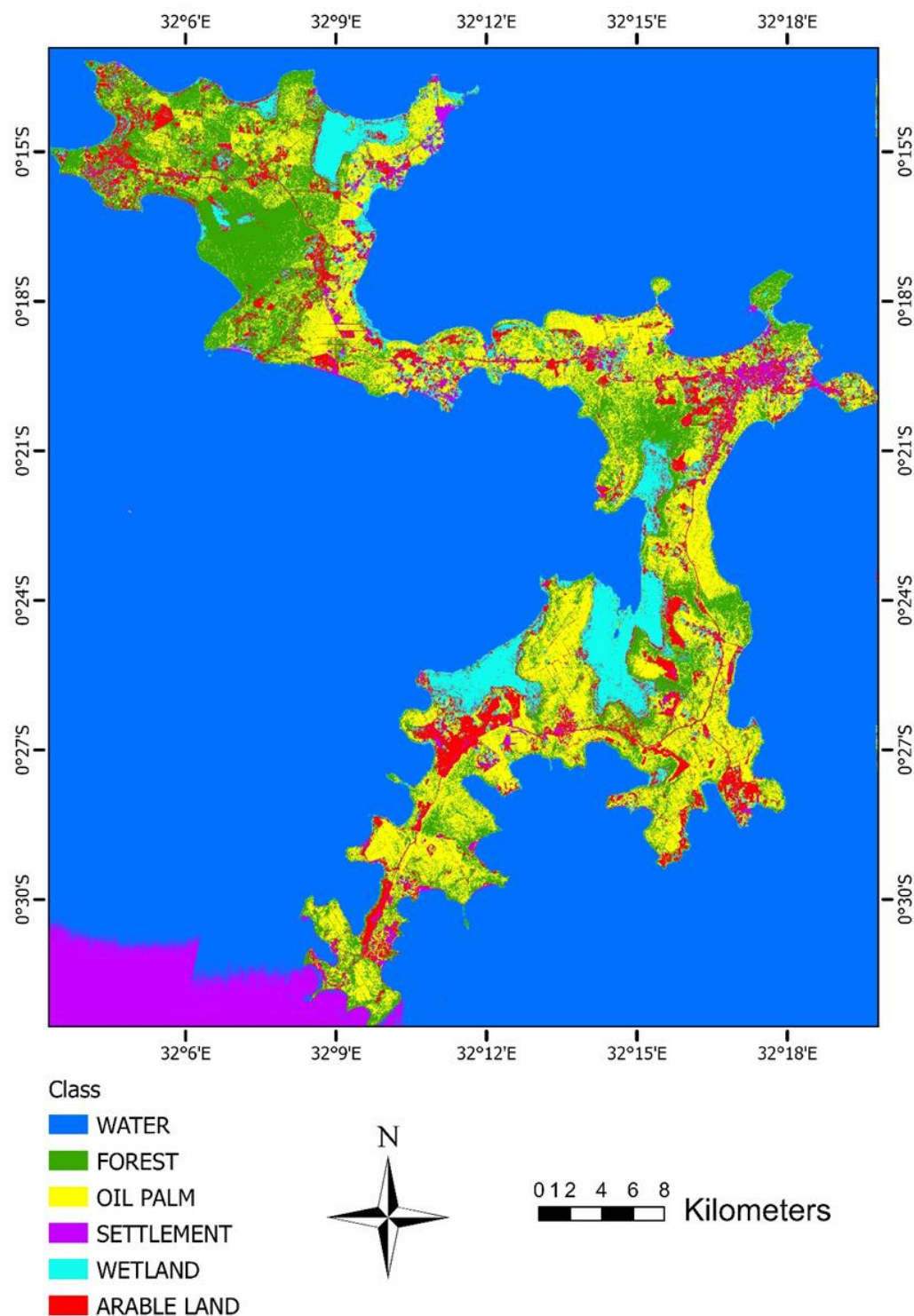
2002 Land Cover by Support Vector Machine Classification



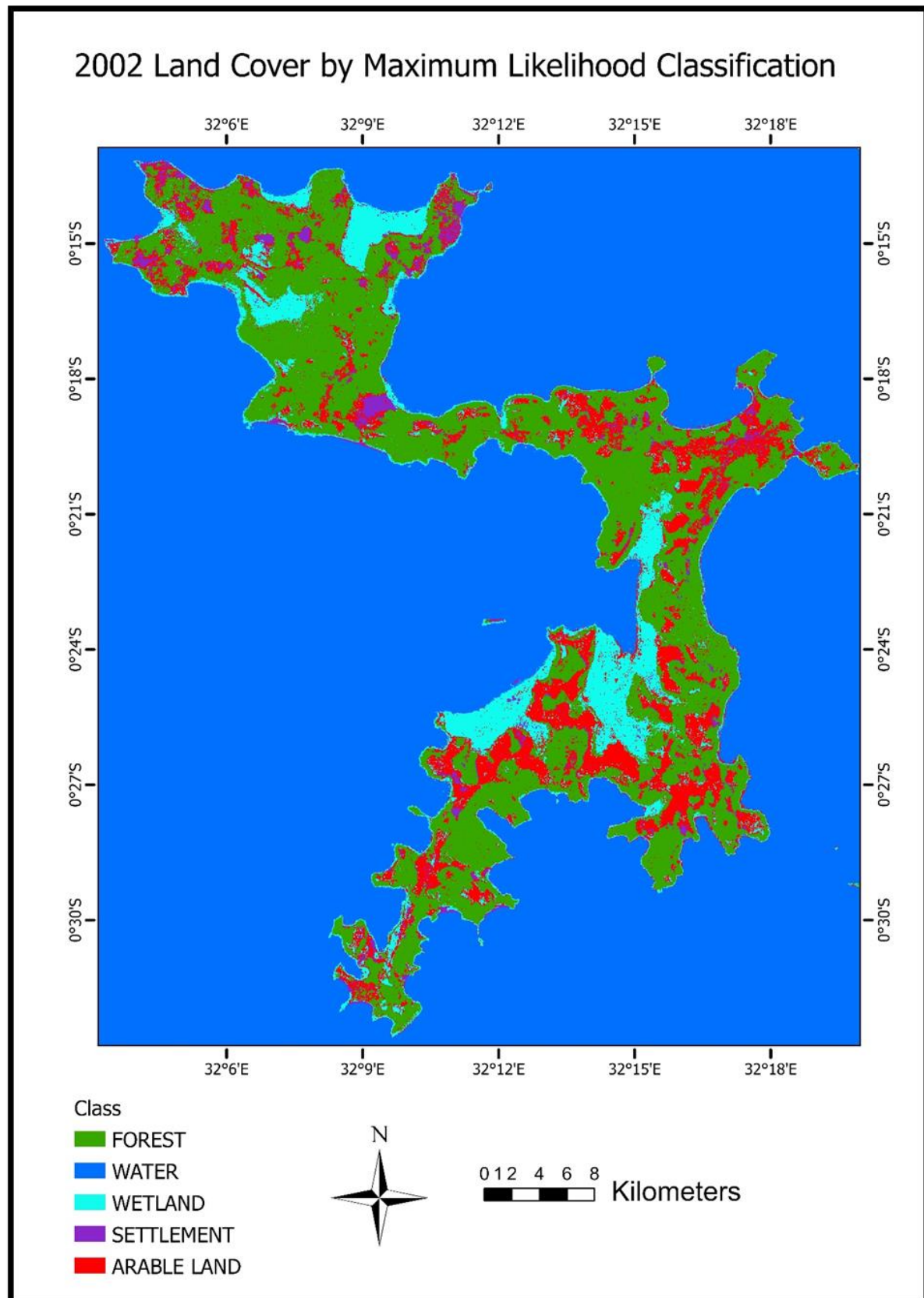
2016 Land Cover by Support Vector Machine Classification



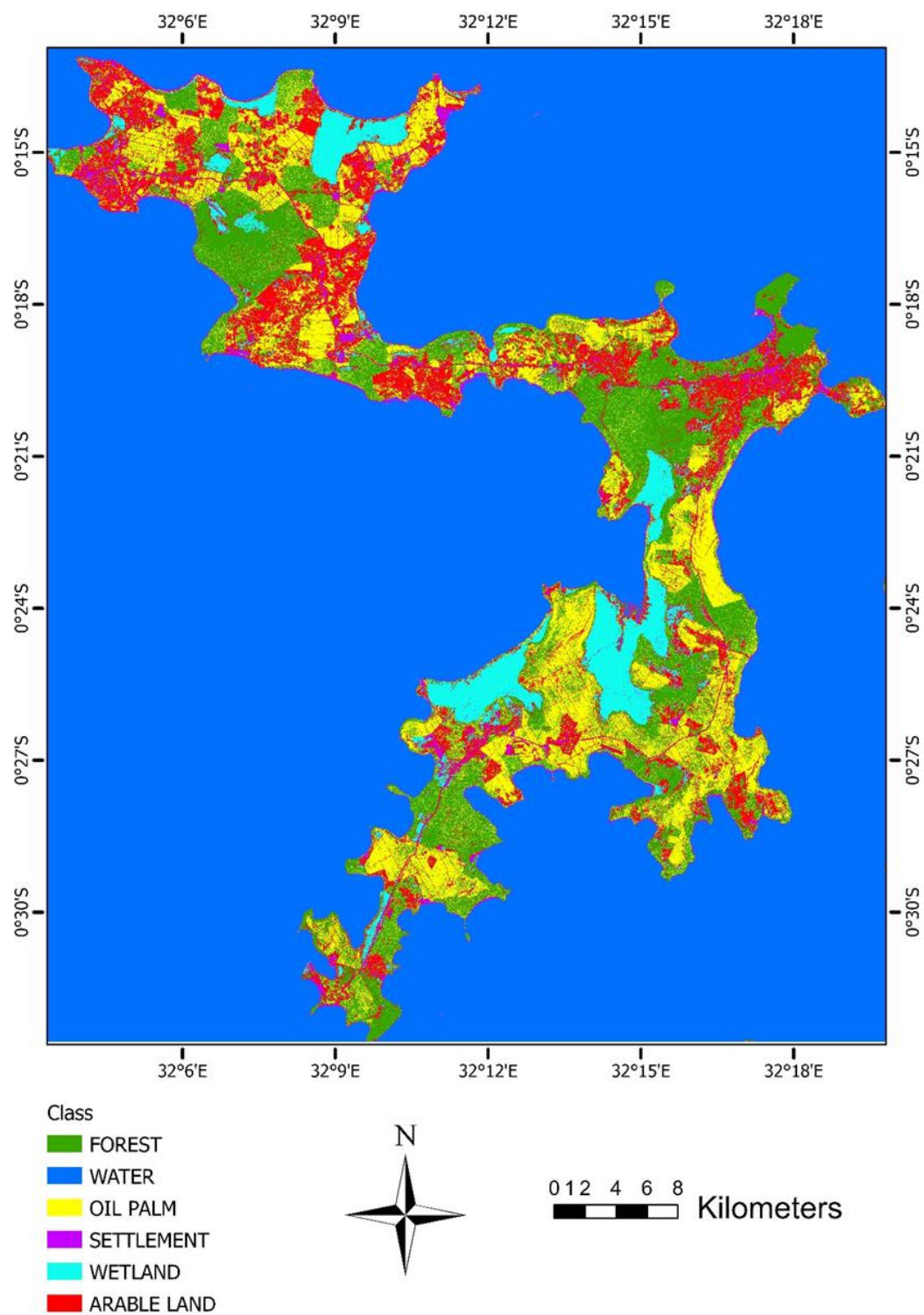
2022 Land Cover by Support Vector Machine Classification



Appendix D : Maximum Likelihood (ML) classified maps



2016 Land Cover by Maximum Likelihood Classification



2022 Land Cover by Maximum Likelihood Classification

